Title
The three-channel Lissajous trajectory of the auditory brain stem response

Author
Martin, William Hal

Publication Date
1984

Peer reviewed|Thesis/dissertation

THE THREE-CHANNEL LISSAJOUS TRAJECTORY OF THE AUDITORY BRAIN STEM RESPONSE

by

William Hal Martin

DISSERTATION

Submitted in partial satisfaction of the requirements for the degree of

DOCTOR OF PHILOSOPHY

in

Speech and Hearing Science

in the

GRADUATE DIVISION

of the

UNIVERSITY OF CALIFORNIA

San Francisco
and Santa Barbara

[redacted]

Date . . . . . University Librarian

Degree Conferred: JAN 02 1984

TIT

CANDI

DEGRE

It is
disse
Micro
be ob

If it
disse
given
yearl
micro
upon

.nles
you i
recro
the c

1.

2.

TABLE OF CONTENTS

ABSTRACT

Auditory brain stem responses (ABRs) are extensively used as tools in basic science research and otoneurological diagnosis. However, ABRs recorded from any single electrode pair are limited in the information they provide. Surface potential mapping studies provide difficult to synthesize applicable meaning from them.

The purpose of this study was to reduce some of these limitations by recording three-single channel click evoked ABRs simultaneously, combining their data, and plotting a single three-dimensional ABR. The use of three orthogonal electrode pairs approximates an infinite number of configurations and therefore combines the investigative power of a mapping study with the simplicity of a single waveform.

Results were as follows: (1) The three-dimensional plot formed a three-channel Lissajous trajectory (3-CLT) of the ABR. Segments of sequential data points of the 3-CLT were planar in configuration. Planar-segments were described in terms of duration, post-stimulus latency, shape and position relative to the voltage axes. The 3-CLT and its planar-segments are reproducible within and across subjects. (2) Planar-segment formation, duration and latency were not affected by changing electrode position. (3) Right ear stimulation produced a mirror-image of the 3-CLT generated by left ear stimulation. (4) The four major planar-segment present at 10 dB differentiated into 12 planar-segments with increasing stimulus level. Some of these segments demonstrated position changes.

On the basis of these results, it can be concluded: (1) Planar-segments provide new information about underlying neurophysiological mechanisms unavailable from any single-channel recording. Planarity of data points suggests similar activity underlying the 3-CLT. (2) The 3-CLT simplifies mapping studies by providing a representation of all of the amplitude, polarity and latency information available in the ABR. (3) Changes in planar-segment position may reflect changes in position of contributing neural generators. (4) The 3-CLT provides more information at low stimulus levels than does the single channel ABR. At 10 dB the 3-CLT offers four planar-segments reflecting activity at different levels of the auditory pathway. Single channel ABRs from equivalent stimuli show only one or two peaks representing more

restricted regions of the brainstem. (5) Increasing the size of the area of activation on the basilar membrane adds new contributing generators to the ABR, and those new generators have different anatomical geometry.

3-CLT analysis is a new technique which provides additional as well as more specific information than the single-channel ABR.

ACKNOWLEDGMENTS

I would like to gratefully recognize some of the many people to whom this thesis truly belongs.

First, to my thesis committee, for their teaching and direction; Dr. Sanford Gerber, for his patience and careful editorial comments, Dr. Michael Merzenich for insight into the ultimate application of this work and for timely encouragement, Dr. John Gardi for his kamikaze inspiration and continual driving energy, friendship and support, and Dr. Don Jewett, my special friend who has shared his commitment to excellence and quest for knowledge with me. I will always be grateful for the privilege of working in the shadow of such a great man. Dr. Richard Flower has made himself continually available throughout my graduate studies with helpful suggestions and support. Dr. Robert Stroud gave much of his precious time to help me understand three-dimensional mathematics. Dr. Hillel Pratt, with whom I will partake in further exploration of the 3-CLT, has been an inspiration and example to me. Dr. Haim Sohmer has supported me during this time by understanding in a very personal way my desire to know God and study His creation. Dr. Arnold Starr, who adopted me at the Laguna Beach Free Clinic several years ago, has become my 'Godfather'. He gave me the initial opportunity to study ABRs and is one who has continually given me fair and good advice in career and personal matters. I only hope that my career in science will be a tribute to his concern towards me. To these men of science, whom I humbly join in the exploration of unknown frontiers, I offer my appreciation.

I am also grateful to the individual friends who have sacrificed their own time and resources to bring this work into existence. Scooter Morris--"Mr. UNIX"--is responsible for the vast amount of programming necessary to complete this work. He has also helped greatly in the production of this text. Mike Randolph, who has worked with me side by side throughout the majority of this project, was without question, the most helpful, available, and willing friend I could have asked for. He was also the best graduate student I have ever had. Goalie Alan Weatherhead and Ed Cuba Martinez rescued me numerous times in my hour of need and shared one long night with me. Laury Fisher, Bill Garrett and Yvonne Sininger have all contributed to the numbers and pictures which are presented in

this work.

Finally, I would like to thank those friends who have stood faithfully beside me through many personal traumas during my studies and have given me the courage to go on. The prayer people, interceding continually on my behalf; Chopper, Sandy Quinn, and Bridget O'Neill. Zelda and Oolee have been my faithful and patient friends, always there in support and love. Dr. Jim Leo, my brother, as well as the Wednesday night Bible Study gang have given me additional spiritual support, especially in the rough spots. Above all my mother, father and family, who never lost faith in me deserve credit and appreciation for being what a family should be.

This work is dedicated to the Lord Jesus Christ, in hope that He might be glorified in all things.

CHAPTER 1

INTRODUCTION

The following corpus consists of three papers. These combined papers present a definitive report on the three-dimensional auditory brain stem response (ABR) also known as the three-channel Lissajous trajectory of the ABR. To date, only a preliminary report by Williston et al (1981), presenting a qualitative description of their results using guinea pigs, had been published. In that report three single-channel ABRs were recorded from orthogonally located electrode pairs. The three waveforms were then plotted three-dimensionally using a plastic, string and colored yarn model. The authors noted that specific sections of the plot appeared to lie in discrete planes.

Planarity of a physiologic response was first noted by Schellong et al (1937), an early investigator in the field of vectorcardiography. He reported that the QRS loop of the three-dimensional vectorcardiogram was planar in configuration. Later, the degree of planarity (i.e., how well the data points conformed to a single plane), the position of the plane relative to the anatomical axes, and the shape of the loop formed by the data points were all found to improve diagnosis of cardiopathology (Burger and

Vaane, 1958; McFee et al, 1961; Pipberger and Carter, 1962; Abel, 1965; Mark and Arbeit, 1965; and Hannien 1967). It is possible that planarity is a phenomenon which can be used to improve our diagnostic capabilities in otoneurology as well.

The purpose of the following studies was to provide a detailed description of the 3-CLT in the cat and to present an experimentally based understanding of the relationship among planar-segments and their neural generators. This was approached at three levels, hence three papers.

The first level was purely descriptive. A group of cats were studied using the most similar experimental conditions possible. The paradigm was simple; monaural stimulation, one stimulus intensity, one stimulus rate, one recording bandwidth, one recording electrode configuration, and one analysis procedure. The 3-CLTs recorded from the cats were described in terms of six indices; number, apex-latency, boundaries, duration, shape, and position in voltage space. The within-animal and across-animal variability in each of these indices was determined. A detailed description of the recording method and planar analysis technique was presented as well as the nomenclature and definitions of this new field.

The second level was an attempt to determine experimentally the relationship between recording electrode location and the 3-CLT. 3-CLTs recorded using various orthogonal and non-orthogonal electrode configurations were compared by using the planar-segment indices mentioned above. Three-channel data were compared to single-channel data in terms of variability with electrode location. This experiment was performed to determine if planar-segments are electrode location dependent, or neural generator dependent.

At the third level, the stimulus intensity was systematically varied to determine the effects of stimulus level on the different characteristics of the planar-segments. Stimulus intensities were raised from near threshold intensities to high levels at small increments in order to observe sequential transitions in the 3-CLT waveform.

CHAPTER 2

PLANAR-SEGMENT FORMATION, ANALYSIS, AND RELIABILITY

INTRODUCTION

The advent of the computer has increased our capabilities for signal processing and therefore expanded and strengthened scientific methodology. High resolution sampling has been combined with averaging to permit recording of low voltage short duration signals which were previously inaccessible using earlier techniques. Such technological improvements allow the recording of neurophysiological responses which are time locked to a sensory stimulus. Sohmer and Feinmesser (1967) noted four negative peaks while recording cochlear potentials using surface electrodes. They postulated that the first two were the N1 and N2 components of the cochlear potential and that the second two were either repetitive firings of the auditory nerve or activity generated in auditory brainstem nuclei. Jewett (1969, 1970), was the first to demonstrate that activity arising from the brain stem could be recorded from electrodes placed on the scalp. Jewett and his associates (Jewett et al, 1970; Jewett and Williston 1971) recorded these potentials in humans and referred to this technique as "far-field" recording. This activity elicited by short duration click stimuli has become known

as the auditory brain stem response (ABR). Following publication of these early reports, other laboratories began to apply ABRs as tools in basic science and clinical medicine.

Sohmer and Feinmesser (1973) and Hecox and Galambos (1974) employed the ABR as a means of studying the auditory system in vivo in man and established a basis for application to audiological evaluation of difficult-to-test children, infants, and neonates. Starr and Achor (1975) studied neurologically impaired patients using ABRs which furthered the understanding of the response and its clinical applicability. Within a decade of its discovery, the ABR has gained wide acceptance and is currently used as a standard clinical procedure and research tool. In audiology, ABRs have been used to evaluate hearing in infants and difficult-to-test patients (Sohmer and Feinmesser, 1973; Starr et al, 1977) and to improve site of lesion testing, specifically for cases of acoustic neuroma (Sohmer et al, 1974; Starr and Hamilton, 1976; Stockard and Rossiter, 1977). ABRs have also been applied in (1.) assessment of brainstem pathologies resulting from neurological disease, metabolic disorder and trauma (Starr and Achor, 1975; Stockard and Rossiter, 1977); (2.) research in cochlear prosthetics (Starr and Brackmann, 1979); (3.) studying neonatal development (Jewett and Romano, 1972;

Shipley et al, 1980) and in neuroanatomical and neurophysiological testing in man and animals (a thorough review is found in Moore 1983).

The usefulness of ABRs is easily demonstrated: however, there are limitations to the amount and type of usable information which can be derived from a response recorded from any single electrode pair. One limitation arises from the lack of understanding about the physiology underlying the response and its precise neural generators. There is argument as to whether the ABR is from somatic or axonal generators (Buchwald, 1983). ABRs have also been considered of limited value for assessing the auditory system because standard methods typically employ a brief acoustic transient or a "click" stimulus (Davis, 1976). Click stimuli have a broad spectrum and therefore do not provide frequency specific information about the auditory system. However, recent studies on tone-pip evoked ABRs and ABRs recorded in the presence of derived-band, masking stimuli indicate that frequency specific responses may be realized (Kodera et al, 1977; Don and Eggermont, 1978).

Another limitation in the use of ABRs for clinical purposes is that the time-voltage waveform varies with electrode configuration. The distribution of scalp-recorded surface potentials has been approximated by

detailed mapping studies: moving either of the active recording electrodes can change the latency, amplitude and even polarity of the peaks and valleys which characterize the ABR (Plantz et al, 1974; Terkildsen et al, 1974; Streletz et al, 1977). The amount of waveform change is dependent upon the direction and distance the electrodes are moved. ABRs have been typically recorded from electrodes placed at the vertex and at the mastoid or ear lobe ipsilateral to the stimulated ear. These electrode positions have been used because they are easy to determine anatomically, and because they selectively accentuate specific peaks in the averaged ABR. The vertex position tends to maximize the amplitude of Wave V (Coats and Martin, 1977), allowing it to be recorded at near-threshold stimulus levels. Electrode positions near the stimulated ear maximize the amplitude of waves I and II, and therefore provide information from peripheral generators, including the acoustic nerve (Coats and Martin, 1977).

Investigators have found that other useful information can be obtained using alternative electrode configurations. Coats and Martin (1977) have shown that Waves I, II, and IV-V in man were accentuated using a vertex-mastoid recording pair while waves II and III were enhanced using a nasopharyngeal-mastoid scheme. Prasher and Gibson (1980) determined that asymmetries in

peripheral generator activity could be identified by recording ABRs from linked reference electrodes placed on both mastoids. These variations in electrode placement suggest that additional useful information (including information concerning brain stem pathologies) may be more readily identified by specific electrode configurations.

The potential increase in information gained from multiple electrode arrays was appreciated during the development of vectorcardiography (VCG). Early VCG studies revealed that when electrocardiogram (ECG) voltages, obtained from three electrode pairs placed orthogonally around the heart, were plotted in three-dimensional voltage space, regularly shaped ellipses were observed. Each ellipse appeared to be planar and corresponded in time with the familiar T wave and QRS complex observed in the ECG (Schellong et al, 1937; Schellong, 1938; Burger and Vaane, 1958). But, by plotting voltage in three-dimensional space, an additional observation was made--specific arrangements of loops in space were associated with normal healthy heart function whereas distorted loop patterns were associated with pathological heart function. In many cases, these disease processes would not have been easily diagnosed using standard single electrode pair ECG techniques (Wartak, 1970). Thus, vectorcardiography has been used as an adjunct to twelve-lead ECG techniques in

diagnosis of abnormal patterns of electrical activity in the heart, hypertrophy of the heart muscle, ventricular conduction defects, myocardial infarction, and injury ischemia (Wartak, 1970).

No single recording channel is always capable of accurately representing all ABR activity. For example, if neural activity is recorded as equal voltages at both recording electrodes, the differentially amplified signal will be zero. This occurs whenever the algebraic sum of neural activity at both the positive and negative recording electrodes is equal to zero. In this case, the averaged response indicates that there is little or no activity, when in fact, there can be (see Martin et al, 1983b). Therefore, when using any single electrode pair to record a "far-field" evoked potential, the averaged response may misrepresent true neural activity.

Recording ABRs from multiple electrode pairs provides a more complete and accurate estimate of the generator activity; however, correlating data from each pair (as in mapping studies) is tedious, difficult, and impractical. Besie how many additional pairs and in what orientations should they be placed to provide "enough" information about the integrity of the auditory system to be diagnostically useful.

Under ideal conditions, three orthogonal electrode pairs can provide a first approximation of equivalent dipole activity and orientation (Pratt et al, 1983). These channels can then be combined and plotted simultaneously on voltage axes resulting in a three-dimensional Lissajous figure. Lissajous curves or figures are defined as the combination of two or more simple harmonic motions. The path which the ABR follows in voltage space is referred to as a three-channel Lissajous trajectory (3-CLT). The 3-CLT has been observed in guinea pigs (Williston et al, 1981) and man (Pratt et al, 1983).

By combining the additional information obtained from simultaneously recorded multi-channel data with our knowledge of physics and physiology, some of the present limitations of the ABR can be reduced. The 3-CLT may give more useful information about the interaction between the neural generators of the ABR than single channel recording. It may also reflect coding mechanisms along the basilar membrane (see Martin et al, 1983c). Finally, the 3-CLT may allow representation of large quantities of surface potential information in a simplified and useful form (see Martin et al, 1983b).

The purpose of this paper is twofold: First to describe in detail the 3-CLT of the ABR recorded from the

cat, and second to provide the information necessary to record, analyze and define 3-CLT planar-segments.

Nomenclature

The primary observation of Williston et al. (1981) was that the 3-CLT recorded in the guinea pig could be be divided into sets of consecutive planar data points. A set of consecutive data points (usually more than 15) which lie in a plane is described as a PLANAR-SEGMENT of the 3-CLT. Segments of the 3-CLT are identified by lower case letters ('a', 'b', 'c', etc.) with arabic numbers for sub-divisions. When a segment statistically approximates a plane, that plane is referred to as the BEST-FIT PLANE. For the purposes of this paper, data points of a segment were considered planar if they remained in the best-fit plane within + 2 standard deviations of the pre-stimulus baseline noise level. The baseline noise used for statistical comparison was rotated to the same angles as the best-fit plane to account for different noise levels in each of the three contributing single channels.

The APEX of a segment is the point of sharpest curvature. The APEX-LATENCY of a segment is the time in milliseconds from the stimulus onset to the apex of the segment. The DURATION of a planar-segment is the time in milliseconds during which the segment remains in the

best-fit plane. The method of analysis employed in this study is called PLANAR ANALYSIS and differs from other multichannel analysis methods (Ino and Mizoi, 1980; Cohen, 1982; Szelenberger, 1982).

METHODS

Subjects

Ten adult cats were anesthetized initially with ketamine hydrochloride/acepromazine malate (.6mg/Kg, 70/30 mixture, I.M.). Anesthesia was maintained by sodium pentabarbitol (40mg/Kg, I.V.). All animals were immobilized in a head holder in a sound-reduction, electrically shielded test chamber (IAC). Rectal temperature was maintained between 37 and 39 degrees C by a water-bath heating pad.

Stimulation

Stimuli were computer-generated square waves (100 usec duration) which, when presented through a shielded headphone (Stax model SR84), produced a 70 dB impulse SPL rarefaction click. The headphone was coupled to a plastic earbar inserted into the right ear of each cat. A fast Fourier transform of the stimulus indicated that peak

energy was between 3 and 5 kHz (for FFT and time/pressure waveform see Martin et al, 1983c). Stimulus calibration was obtained using a precision Sound Level Meter (Bruel and Kajer, Model 2209). The sound level meter was equipped with a 1/2 inch microphone and coupled directly to the output of the plastic earbar.

Recording

Silver-silver chloride wire electrodes were inserted subcutaneously for each recording channel. The X channel electrodes were placed at the bridge of the nose (+) and occiput (-). The Y channel electrodes were placed at the left (+) and right (-) mastoids, immediately below the pinna. The Z channel electrodes were placed at vertex (+) and midline throat (-). These channels are referred to as the RECORDING AXES (Figure 1). The electrode-skin impedance was measured using a Grass electrode impedance meter and was less than 3 kohms in all cases. The activity from each channel was band-pass filtered from 10 Hz to 3 or 10 kHz (3dB down at 6dB/oct rolloff) and amplified 100,000 times (WPI Model DAM 6-A modified to give 100,000 gain). Lowering the high frequency cut-off did not change the latency or amplitude of the single-channel responses, but provided results which were more easily analyzed through planar analysis. Five-hundred sweeps of 15 ms each were averaged on line using a Nova 3 computer.

The data were sampled every 25 usec (23 usec for cat 01) and digitized with a 12 bit A/D converter. In order to maintain such high sampling rates, the ABRs from each channel were recorded sequentially rather than simultaneously. This was deemed possible because single-channel ABR test-retest reliability was very good (Figure 2).

Analysis

Describing the three-dimensional characteristics of the 3-CLT with two-dimensional plots is very difficult. Our laboratory has experimented with stereoscopic photographs, 16mm movies, plastic and string models, and three single-channel plots of the 3-CLT. Each of these methods provided qualitative information about the 3-CLT, but provided little quantitative information about the position, duration and shape of planar-segments. The analysis method in this study was an off-line procedure in which the 3-CLT was displayed on an oscilliscope and rotated manually by keyboard input. Any set of consecutive data points could be analyzed for planarity. When a segment appeared visually to be planar, the observer initiated a program which determined if the sequence of points lay within + 2 standard deviations (re baseline noise) of the best-fit plane. This program determined the endpoints of the planar-segment from which duration values were calculated. The criterion for an endpoint was that the next

nine points following an endpoint must all lie out of the best-fit plane.

The shape of the planar-segment was qualitatively represented by a plot of the data points from a view normal to the best-fit plane in which the segment lies. This is referred to as the "broadside" view. The apex latency for each planar-segment was determined by visually selecting the apex of the segment in the broadside view. The variance in and out of the best-fit plane was also plotted (Figure 3).

The position of the best-fit plane in three-dimensional voltage space was also calculated. To describe the position of a plane, a set of analysis axes had to be defined. The X, Y, and Z channel data are plotted on X, Y, and Z voltage axes. These are referred to as the ANALYSIS AXES. The convention for the orientation of these axes is taken from the Handbook of Chemistry and Physics' section on analytic geometry (Hodgman, 1960). The convention follows the right hand rule. Thus, the extended index fingertip is positive X, the middle finger to the left is positive Y, and the thumb pointed upward is positive Z. The intersection of the fingers and thumb is the origin (or zero voltage point).

In these experiments, the ABR from the nose-occiput channel is plotted in the X direction, the ABR from the left-right mastoid channel in the Y direction, and the ABR from the vertex-throat channel in the Z direction. Both recording and analysis axes follow the right hand rule. A distinction is made between recording and analysis axes, because analysis axes need not in any way be related to anatomical location.

The position of the best-fit plane relative to the analysis axes can be described mathematically in many ways. One of these methods was applied in this study and others are referred to in the discussion section. The method we chose describes the position of the best-fit plane by defining the unique vector which is normal to the plane and passes through the origin. This vector is called the SIGHT VECTOR since it is determined by visually rotating the data points during analysis. The sight vector is described in terms of its length (distance) and by two angles relative to the analysis axes. This method is based on a modification of the spherical coordinate system (Hodgman, 1960). The first angle, the AZIMUTH, is the angle between the sight vector and the positive X axis, around the Z axis. Positive angles (toward the +Y axis) range in value from 0 to +180 degrees. Negative angles (towards the -Y axis) range from 0 to -180 degrees. The

second angle, the ELEVATION, is the angle between the sight vector and the positive Z axis. Elevation values range from 0 to +180 degrees. An analogy to spherical coordinate angles is that of longitude and latitude; the former equivalent to azimuth and the latter to elevation. The distance is measured in microvolts from the origin and is the length of the sight vector. This method was adopted for this study because it provides the most intuitive means of visualizing the position of a plane relative to the analysis axes (Figure 4). To compare sight-vector positions, the included angle between two sight vectors was calculated using the formula (Hannien 1967):

$$\text{Included angle} = \cos^{-1} \frac{X_1X_2 + Y_1Y_2 + Z_1Z_2}{\sqrt{X_1^2 + Y_1^2 + Z_1^2}\sqrt{X_2^2 + Y_2^2 + Z_2^2}}$$

Where X, Y, Z are the coordinates of any points along the sight vectors of the planar-segments being considered (Figure 5). The included angle lies in the plane made up of the two sight vectors intersecting at the origin.

Statistical analysis of sight vector comparisons was performed using Hotellings' t-square (Morrison, 1976) on X, Y, and Z values of the sight vectors for each adjacent pair of planar-segments. This method does not compare within trial pairings of adjacent sight vectors as does the graphic display in Figure 13, but pools all X, Y, and

Z values and compares them to adjacent sight vector X, Y, Z values. The values are pooled because X, Y, and Z values are interdependent and therefore sight vector position comparisons must consider all three values as one functional unit.

RESULTS

Three two-dimensional views of a typical 3-CLT are displayed in Figures 6a, b, and c. The X, Y, and Z channels which were combined to form this 3-CLT are illustrated in Figure 2. Figures 6a, b, and c are the results of plotting all of the possible combinations of the single-channel ABRs in Figure 2 as two-dimensional Lissajous figures. The voltage trajectory begins at the origin, but never passes through the origin again. Time is not explicitly plotted, but is represented by the distance between data points (Williston et al, 1981).

Planar-Segment Formation

The 3-CLT illustrated in Figure 6a, b, c can be divided into 12 planar-segments. These segments have been named a1, a2, b1, b2, c1, c2, c3, c4, d1, d2, d3, and d4. This breakdown is based on the relation of the grouped planar-segments at 70 dB to those observed at lower

stimulus levels (see Martin et al. 1983c). Figures 7a-e indicate the planar-segment boundaries for each of the 12 planar-segments. Figure 7a displays the X, Y, and Z single channel ABRs and the boundaries for the four groups of planar-segments ("a", "b", "c","d"). The boundaries for each individual planar-segment are presented in figures 7b, c, d, e. All planar-segments in these examples overlap (i.e., they share data points) with adjacent planar-segments except d1-d2 and d3-d4 (See Figure 7e). Planar-segment boundaries do not necessarily correspond with any specific characteristic of single-channel waveforms, such as positive or negative peaks.

Typical examples of each planar-segment are plotted in Figures 8a, b, c, d. The variance in and out of the plane is plotted with the beginning and ending points (in milliseconds) for each segment. "Non-planar" data points have been added at each end of the planar-segment as an indicator of the loss of planarity outside the boundaries. Broadside views are also plotted to illustrate the variety of shapes and sizes of planar-segments. The azimuth, elevation, and distance for each planar-segment is presented.

Planar-segments a1, a2, and b1 correspond roughly with the vertex potential, Jewett Wave I. B2, c1 and c2 correspond to Wave II, and c3 and c4 correspond to Wave

III. Planar-segment d1 begins on the falling slope of III and ends on the rise of IV. D2 begins on the rise of IV and continues to the rise of V. Wave V corresponds to planar-segments d3 and d4.

Planar-Segment Variability Within and Across Subjects

Similar three-channel ABRs were obtained when recording from one cat eight times over a six hour period at using a 70dB impulse SPL click stimulus. In each case, a 3-CLT was recorded which could be divided into 12 planar-segments using planar analysis. Figure 9 graphically illustrates the distributions of planar-segment boundaries, apex latencies, and durations within one cat over the six hour period. The median boundaries indicate that planar-segments typically overlap. The apex latency of a1 was not reported because the shape of the segment often approximates a line and it is very difficult to define an apex in such a planar-segment. The durations of planar-segments a1 to d1 were usually slightly less than .5ms each, however, planar-segments d2 to d4 were two to four times longer. These later planar-segments are not only longer in duration, but are more variable in duration than earlier planar-segments. Figure 10 is an example of the maximum variability for a particular planar-segment (in this case c3) recorded within one animal. Planar-segment c3 was selected because it illustrates as specific type of

variability occasionally observed. In the case shown on the right, c3 and c2 are combined to form one planar-segment, therefore changing the shape and increasing the duration of c3. The apices of c2 and c3 are marked and if the data points which form c2 are ignored, both the shape and duration of c3 remain comparable to the two other examples of c3 presented.

Figure 11 plots the boundary, latency, and duration distributions for all planar-segments recorded across 10 subjects at one stimulus intensity, 70dB. Across-animal latencies were normalized to account for differences in hearing across subjects. This was done by determining an average Wave V latency from all cats and then correcting single-channel ABRs from each cat to normalized values by adding or subtracting latency. This correction was considered reasonable because inter-apex latencies and planar group durations changed minimally at stimulus levels from 10 to 70dB (Martin et al, 1983c). As observed in the within-subject data, there is boundary overlap between adjacent planar-segments. Also, there is a marked increase in duration and duration variability of planar-segments d2, d3, and d4 compared to earlier segments. Variability in shape of planar-segment c3 across animals is illustrated in Figure 12. Although the positions of the plots are different, the shapes are basically the

same. This is generally true for all planar-segments when compared across animals.

Sight Vector Position

Average sight vector positions for each planar-segment were calculated as well as their distribution in voltage space. These values recorded from one cat over a six hour experimental period are presented in Table I. Average sight vector positions required the calculation of the cartesian coordinate values X, Y, and Z of the point at which the sight vector intersected the best-fit-plane. For a given planar-segment, the X, Y, and Z values for all of the trials were averaged and then converted back to azimuth and elevation values. The distribution of sight vectors for a given planar-segment around the average sight-vector is reported as an included angle. This value was determined by calculating the included angle between the average sight vector and the sight vector recorded during each of the eight trials. The percentile values reported indicate the percentage of the total sight vectors observed which were within a specific radius (in degrees of included angle) around the average sight vector. For example, 50% of the observed sight vectors for planar segment a1 were within 7 degrees radius of the average a1 sight vector in any azimuth or elevation

direction. Therefore, the larger the included angle value for a given percentile, the greater the variability in the position of the sight vector for that specific planar-segment. For example, planar-segments a1, a2, and c1 have little variability in position for this animal while b1 (especially) and d1 are the most variable.

Average sight vector positions and their distributions recorded from 10 different cats are presented in Table II. The variability of sight vector position across animals was typically two to three times greater than the variability within one animal over a six hour testing period with one exception: b1 was much more variable in one animal over a six hour testing period than it was across the eight subjects.

Sight Vector Distance

Median and quartile distance values for sight vectors recorded within and across subjects are presented in Table III. In cases where the distance is very small, the sight vector approximates zero magnitude. However, since the sight vector is normal to the best-fit plane, it may have a direction or sense even at zero magnitude. The "typical" sense of each sight vector was determined by choosing the sense most consistently observed across the ten sub-

jects. In cases where distances were small and therefore the sense of the sight vector was ambiguous (e.g. a1, c1, and d1), the typical sense was adopted. This procedure maintained consistent azimuth and elevation values but resulted in negative median distances for planar-segments c2 and d2 in the within-animal distance data. Both within and across animals quartile distance values rarely exceeded 2 uv, and median values were usually less than 1uv.

Number of Planar-Segments

Twelve planar-segments were visually identified in all animals. However, it was necessary to define some criterion to determine if two adjacent segments of the 3-CLT could be identified as separate planar-segments. The criterion selected was the position of each sight vector relative to its adjacent counterpart. The position difference between each pair of adjacent sight vectors was quantified by measuring their included angle (e.g., a1 vs. a2, a2 vs. b1, b1 vs. b2, etc.) for all experimental trials. Included angles observed between adjacent sight vectors are presented in Figure 13 for both within and across-subject testing. This figure illustrates the difference in position of adjacent sight vectors. Median and quartile included angle values describe the relative

difference in position between any two sight vectors from sequential planar-segments. The smaller the included angle, the closer the positions of adjacent sight vectors. Also presented in Figure 13 are test-retest included angle values for each individual sight-vector from two sequential trials within one subject as a comparison of normal sight-vector variability. Operator analysis error was always less than test-retest variability. This was determined by reanalyzing the same data six times over a period of several months and determining the maximum included angle between any pair of the six sight vectors for a given planar-segment. The maximum operator error included angle was then compared to included angles determined by the same operator analyzing repeat tests within the same animal. By comparing adjacent pairs of sight vectors, median adjacent included angle values ranged from 26 degrees (c4 vs d1, within animal) to 159 degrees (a1 vs a2, within animal). In three cases, the included angle between adjacent planes was so small that data points of both adjacent planar-segments were within + 2 standard deviations of the rotated baseline noise (i.e. within the limits defined as "planar"). This suggested that only one planar-segment existed, although two were usually observed. This was the exception rather than the rule. Only two of 110 adjacent included angles derived from across-subject data (c4 vs d1, and d2 vs d3) and one of 88

derived from within-subject, demonstrated (d3 vs d4) included angles of zero. In these cases however, it was still possible to determine apex-latencies and therefore identify planar-segments. An example of this was the combination of c2 and c3 into one planar-segment while their apices could still be identified (Figure 10).

All but two of the adjacent sight-vectors, both within and across animals, were demonstrated to be in significantly different locations using Hotellings' t-square test ($p < 0.05$). The two which were not found to be significant by this test were the c4 vs. d1 within-animal comparison ($p=.07$) and the d2 vs. d3 across-animal comparison ($p=.80$). However, Figure 13 illustrates that c4 and d1 within one animal as well as d2 and d3 across animals were usually reported to be in different locations.

In summary, most of the time, twelve sequential planar-segments were observed using planar-analysis. Each differed in position and shape from those adjacent to it. Planar-segments with short apex-latencies had short durations, while planar-segments with latencies greater than about 4 milliseconds post-stimulus were two to three times longer in duration.

DISCUSSION

The results of this study support the work of Williston et al. (1981) using guinea pigs. Combining three single-channel ABRs recorded from orthogonally placed electrode pairs results in a three-dimensional Lissajous figure in the cat as well as the guinea pig. The path of the 3-CLT begins at the origin. But, as in the guinea pig, does not return to the origin. Williston et al. (1981) pointed out that this is not observed in the three-dimensional plot of the vectorcardiogram. This phenomenon could be due to postsynaptic potential, slow wave activity reflected in the ABR. Williston et al. (1981) also noted that at least three segments of consecutive data points were planar when plotted. Planar-segments are also observed along the 3-CLT of the cat. However, the number of planar-segments observed in the cat is four times that reported in the guinea pig. The difference in number of planar-segments between cats and guinea pigs may be partly physiological. The single-channel ABR of the guinea pig has at most four peaks in the Z trace, whereas a similar recording in the cat shows five positive peaks, possibly six, because Wave I in the Z channel forms two positive peaks (see Figure 2). The more probable reason for the discrepancy is the difference in analysis techniques. Williston et al. (1981) were limited

to visual appraisal of a string model for their analysis. Computer analysis employing statistical criteria for planar-segment determination has enabled us to increase the sensitivity of planar-analysis.

The consistent finding of 12 planar-segments, each with similar durations, latencies, boundaries, and locations in voltage space, observed across all subjects, indicates that planar-segment formation is a general phenomenon which reflects neural generator activity. Planar-segment formation is also observed in vectorcardiography which records cardiac activity with three orthogonally placed electrodes. When plotted in three dimensions the QRS complex and T wave form loops which are planar (Wartak, 1970). The generators of VCG planes are the cardiac muscles. Asynchronous firing of heart muscle due to pathology can result in a disruption of planar-loops in the VCG (DePasquale and Burch, 1960; Frimpter et al, 1958; Hugenholtz et al, 1961; Mayer et al, 1963), and changes in planar position (Pipberger and Carter, 1962; Abel, 1966; Mark and Arbeit, 1966) and loss planarity (Pipberger and Carter, 1962; Mark and Arbeit, 1966). Disruption of the neural firing pattern, either within one or between generators apparently modifies the formation of planar events recorded from the heart. Analogous disruptions of neural synchrony should have equal effects on ABR

planar-segments.

The increase in variability of sight vector position across animals compared to within animals primarily reflects variations in single-channel waveforms which contribute to 3-CLT formation. Jewett and Williston (1971), Starr and Achor (1975), Rowe (1978), and Stockard et al. (1979) have reported that amplitude and general waveform appearance vary from subject to subject more than latency values. Planar-segment position is an amplitude related function and thus the increased variability in position across subjects would be expected. In one case in which within-animal sight vector distribution values for planar-segment b1 exceeded across-animal distribution values, the increase in variability was introduced by the last three recordings obtained over the six hour period. It should be noted that over long testing periods during which the animal was maintained under anesthesia, the position of the sight vector for planar-segment b1 varied much more than other sight vector positions. This suggests that some planar-segments may reflect activity which is particularly sensitive to subject state.

Overlapping of planar-segment boundaries may be partly due to the methodology employed in planar-analysis. To be considered planar, data points had to lie within + 2

standard deviations of the rotated baseline noise. This range could permit a few data points at each end of a planar-segment to be accepted when in actuality the 3-CLT had begun to leave one plane and enter a new one. The points at the transition between adjacent planar-segments would then be included within the boundaries of both adjacent segments. The criteria of ± 2 standard deviations of baseline noise assumes that each data point is independent of the points immediately before and after it. This, however, is not the case, and errors resulting from this assumption will tend to increase the overlap of adjacent planar-segments. Overlapping could also be caused by decreasing activity from the generators forming one planar-segment interacting with increasing activity of generators forming the next planar-segment. In this case, the overlap would result from the simultaneous activity of sequential generators during a transition period.

Planar-segment duration increased as a function of planar-segment latency both within and across subjects. This trend reflects the fact that the auditory pathway is a divergent system, branching and increasing in complexity at each synaptic junction. The ABR is the algebraic sum of all simultaneous activity synchronized to the acoustic signal as a function of time. At shorter latencies (reflecting more peripheral activity centers) planar-

segments may represent the activity of fewer, more discretely located generators than at longer latencies. These short latency generators would have a high degree of synchrony and little overlap with earlier or later generator activity. Longer latency planar-segments may have longer durations because of the overlap of neuronal activity due to divergence.

Variability in planar-segment boundaries and duration values was related to the included angle between adjacent sight vectors. When two adjacent segments have a small included angle, their best-fit planes are approximately the same. Planar analysis may indicate that the two planar-segments form one longer segment (still planar) thereby increasing the duration and altering the boundaries of each contributing planar-segment. However, the apex of the segment remains unchanged and thus the apex latency as well.

The twelve planar-segments identified were usually located in significantly ($p < .05$) different positions as defined by their sight vectors with the exception of two cases. In both cases the included angles between adjacent plane-segments were small (c4 vs d1 within subject = 26 degrees, d2 vs d3 across subject = 28 degrees). It was

also determined that in three out of 198 cases, include angles between two planar-segments were zero, suggesting that both planar-segments were in the same best-fit plane. This could possibly occur when adjacent included angles are small enough that data points lie within the planarity criteria used (i.e. less than $\pm$ 2 standard deviations of rotated baseline noise). Therefore, the number of planar-segments will be less than 12 when the included angle between two adjacent sight vectors is so small that the difference in sight vector position is considered due to random variation in electrical or physiological noise. In general, however, the results suggest that adjacent planar-segments are in different positions in voltage space.

The significance of spatially separated planar-segments is that the location of segments in voltage space appears to be dependent upon neural generator activity (Martin et al, 1983b and c). Therefore, changes in planar-segment position may provide information about changes in generator orientation or the time-course of activation unavailable in single-channel ABRs (Martin et al, 1983b). This information would be clinically useful for identifying site of lesion and following progressive changes in neuronal generators as a function of disease.

The presentation of three-dimensional characteristics of the 3-CLT in a two-dimensional format is difficult to achieve. The method used in this paper is not the only method available. Another method is to present the Cartesian coordinate values of the point (i.e., X, Y, Z) at which the sight vector intersects the best-fit plane. A third technique involves describing the best-fit plane of a planar-segment by its equation $Ax + By + Cz + D = 0$ where A, B, and C are the coefficients of the plane and D is the distance of the plane from the origin. A fourth way of presenting 3-D data employs polar coordinate axes definitions rather than spherical coordinate definitions. This method uses three angles and a distance to describe the sight vector instead of the two angles and a distance which we have used. A fifth technique uses the unmodified spherical coordinate method, in which azimuth values are measured from 0 to 360 degrees. All of these methods are mathematically equivalent and none provides more information than any other. They merely differ in method of presentation. We have chosen to present azimuth angles in positive and negative values to more clearly illustrate symmetry in responses obtained from stimulating opposite ears. For example, if a sight vector has an azimuth of +50 degrees with right ear stimulation, one would expect the equivalent sight vector from left ear stimulation to have an azimuth value of -50 degrees and therefore a

mirror image of the opposite sight vector.

There are several advantages in using planar analysis of the 3-CLT instead of single-channel ABRs. The first is that data from three separate recording configurations can be presented in a concise format, unlike mapping studies. Another benefit is that by using orthogonally placed electrode pairs, the possibility of recording unrepresentative activity is greatly reduced. Activity which may have a net differential potential of zero in one channel, will be recorded by one or both of the other channels and therefore represented in the 3-CLT.

A sight vector defines the position of the best-of fit plane of the data points which comprise a planar-segment, but does not provide any direct information about the location of the actual data points in voltage space. An additional index of spatial position would be to calculate the center of gravity of each planar-segment. This would be the mean of all X, Y, Z values for data points within a given planar-segment. The center of gravity could be described by the azimuth, elevation, and distance of the vector from the origin to the center of gravity point, similar to the way in which sight vectors are described.

Present clinical measures for single-channel ABRs are dependent upon one or two data points for each measure (e.g., the peak of Wave V). Apex-latencies are also determined from a single point, but that point is the net activity of three recording channels, therefore representing a more complete picture of time specific information in the ABR. Planar-segments consist of groups of data points (usually 15 or more), all of which share one common property; the points are generated in such a way that they fulfill the requirements $Ax + By + Cz + D = 0$ and as a result form a plane. This provides us with information regarding the duration of underlying neural events which is unavailable from single-channel recorded ABRs. This proposition is further supported by the fact that planar-segment boundaries do not correspond directly to peaks or valleys of any specific single-channel ABR.

The study of planar-segments may also increase our understanding and utilization of single-channel ABRs. Clinical research using 3-CLTs may enable us to determine single-channel electrode configurations which maximize the identification and diagnosis of specific neuronal impairments (Martin et al, 1983b).

Finally, if planar-segments do directly represent neuronal activity along the auditory pathway, parametric

studies involving stimulus level and masking manipulation may provide new information about the nature, location and identity of the generators which contribute to the ABR as well as to mechanisms of auditory processing (Martin et al, 1983c).

SUMMARY

Auditory brain stem response (ABR) three-channel Lissajous trajectories were recorded from 10 anesthetized adult cats from three orthogonally placed electrode pairs. Planar analysis, an off-line procedure, defined planar-segment boundaries, durations, apex-latencies and sight vector positions relative to the analysis axes. Planar-analysis indicated that sets of sequential data points along the 3-CLT formed 12 distinct planes in three-dimensional voltage space. Within- and across-subject variability was described. Alternative methods for describing planar-segment position in voltage space were presented. Planarity of data points suggests that some common underlying neurophysiological factor such as neural synchrony may be responsible for the formation of planar-segments in voltage space. These results also suggest that data obtained from three orthogonally placed electrode channels provides information about the distribution of surface potentials unavailable from any single-channel

ABR.

TABLE LEGENDS

Table I

Within animal sight vector distribution. The mean sight vector position as well as its range of distribution are presented for data recorded from one cat eight times over a six hour period. All values are in degrees. The percentile values indicate the included angle away from the average sight vector in which a certain percent of the total sight vectors was located. For example, 75 percent of all al sight vectors in this cat were within 9 degrees of the average al sight vector (azimuth=40, elevation=131). Therefore the size of the percentile included angle is dependent upon the variability in sight vector position.

Table II

Across animal sight vector distribution. The same as Table I except the data were compiled from planar-segments recorded from 10 different cats.

Table III

Within and across animal sight vector distance values (in microvolts). Median distances and quartile ranges are

presented for each planar-segment.

FIGURES

Figure 1

Recording axes for the 3-CLT. Electrode pairs are orthogonal in relationship, i.e., perpendicular and at right angles to each other. X electrode locations are bridge of nose (positive) and occiput, Y locations left (positive) and right mastoids, Z locations Cz (positive) and midline throat.

Figure 2

Single channel traces recorded from the X, Y and Z electrode pairs. The double tracings indicate the within-animal test-retest reliability for each electrode pair location. Each plot is of two traces recorded one hour apart. Arrows indicate stimulus onset at the left of each trace.

Figure 3

Hypothetical example of planar-analysis plots. Above, data points 1-8 are plotted ordinate vs. variance in and out of the best-fit-plane. The lines at each end of the variance plot represent the best-fit-plane. Points which are less than two standard deviations of the rotated

baseline noise above or below this line are considered within the plane. The lower portion of the illustration plots the normal to best-fit-plane view of the same data points. The comma represents the first data point and the arrow points the direction of the trajectory. The 0 is the point at which the sight vector intersects the best-fit plane of the planar-segment.

Figure 4

Analysis axes with example of a sight vector. Azimuth is the angle between sight vector and the X axis, elevation is the angle between the sight vector and the Z axis. The length of the sight vector is the distance. The polarity of the analysis axes is consistent with the "right hand rule". Also shown are the data points of planar-segment "P" (figure 3) in their best-fit plane. The sight vector is normal to the best-fit plane and intersects the origin. The thickness of the best-fit plane is determined by + two standard deviations of the baseline noise rotated to the same position as the sight vector.

Figure 5

Example of included angle in voltage space. If a and b are sight vectors for two different planar-segments, the difference in position of the two planar-segments may be

described by the angle between their respective sight vectors.

Figure 6a

The 3-CLT to right ear stimulation, superimposed upon analysis axes. The trace begins at the open circle near the origin. Stimulus intensity was 70 dB impulse SPL. Positive Y is to the viewer's right, positive Z at the top of the figure, positive X (not shown) coming at the viewer from the plane of the figure.

Figure 6b

Analysis axes have been rotated to the right 90 degrees around the Z axis relative to 6a. Positive Y (not shown) is coming out of the plane of the figure away from the viewer.

Figure 6c

Analysis axes have been rotated down towards the viewer 90 degrees relative to 6b, so that positive Z (not shown) is now coming out of the plane of the figure towards the viewer.

Figure 7a

Single-channel traces with the 4 major planar groups, "a", "b", "c" and "d". The vertical cursors demarcate the boundaries of each major planar group. Traces were

recorded with right ear stimulation at 70 dB, the same as in figs. 2, 6 and 8.

Figure 7b

Single-channel traces with planar-segments. The vertical cursors demarcate the planar-segments within major planar group a. Note the overlap of boundaries between adjacent segments. Arrowheads indicating boundaries of planar-segment b1 are included to show overlap between a2 and b1.

Figure 7c

Single-channel traces with planar-segments. The vertical cursors demarcate the planar-segments within major planar group b.

Figure 7d

Single-channel traces with planar-segments. The vertical cursors demarcate the planar-segments within major planar group c.

Figure 7e

Single channel traces with planar-segments. The vertical cursors demarcate the planar-segments within major planar group d. In this example, d1-d2 and d3-d4 do not overlap.

Figure 8a

An example of planar analysis for planar-segments a1 and a2 recorded from a cat (compare to Figure 3). The upper traces are the variance in and out of the best-fit plane. Arrowheads mark the planar-segment beginning and ending points (values in post-stimulus ms). Additional points outside the planar boundaries are displayed to indicate the degree to which the data points before and after a planar-segment deviated from the best-fit plane. The lower traces plot the broadside view of the same data points. Arrowheads mark the boundaries of the planar-segment whose points have been connected by a line to more clearly indicate planar-segment shape. The arrow alongside the planar-segment indicates the direction of the trajectory. The comma is the first data point of the planar-segment, and the O is the point at which the sight vector intersects the best-fit plane. Below are the azimuth, elevation (in degrees) and distance values (in microvolts) for each planar-segment.

Figure 8b-d

The same as in Figure 8a, but for planar-segment groups b-d.

Figure 9

Within animal distributions of planar-segment boundaries, apex-latencies, and durations. Results from one cat over a six hour testing period are plotted. On the LEFT side of the figure, boundary and apex-latency data are presented. Dotted vertical lines represent the median beginning or ending point of each planar-segment. The shaded region indicated the quartile distribution of the boundary values. Quartile ranges for apex-latency are indicated by vertical half-lines near the arrowheads. The arrowheads indicate median apex-latency values. Note the overlap of adjacent segment boundaries. The values above and below the LEFT side are post-stimulus millisecond units. On the RIGHT side of the figure duration data for each planar-segment are presented. The dotted vertical line is the median duration value and the shaded area is the quartile range. Note the increase in duration of planar-segments d2 to d4. The values above and below the RIGHT side are in milliseconds duration.

Figure 10

An example of planar-segment variability within one animal. The upper plots are of the variance in-and-out of the best-fit plane. Arrowheads indicate the planar-segment boundaries in post-stimulus milliseconds. Planar-segment c3 is displayed from recordings near the

beginning, middle, and end of a six hour recording session. The maximum difference in position at any time was 27 degrees. The shape of c3 remains relatively constant throughout the recording session, but in the trace at the far right the duration is increased by 0.2 ms. This is because the included angle between c2 and c3 has become so small that c2 points are added to the beginning of the c3 planar-segment. These points (as well as the apex of c2) can be identified in the broadside view.

Figure 11

Same as Figure 9, but data taken from 10 different cats. Latencies have been normalized for Wave V latency.

Figure 12

An example of planar-segment variability across animals. The three most different c3 planar-segments recorded from 10 animals are displayed. They differ in shape (normal to the plane view), position, and duration, but are still readily identified using planar-analysis techniques. The maximum difference in position between any two c3 sight vectors across animals was 57 degrees.

Figure 13

Included angles between sight vectors of adjacent planar-segments. The top of the shaded bars indicate the

median adjacent included angle for eight trials within one cat. Also indicated are the quartile ranges at the top of each bar. This shows the difference in positions of any two sequential planar-segments. The unshaded bars represent the same information recorded across 10 individual cats. For comparison, test-retest variability scores (back to back recordings) within one cat are presented for each individual planar-segment (black bars). An asterisk over a bar indicates that the two planar-segments were in significantly different locations ($P < .05$) as determined by Hotellings' t-square test. P values for non-significant pairs are presented.

TABLE I.

WITHIN ANIMAL SIGHT VECTOR DISTRIBUTION

(in degrees)

Planar Segment	Average Sight Vector		50%	75%
	Azimuth	Elevation		
a1	40	131	7	9
a2	-162	50	5	9
b1	-146	112	32	44
b2	-13	111	11	15
c1	-35	97	5	6
c2	-126	60	9	19
c3	161	54	18	19
c4	-49	101	9	13
d1	-35	123	26	33
d2	-76	105	13	17
d3	-122	65	13	23
d4	-166	56	6	12

TABLE II

ACROSS ANIMAL SIGHT VECTOR DISTRIBUTION

(in degrees)

Planar Segment	Average Sight Vector Azimuth	Elevation	50%	75%
a1	43	131	12	25
a2	-177	28	7	17
b1	-127	115	11	17
b2	-2	113	17	25
c1	-19	75	25	38
c2	-133	27	31	31
c3	130	42	20	33
c4	-65	97	13	23
d1	-55	103	35	42
d2	-72	93	23	28
d3	-65	98	21	31
d4	150	73	51	72

TABLE III

WITHIN AND ACROSS ANIMAL SIGHT VECTOR DISTANCES

(microvolts)

Planar Segment	Within			Across		
	Median	Quartile		Median	Quartile	
a1	0.0	0.0	0.1	0.2	0.0	0.3
a2	0.7	0.5	0.8	1.6	1.0	1.9
b1	0.1	-0.2	0.5	0.0	-0.1	0.4
b2	0.5	0.4	0.6	1.3	1.0	2.4
c1	0.0	-0.1	0.2	0.3	0.0	1.0
c2	-0.1	-0.6	0.0	0.9	0.5	1.1
c3	1.2	1.0	1.6	1.7	0.9	2.7
c4	0.5	0.4	0.7	1.0	0.7	1.2
d1	0.0	-0.2	0.5	0.8	0.4	1.2
d2	-0.9	-1.2	-0.4	1.6	-1.2	0.3
d3	1.4	1.3	1.6	0.4	-1.2	1.2
d4	1.5	1.2	1.6	0.9	-0.5	2.3

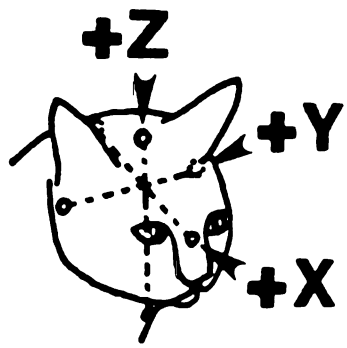

Figure 1.

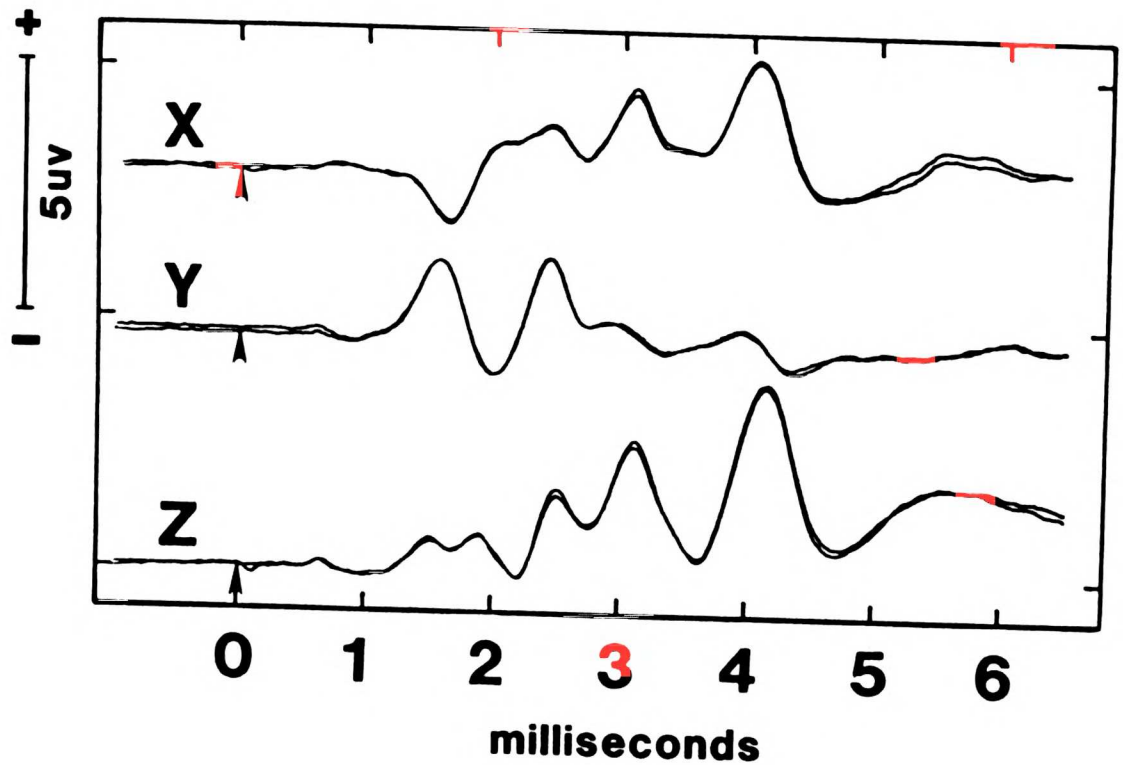

Figure 2.

PLANAR-ANALYSIS

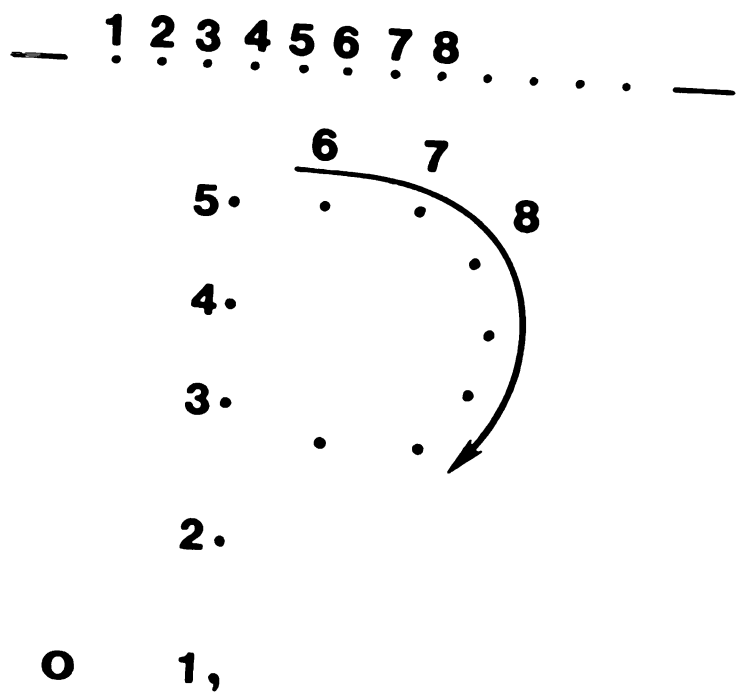

Figure 3.

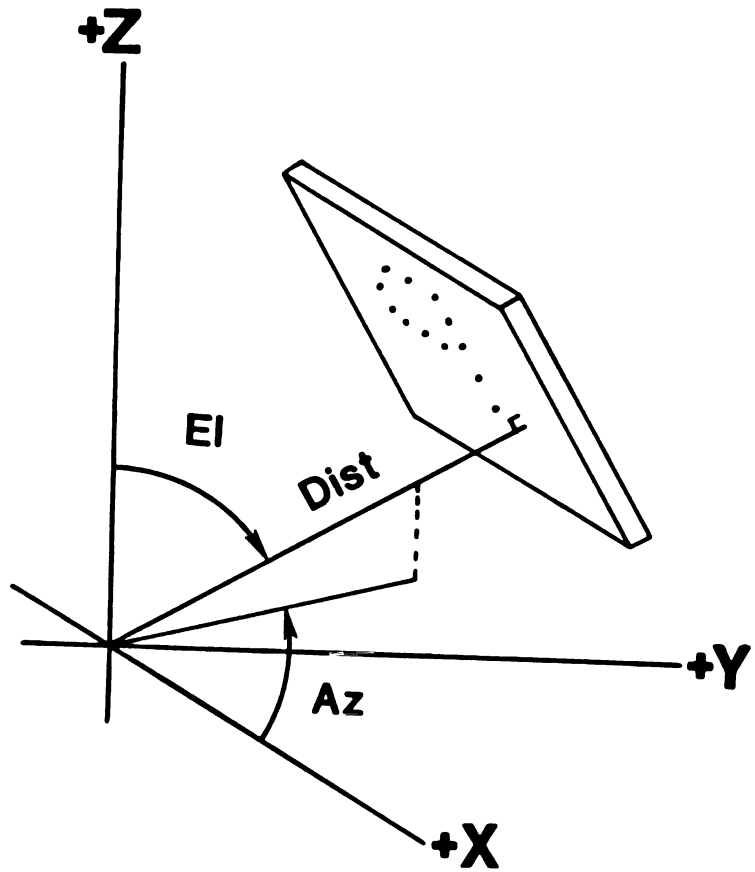

Figure 4.

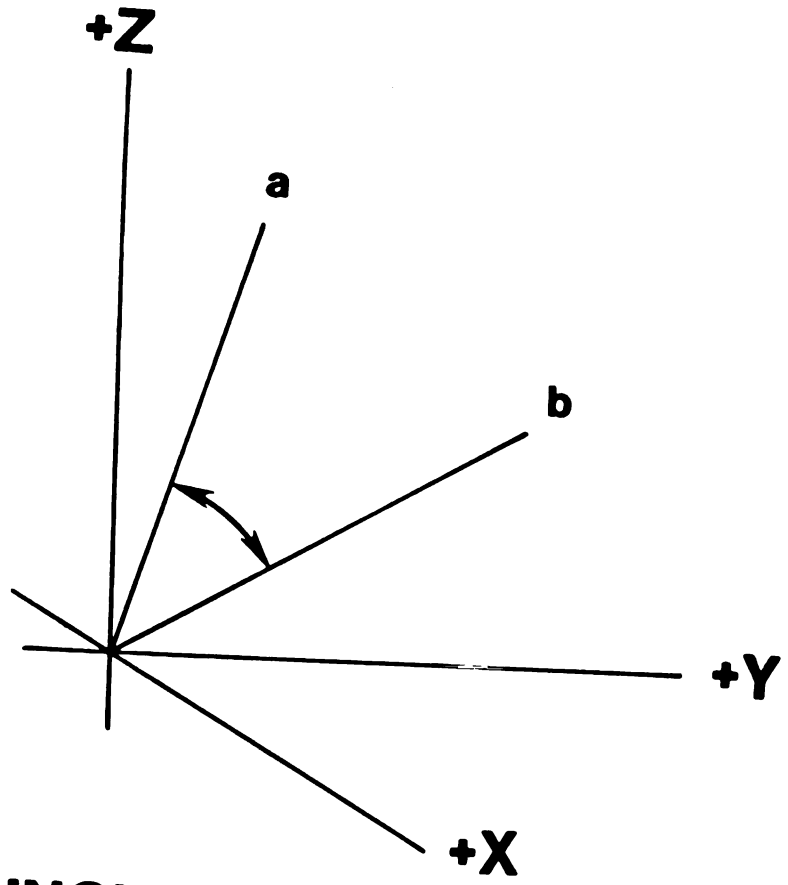

INCLUDED ANGLE

Figure 5.

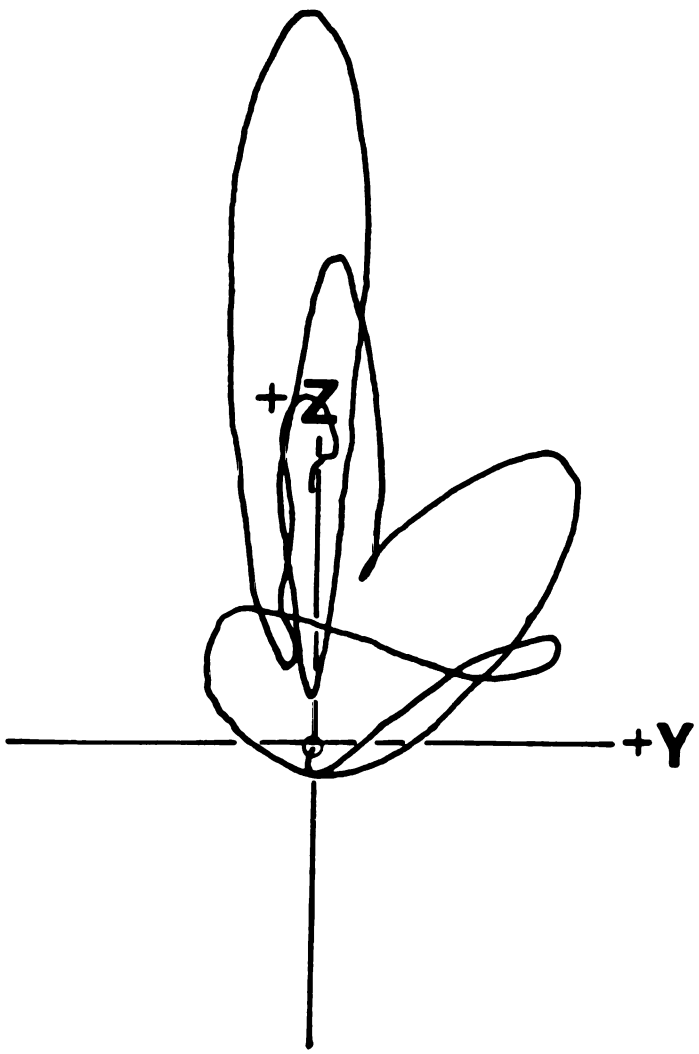

Figure 6a

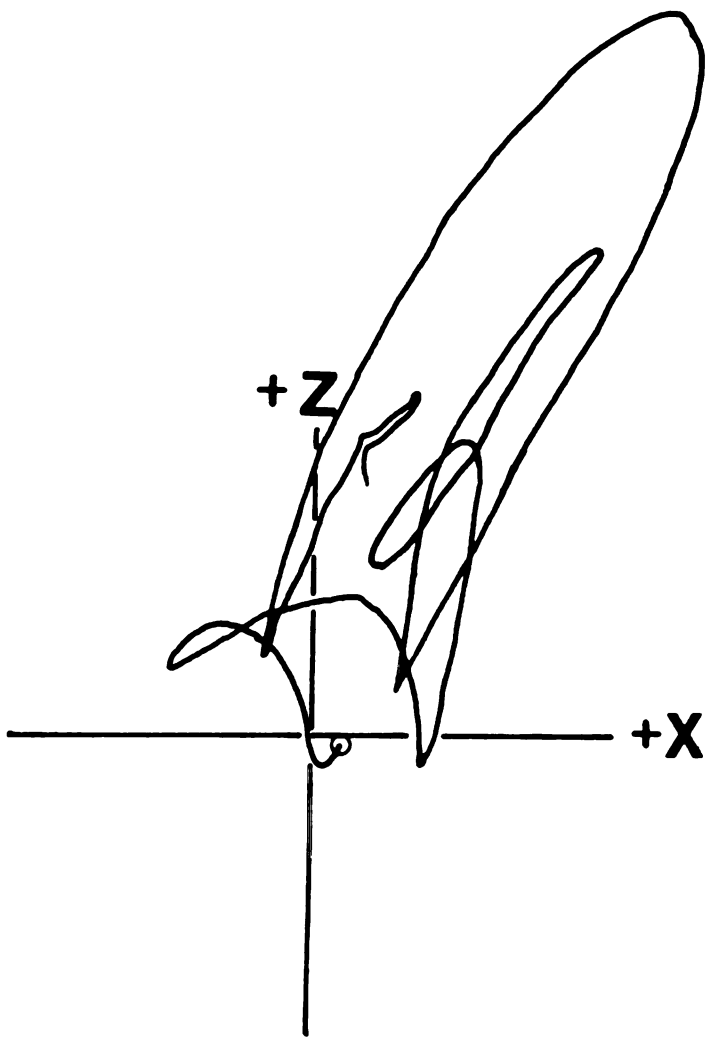

Figure 6b

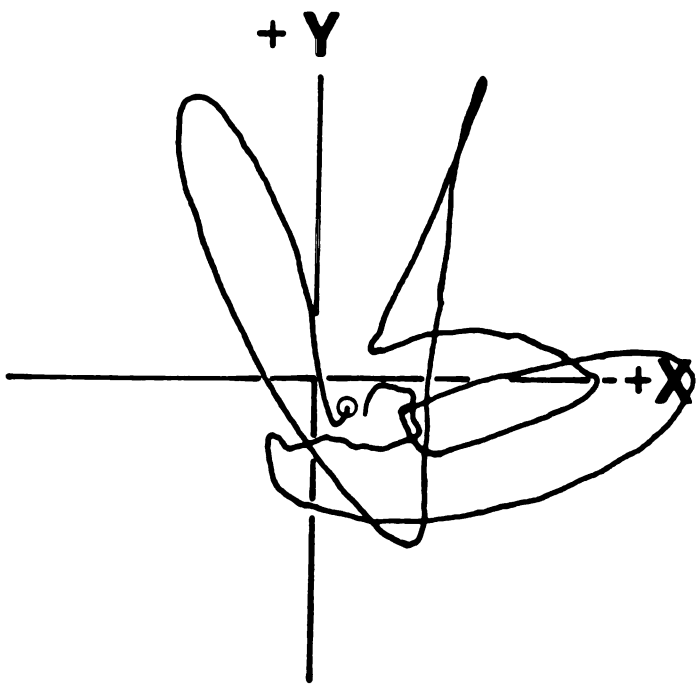

Figure 6c

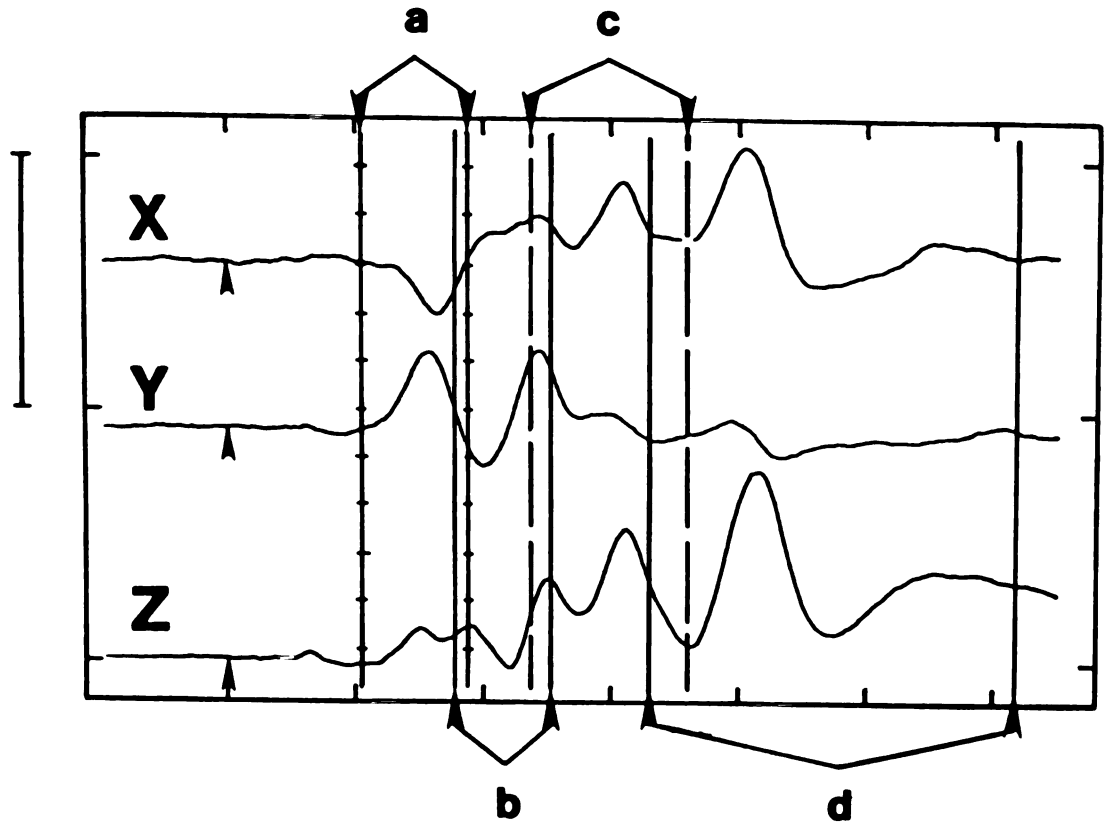

Figure 7a

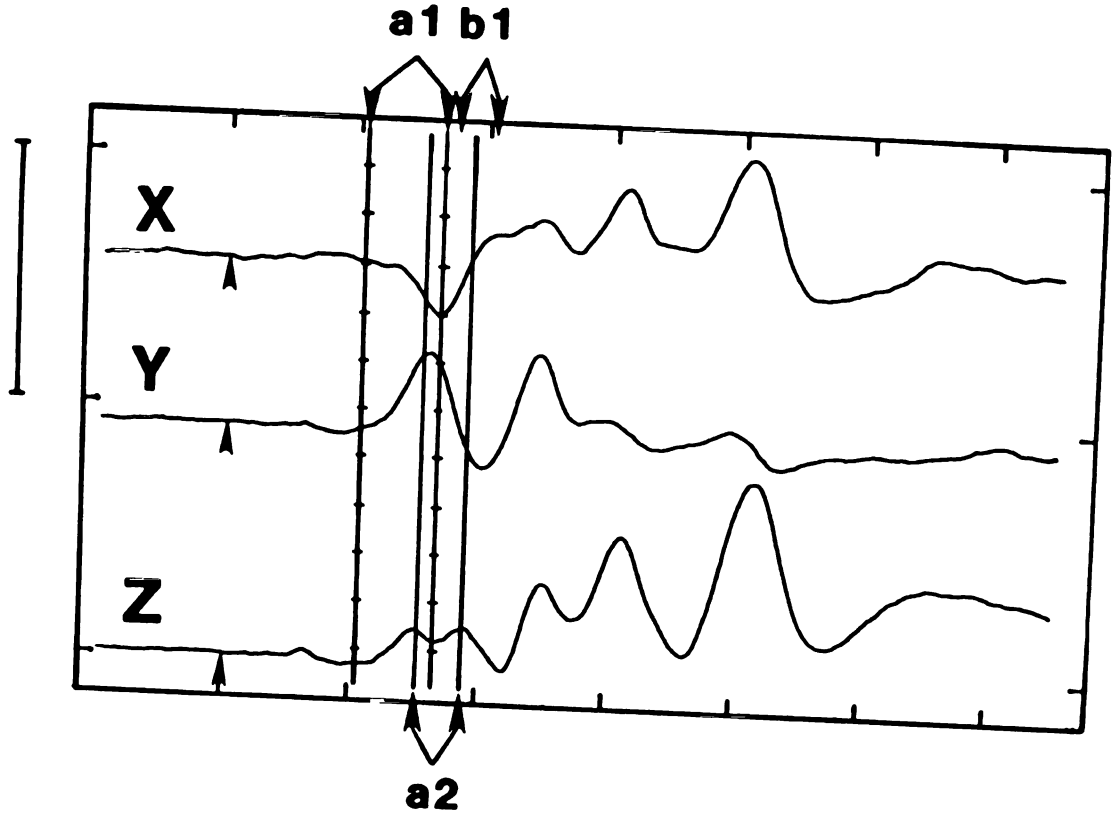

Figure 7b

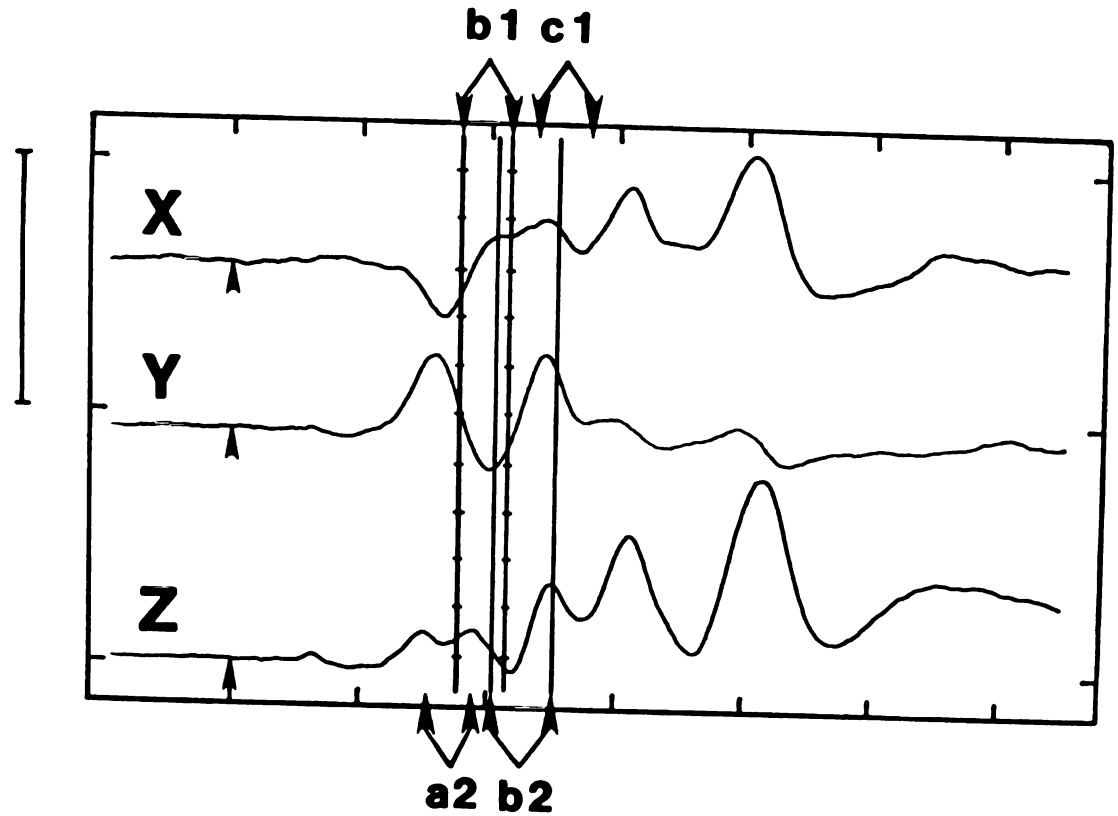

Figure 7c

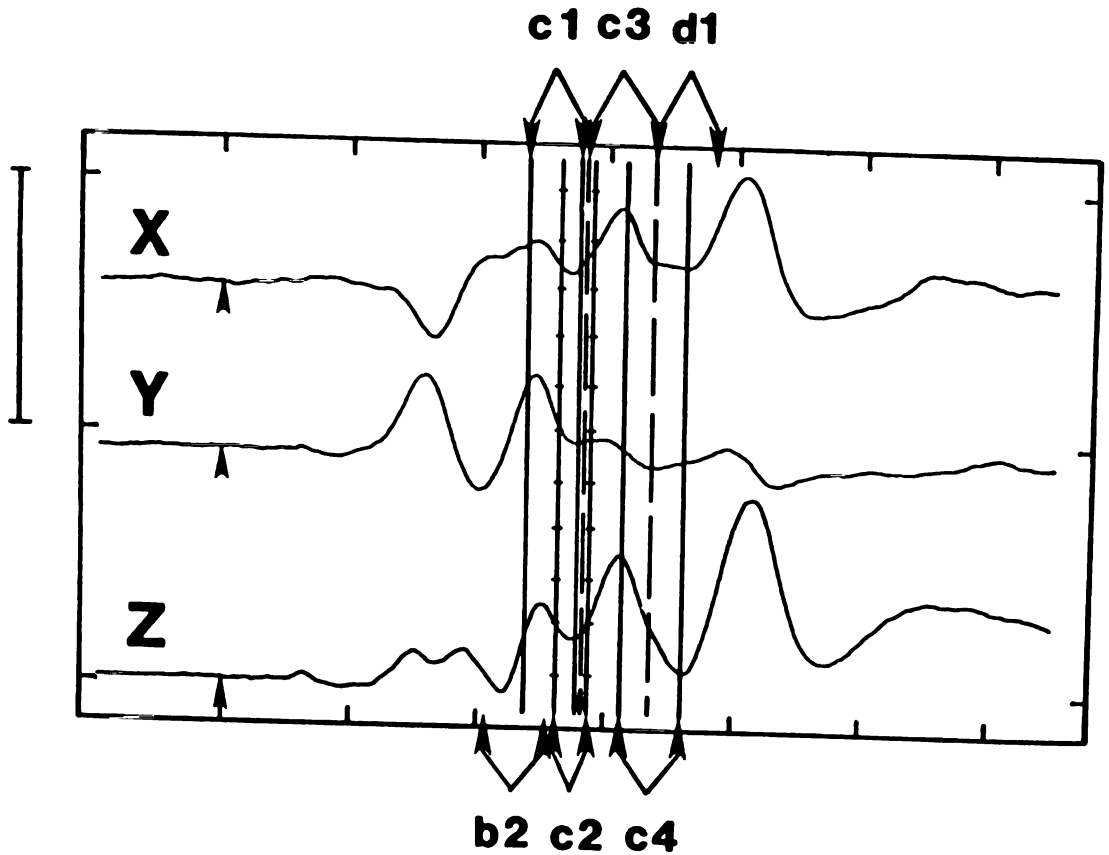

Figure 7d

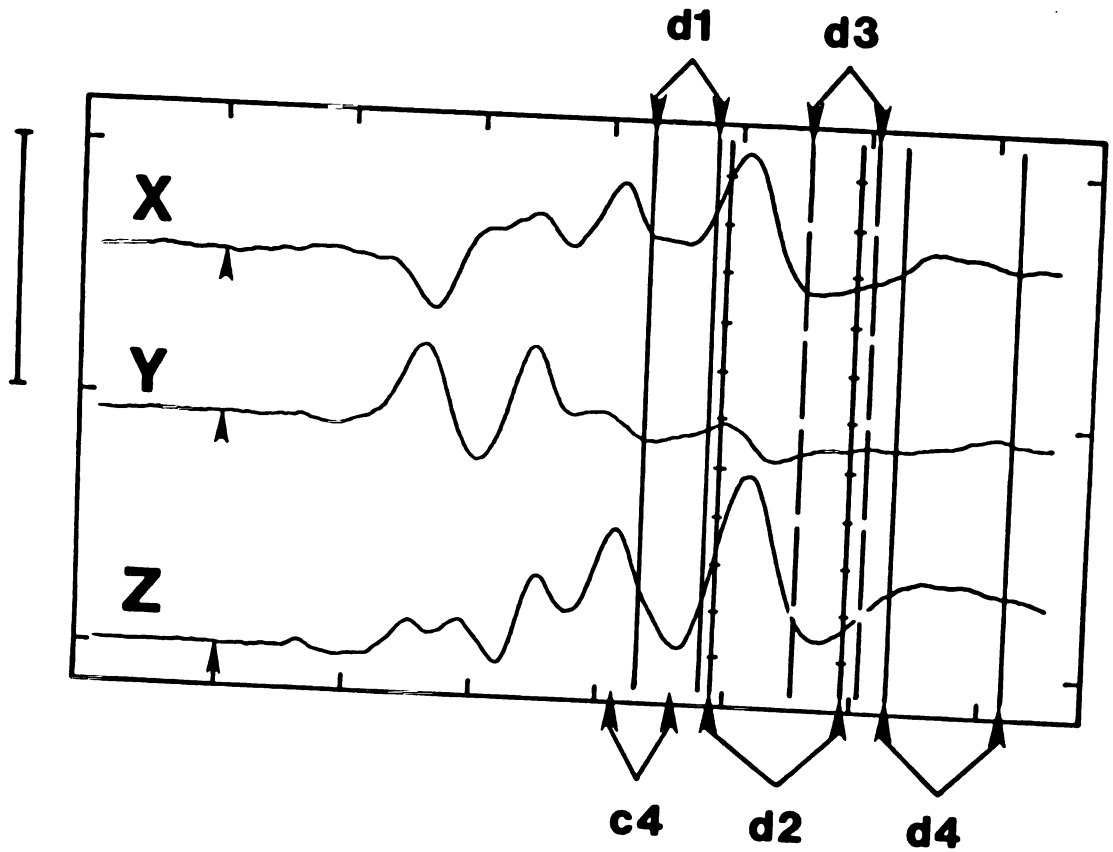

Figure 7e

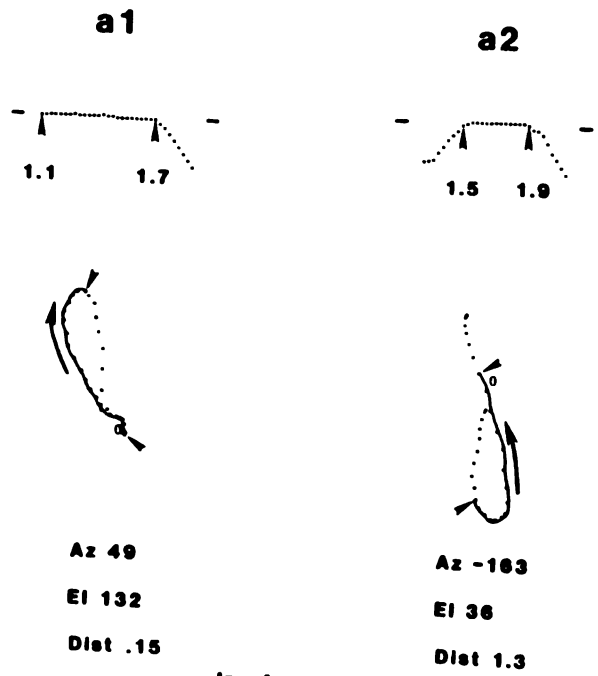
a1
a2
1.1
1.7
1.5
1.9
Az 49
El 132
Dist .15
Az -163
El 36
Dist 1.3
Inc Angle 24

Figure 8a

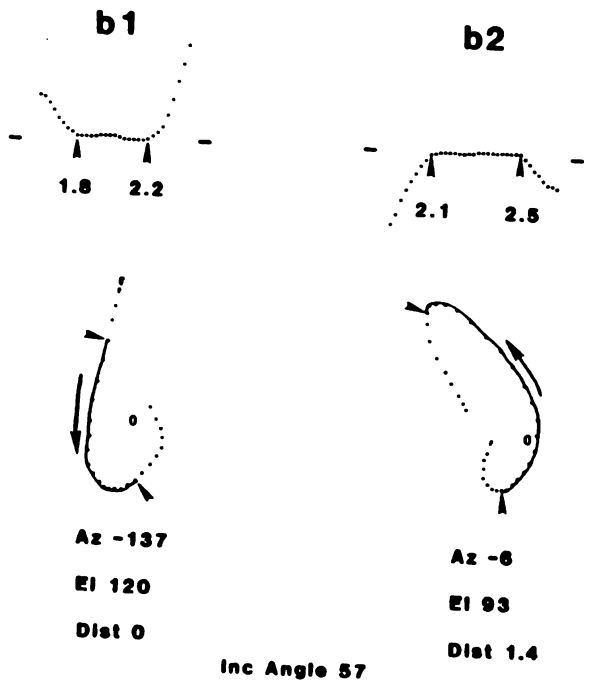
b1
b2
1.8
2.2
2.1
2.5
Az -137
El 120
Dist 0
Az -6
El 93
Dist 1.4
Inc Angle 57

Figure 8b

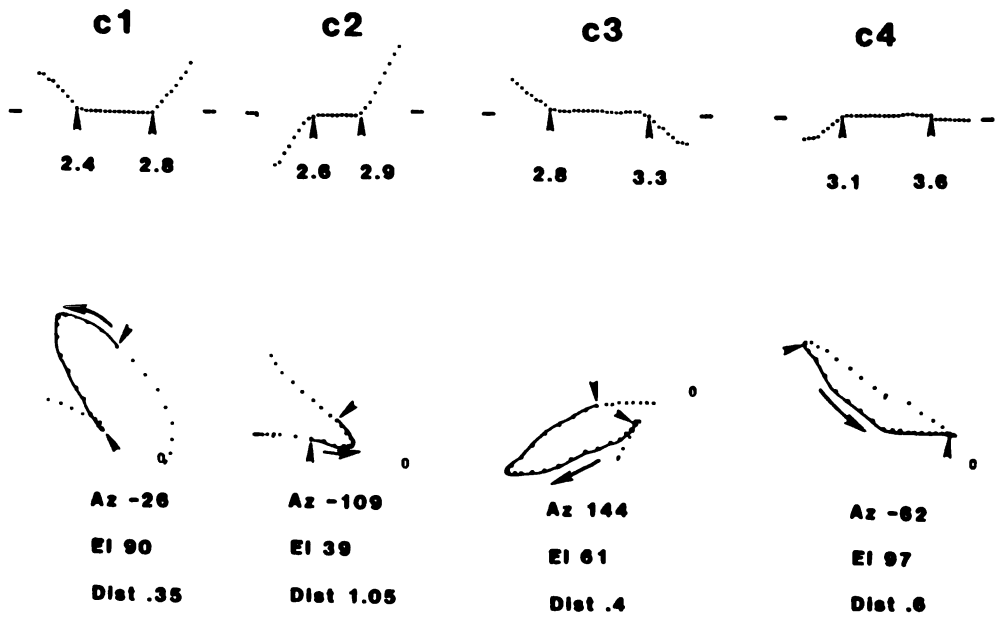
c1
c2
c3
c4
2.4
2.8
2.6
2.9
2.8
3.3
3.1
3.6
Az -26
El 90
Dist .35
Az -109
El 39
Dist 1.05
Az 144
El 61
Dist .4
Az -62
El 97
Dist .6
Inc Angle 86
Inc Angle 78
Inc Angle 33

Figure 8c

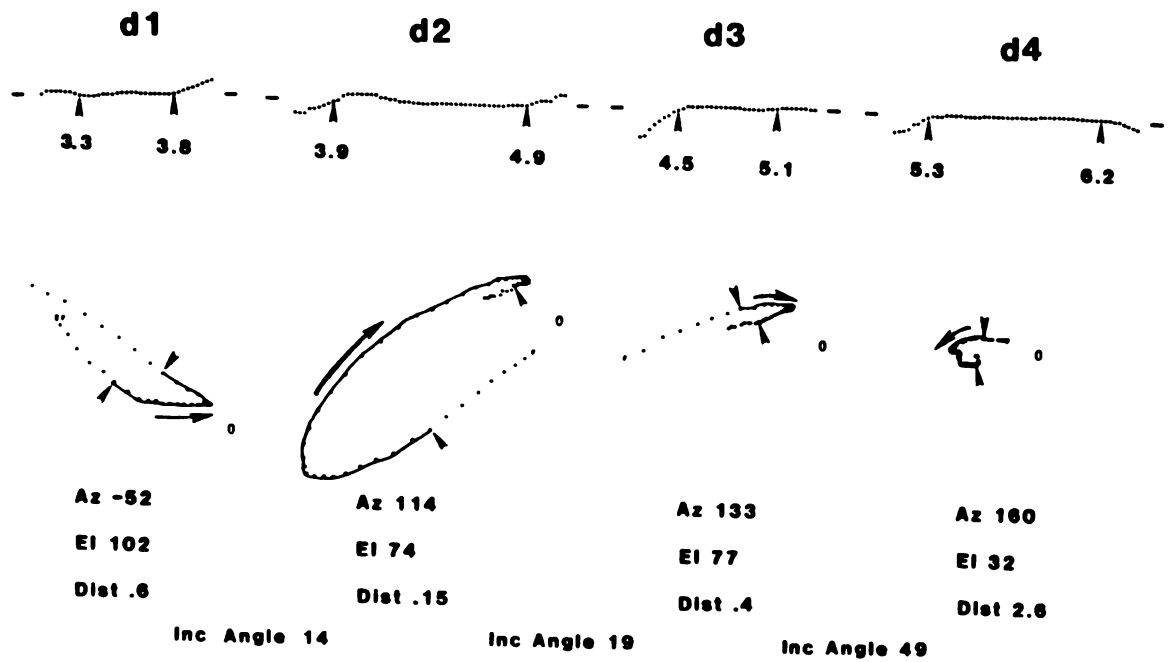
d1
d2
d3
d4
3.3
3.8
3.9
4.9
4.5
5.1
5.3
6.2
Az -52
El 102
Dist .6
Inc Angle 14
Az 114
El 74
Dist .15
Inc Angle 19
Az 133
El 77
Dist .4
Inc Angle 49
Az 160
El 32
Dist 2.6

Figure 8d

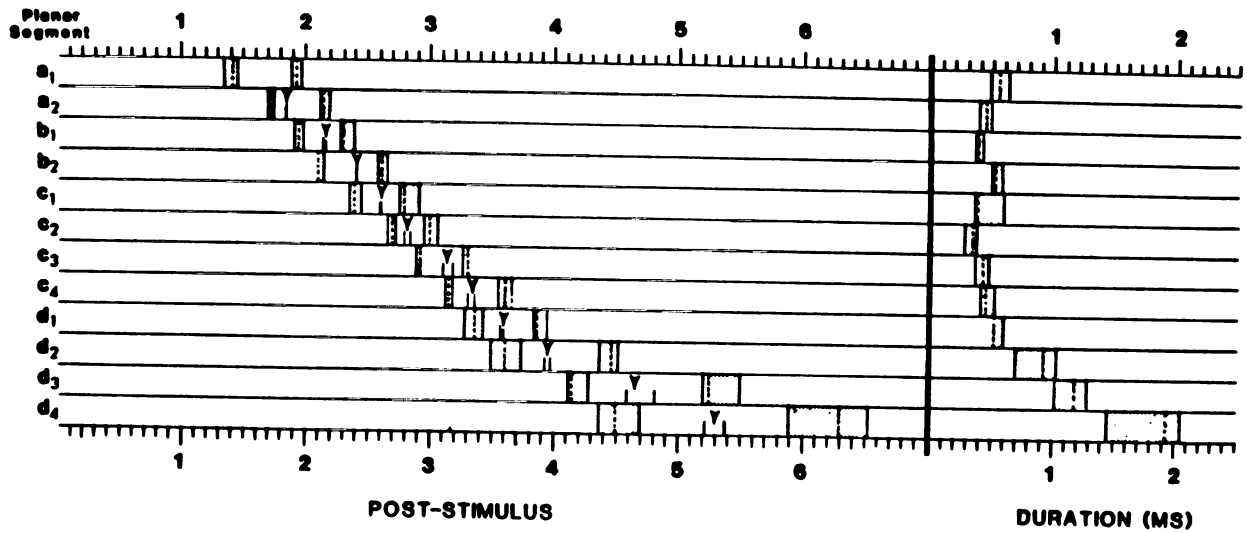
WITHIN-ANIMAL BOUNDARIES
APEX-LATENCIES AND DURATIONS
Planar Segment
1
2
3
4
5
6
1
2
a_1
a_2
b_1
b_2
c_1
c_2
c_3
c_4
d_1
d_2
d_3
d_4
1
2
3
4
5
6
1
2
POST-STIMULUS
DURATION (MS)

:Figure 9.

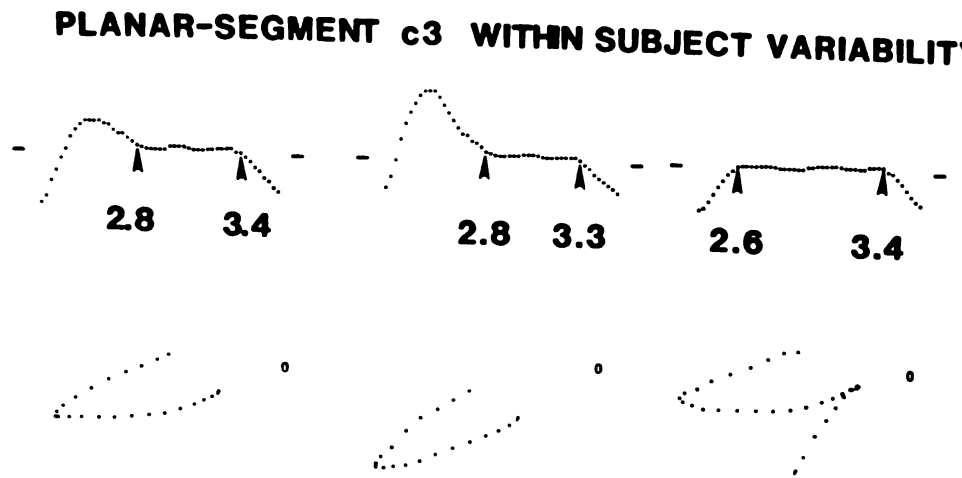
PLANAR-SEGMENT c3 WITHIN SUBJECT VARIABILITY
2.8
3.4
2.8
3.3
2.6
3.4
Az 162
El 52
Dist .62uv
Dur .58
Az 144
El 61
Dist .4
Dur .53
Az 174
El 51
Dist .7
Dur .78
Max Included Angle 27

Figure 10.

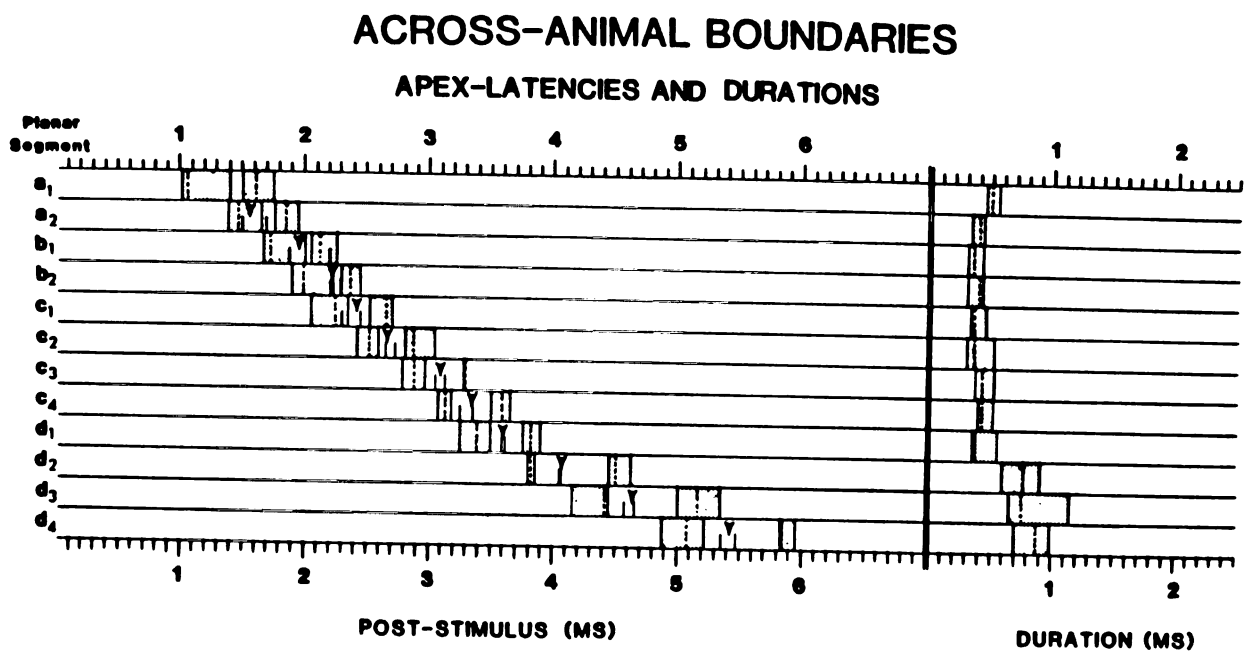
ACROSS-ANIMAL BOUNDARIES
APEX-LATENCIES AND DURATIONS
Pioneer Segment
1
2
3
4
5
6
1
2
a_1
a_2
b_1
b_2
c_1
c_2
c_3
c_4
d_1
d_2
d_3
d_4
POST-STIMULUS (MS)
DURATION (MS)

Figure 11.

PLANAR-SEGMENT c3 ACROSS SUBJECT VARIABILITY

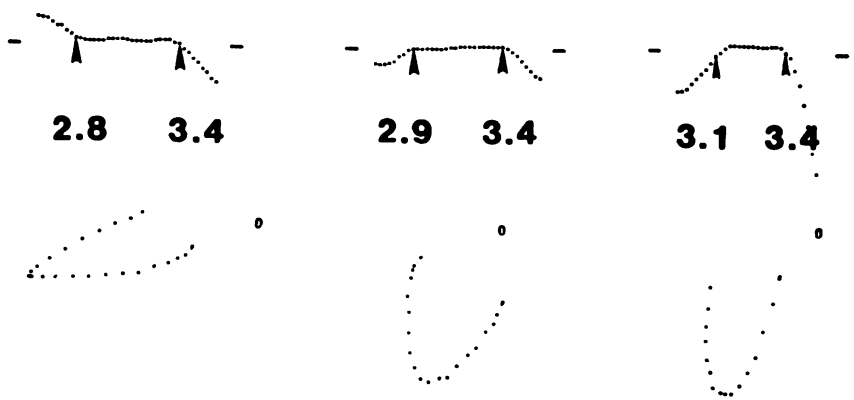

Figure 12.

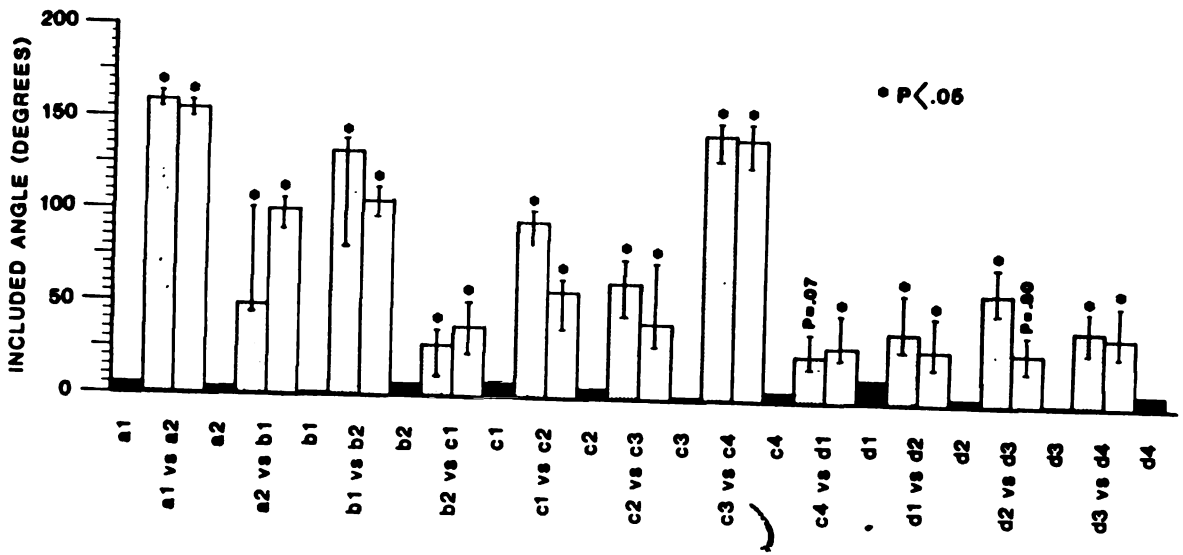
INCLUDED ANGLE (DEGREES)
200
150
100
50
0
• P<.05
P=.07
P=.06
a1
a1 vs a2
a2
a2 vs b1
b1
b1 vs b2
b2
b2 vs c1
c1
c1 vs c2
c2
c2 vs c3
c3
c3 vs c4
c4
c4 vs d1
d1
d1 vs d2
d2
d2 vs d3
d3
d3 vs d4
d4

Figure 13.

CHAPTER 3

THE EFFECTS OF ELECTRODE PLACEMENT

INTRODUCTION

The auditory brain stem response (ABR) is the scalp-recorded electrical potential resulting from the sequential activation of the auditory pathway in response to an abrupt auditory stimulus. The potential recorded at any instant in time represents the algebraic summation of activity from all simultaneously active generators (Jewett, 1970; Jewett and Williston, 1971). Simultaneous three-channel representation of ABRs reveals a Lissajous figure resulting from the path of the potential in three-dimensional voltage space (Williston et al, 1981; Martin et al, 1983a). The primary observation concerning the ABR three-channel Lissajous trajectory (3-CLT) is that sets of sequential data points form planar-segments. Planar-segments have been reported in the guinea-pig (Williston et al, 1981), cat (Martin et al, 1983a), and man (Pratt et al, 1983). Twelve planar-segments have been recorded from the cat and have been described in terms of their apex latency, boundaries, duration and sight vector position in voltage space (see Martin et al. 1983a). There was no direct correlation between planar-segment duration or apex-latency and specific peaks and valleys of ABR

activity recorded across any single electrode pair, however, all twelve planar-segments were reproduced within and across animals. It was hypothesized that planar-segment measures provide more accurate and complete detection of the ABR generators than activity recorded across any single electrode pair. The purpose of this study was to determine effects of electrode placement on 3-CLT waveforms and on planar-segment boundaries, duration, apex-latencies, and sight vector positions.

Several mapping studies have reported that auditory evoked potential waveforms vary with electrode placement. These potentials have been found to have widespread scalp distribution, asymmetrical with monaural stimulation (Plantz et al, 1974) but bilaterally symmetrical with binaural stimulation (Martin and Moore, 1978; Streletz et al, 1977; Ino and Mizoi, 1980; Dum et al, 1981; Hashimoto et al, 1981; Szelenberger et al, 1981). No areas of the scalp were found to be electrically neutral during the ABR (Plantz et al, 1974). Large changes in electrode position resulted in ABR waveform changes including: 1) changes in peak latencies (Plantz et al, 1974; Allen and Starr, 1978; Prasher and Gibson, 1980; Hashimoto et al, 1981; Starr and Squires 1982); 2) changes in peak amplitudes (Plantz et al, 1974; Streletz et al, 1977; Prasher and Gibson, 1980; Dum et al, 1981; Parker, 1981); and 3) changes in peak

polarity (Picton et al, 1974; Plantz et al. 1974; Terkildsen et al, 1974; Streletz et al, 1977; Parker 1981; Cohen, 1982; Starr and Squires 1982). Similar changes have been reported from mapping studies recording frequency following responses (Stillman et al, 1978; middle latency responses (Picton et al, 1974; Streletz et al, 1977; Cohen, 1982) and late cortical responses (Picton et al, 1974; Streletz et al, 1977). In all of the above mentioned studies, care was taken to experimentally verify that non-cephalic reference sites were neutral when used.

If waveform variability is not due to variations in the volume conduction properties of head tissues, as proposed by Plonsey (1969), then peak latency, amplitude and/or polarity changes must reflect temporo-spatial properties of ABR generators (Plantz et al, 1974; Jewett, 1983). These properties may include generator movement (Starr and Squires 1982), equivalent dipole orientation (Prasher and Gibson, 1981) and/or number of generators (Hashimoto et al, 1981).

Variations in ABR waveform related to electrode position have led to studies designed to determine "optimal" recording configurations (Terkildsen et al, 1974; Parker, 1981), while other studies simply employed additional channels for additional clinically relevant information

(Stockard et al, 1977; Prasher & Gibson, 1980). Hashimoto et al, (1981) recording between the ipsilateral ear and the sternum, reported that Wave II polarity was abnormally inverted in patients with brain stem gliomas, whereas Wave III polarity was abnormally inverted in patients suffering from medulloblastomas. This result suggests that specific electrode configurations are more effective for recording waveform changes resulting from certain pathologies. It follows that the clinical utility of the ABR to detect potential pathology may be limited if confined to one electrode pair.

Collectively, these mapping studies point out the vulnerability of using established clinical criteria that rely solely on peak latency and amplitude values. Changes in peak amplitudes and latencies which result from recording ABRs from different surface locations indicate that the peaks and valleys of a single-channel ABR are electrode position dependent and not directly generator dependent. It is possible that the ABR 3-CLT and its planar-segments may also be electrode position dependent. This study was designed to determine the effects of electrode placement on 3-CLT formation under two conditions. In the first experiment the position of recording axes relative to the scalp was changed while their relative orthogonality was maintained. This study was done to determine

whether or not planar-segment formation and position in voltage space was dependent upon orientation of orthogonal recording axes. The changes in electrode placement selected for this experiment maximize two possible sources of 3-CLT distortion: 1.) the "near-field" effect of recording near the cochlear nerve, and 2.) the interruption of volume conduction pathways in the cranium by oral and nasal pharyngeal air spaces. In the second experiment, non-orthogonal recording axes were used to address the question: Are planar-segment formation and position dependent upon orthogonal recording axes? This question is answered at two levels. The simpler case compares 3-CLTs acquired using orthogonal recording axes with 3-CLTs acquired using recording axes in which only one axis is non-orthogonal. The specific variations in electrode position for this experiment were chosen because they maximize the effects of non-orthogonal placement while requiring a relatively small change in scalp location. Specifically, Plantz et al, (1974) reported that movement of an electrode at the throat a few centimeters towards the stimulated ear resulted in polarity changes at that electrode for Waves I, II, and III in the cat when using a non-cephalic reference. In the more complex case, all three axes were non-orthogonal but widely spaced.

METHODS

Experimental Conditions

Six adult cats, from the population reported in our previous study (Martin et al, 1983a), were also used in this study. All experimental conditions are presented in detail in that text.

In this study, electrodes were placed at 14 locations on each cat's scalp. The location of the recording electrodes used was dependent on specific questions to be answered. The ground electrode was located at the back of the neck between C1 and T12 in all experiments.

Analysis

The three single-channel ABRs recorded for each electrode configuration were combined and the 3-CLT plotted on three orthogonal analysis voltage axes, using a computer graphics program. Hard copies of analyzed data were plotted and numeric data for planar-segment duration, apex-latency and position relative to the analysis axes were compared. Planar-segment shape was not considered in this study. For a detailed description of the analysis method and terminology definitions, see Martin et al, (1983a).

RESULTS

Psi vs. Chi

The first experiment required two different orthogonal recording axes. The __psi__ configuration used in this study utilized the same electrode positions described by Martin et al. (1983a); that is, X channel electrodes were placed at the bridge of the nose (+) and occiput (-), Y channel electrodes at left (+) and right (-) mastoids, immediately below the pinna, and Z channel electrodes at vertex (+) and throat (-) (Figure 1). Electrode positions for the chi configuration were the result of a 45 degree clockwise rotation of the psi configuration Y and Z electrode pairs around the X axis (Figure 1). Psi vs. chi comparisons were made on four cats.

Single channel ABRs recorded from both the psi (X, Y, Z) and chi (X, V, W) electrode configurations are shown in Figure 2. The X channel was the same in both configurations. Note the dramatic difference in single channel waveforms which resulted from the new positions of two electrode pairs. All channels recorded show differences in waveform which are a result of recording from new locations. The differences manifested are in peak latency, amplitude, and polarity.

In contrast to the marked changes in single-channel waveforms following rotations of orthogonal recording axes, planar-segment boundaries, apex-latencies, and dura-

tions remained relatively unchanged. The reader should be reminded that planar analysis does not consider peaks or valleys as analysis criteria. Only data points which are statistically planar were considered part of the planar-segments (Martin et al, 1983a). Planar-segment boundaries recorded from both psi and chi configurations are also presented in Figure 2. Segments a1 and b2 are typical examples of boundary changes which resulted from rotation of the recording axes. Planar-segment d4 boundaries were most affected by psi/chi rotation changes and are also presented. Other planar-segment boundaries were less affected than d4 as shown in Figure 2. Note that planar-segment boundaries are minimally affected by the rotation of orthogonal electrode pairs around the X axis. This is further demonstrated in Table I, which compares psi and chi boundaries, apex-latencies and durations for all twelve planar-segments in the same cat. The psi values were recorded over a six hour period. All of the apex-latency values derived from planar-analysis of ABRs recorded with chi electrodes were within the range of values obtained from ABRs recorded using psi electrodes. Eighty percent of all chi planar-segment beginning and ending points were within the range of psi values. Those cases which exceeded the psi range were always either the beginning point or ending point, never both, and never by more than 0.28 milliseconds. Planar-segment durations

were in agreement with results observed for planar-segment boundaries. These results were verified in all four cats.

An example of 3-CLTs recorded from psi and chi electrode configurations as viewed looking down the unchanged X axis (+X toward the viewer) is shown in Figure 3. The chi analysis axes have been rotated 45 degrees to correct for the approximate 45 degree clockwise rotation of the recording axes (see Figure 1). This figure presents a qualitative comparison of psi and chi 3-CLT formation and shows that voltage space waveforms recorded from different orthogonal electrode pairs are remarkably similar. They differ in that the largest vertical loop appears to lie slightly left of the origin in the chi but not the psi recording.

For the psi vs. chi experiment, all chi data was initially analyzed as recorded with no correction made for the 45 degree rotation of the Y and Z channels around the X recording axis. All boundary, latency, and duration values reported are from that initial analysis (Table I). A post-hoc counter-clockwise rotation of 45 degrees around the X axis was calculated for all chi sight vectors for comparison with the unrotated psi sight vectors. This analysis provided an estimate of the relative change in 3-CLT waveform as a function of changing orthogonal

recording electrode positions (Table II).

The equation used for this 45 degree counter-clockwise rotation around +X is:

For the matrix,

$$(X_2, Y_2, Z_2) = \begin{bmatrix} 1 & 0 & 0 \\ 0 & \frac{1}{\sqrt{2}} & \frac{1}{\sqrt{2}} \\ 0 & \frac{-1}{\sqrt{2}} & \frac{1}{\sqrt{2}} \end{bmatrix} \quad \begin{bmatrix} X_1 \\ Y_1 \\ Z_1 \end{bmatrix}$$

Solve the equations,

$$X_2 = a_{11} X_1 + a_{12} Y_1 + a_{13} Z_1$$

$$Y_2 = a_{21} X_1 + a_{22} Y_1 + a_{23} Z_1$$

$$Z_2 = a_{31} X_1 + a_{32} Y_1 + a_{33} Z_1$$

Where: X1, Y1, and Z1 are uncorrected chi values for the the sight vector intercept of the best-fit plane and X2, Y2, and Z2 are the corrected chi values.

The observation derived from Figure 1 is supported by the results in Table II. Chi sight vectors were rotated counter-clockwise 45 degrees to correct for the 45 degree clockwise rotation of the chi recording axes from psi (control) positions. Included angles (Martin et al, 1983a) between corrected chi and psi sight vectors were calculated (the smaller the value, the closer the positions of corrected psi and chi sight vectors). For comparison, the test-retest variability ranges for all sight vectors within the same animal are reported. Ten of twelve corrected chi sight vectors were within the

expected range of psi values, indicating that there is very little change in the 3-CLT waveform as a result of rotating orthogonal recording axes. This was verified in all four animals. Table II also presents the range of across animal included angle values for corrected chi vs. psi sight vectors for all four cats.

Psi vs. Z2

The second experiment required non-orthogonal recording axes. The 3-CLTs from orthogonal recording axes (psi configuration) were compared to 3-CLTs recorded from non-orthogonal recording axes. The -Z electrode in the control or psi configurations is located at the midline of the throat while in the simplest non-orthogonal case, the -Z electrode is moved toward the stimulated ear approximately 3 cm. The latter position is referred to as the Z2 position (Figure 4). Psi vs. Z2 comparisons were made on five cats.

An example of changes in single-channel waveforms that occur when one electrode pair is moved is presented in Figure 5. Recall that the Z2 position reflected movement of the -Z electrode 3 cm toward the stimulated ear. In the planar analysis, the X and Y channels were the same for both Psi and Z2 configurations. The double-peaked

character of Wave I in the psi Z channel was absent in Z2 forming one predominant wave with an inflection on the falling slope. Z2 Wave II was larger in amplitude compared to its psi equivalent, but Waves III,IV, and V in the Z2 configuration were smaller in amplitude. There was little difference in planar-segment boundaries as a result of recording the 3-CLT with one non-orthogonal electrode pair when compared to the orthogonal control. Planar-segment a1 and b2 boundaries are presented as typical examples of the small changes seen between psi and Z2 recording conditions. To illustrate the extreme case, planar-segment d3 boundaries were presented, being the most altered by the use of a non-orthogonal recording configuration. These results are further supported by Table III, which shows the boundaries, apex-latencies, and durations of all planar-segments recorded from one cat using the Z2 electrode placement. For comparison, the range of psi values within the same animal over a six hour period is presented. All but one of the apex latencies for the Z2 planar-segments were within the range of psi values. Also, over 90% of the beginning and ending points of the Z2 planar-segments were within the range of psi values. The duration values reflect the boundary results illustrated in Figure 5. In general, planar-segment boundaries, apex-latencies, and durations were equivalent when recording from orthogonal (psi) or non-orthogonal (Z2)

recording axes.

3-CLT shape differences were dependent upon whether or not the recording axes were orthogonal. These differences were indicated by changes in sight vector positions between data recorded from psi and Z2 conditions. In one animal, 75% of the Z2 sight vectors differed from psi sight vector position test-retest variability scores as determined by included angle measures (Table II). The manner in which the Z2 sight vectors deviated was complex and not predictable from single-channel ABRs.

It was, however, reasonable to expect changes in 3-CLTs recorded using Z2 electrode configurations because Z2 data were recorded using non-orthogonal electrode pairs and analyzed using orthogonal analysis axes. We hypothesize that, if a correction factor were applied to the Z2 data, which accounted for the actual electrode placement, the 3-CLT recorded using the Z2 configuration would be similar to the 3-CLT recorded using orthogonal recording axes, just as shown when comparing the psi and chi 3-CLTs in Figure 3.

The findings reported for one animal in Figure 5 and Tables II and III were supported by the results from all five tested animals.

Psi vs. NO1, NO2

In the more complex case, all recording axes were non-orthogonal, (i.e. none of the axes was perpendicular to each other). 3-CLT records obtained from control configurations (psi) were compared to 3-CLT records obtained under non-orthogonal recording conditions (referred to as NO1 and NO2). NO1 configuration electrodes were placed in the following positions: 1) R channel electrodes were placed above the left eye (+) and behind the right pinna (-), 2) Q channel electrodes were placed on the left mandibular angle (+) and superior to the right pinna (-), and 3) S channel electrodes were placed at the vertex (+) and right mandibular angle (-). Placement of NO2 configuration electrodes was identical to NO1 configuration placement with the exception of the T channel. In this case, electrodes were placed superior to the left pinna (+) and immediately below the right pinna (-) (Figure 6). NO1 and NO2 vs. Psi comparisons were made in one cat.

Results similar to those described in the psi vs. Z2 section were observed when all psi data were compared to data recorded from axes which were completely non-orthogonal; twelve planar-segments were still identified. An example of single-channel ABRs recorded from the psi configuration (X, Y, Z) and two non-orthogonal configurations NO1 (Q,R,S) and NO2 (Q,R,T) are shown in Figure 7.

Single-channel waveforms recorded from each electrode position differed in both peak amplitude and latency measures. However, it was found that planar-segment boundaries were relatively unaffected by electrode configuration. Planar-segments a1 and b2 were typical of boundary differences which resulted from recording with orthogonal or non-orthogonal recording axes. Vertical cursors through X, Y, and Z recordings represent a1 and a2 control boundaries, while vertical cursors through Q,R, and S represent a1 and a2 boundaries for the first non-orthogonal case (NO1). Cursors overlaid on trace T indicate a1 and a2 boundaries for the second non-orthogonal (NO2). Although large changes in single-channel activity occur within the confines of planar-segment boundaries, the boundaries themselves remain relatively unchanged. Planar-segment d3 is presented as an example of the greatest variation that resulted from a change in recording configuration.

Planar-segment boundaries, apex-latencies, and durations for psi, NO1 and NO2 recording configurations are compared in Table IV. No range of variability was available for psi values recorded from this animal; however, 75% of the NO1 and NO2 values were within 0.1 ms of psi values.

The 3-CLT waveforms recorded using different non-orthogonal recording axes varied from one another in a complex manner and were different from CLTs recorded from psi configurations as was the Z2 case above.

DISCUSSION

The formation of planar-segments in voltage space is independent of electrode position. It was possible to record three-channel Lissajous trajectories with full complements of 12 planar-segments in all five of the different recording configurations used in this study.

A change of recording axes from psi to chi orientations provided the simplest case for determining whether planar-segment formation and planar-segment position are dependent upon the orientation of orthogonal recording axes. In the psi configuration, the -Y electrode is placed on the mastoid of the stimulated (right) ear while the -Z electrode is placed at the throat beneath the oral cavity. In the chi configuration, the -V electrode is near the right mandibular angle, away from the potentially active mastoid region, while the -W electrode is near the left mandibular angle, away from the midline of the throat and oral cavity air space. Single-channel ABRs from chi electrode pairs differed markedly from control (psi)

recordings (Figure 4). This could prove important for research and clinical purposes in that planar-segments are not as vulnerable to changes in electrode position as are single-channel ABR peaks and valleys. Planar-segment formation, apex-latency, duration and position were unaffected by rotating orthogonal recording axes. The "near field" effect of the stimulated ear, and the oral-naso pharyngeal air spaces only minimally distorted the trajectory of responses recorded in three dimensions (Figure 5).

Presently, all clinical application relies on latency and amplitude values obtained from single-channel ABRs. It has been demonstrated in this paper (especially by data presented in Figures 2, 5 and 7) and others (Picton et al, 1974; Plantz et al, 1974; Terkildsen et al, 1974; Streletz et al, 1977; Allen and Starr, 1978; Martin and Moore, 1978; Prasher and Gibson, 1980; Dum et al, 1981; Hashimoto et al, 1981; Parker, 1981; Szelehberger et al, 1981; Cohen, 1982; and Starr and Squires 1982) that ABR waveform shape is determined by the location of scalp electrodes. Results from this study suggest that all time dependent (planar-segment boundaries, apex-latency, duration) and amplitude dependent (3-CLT shape) information is maintained with orthogonal recording axes, regardless of position of recording electrodes.

Furthermore, formation of planar-segments, apex-latency and duration are independent of orthogonality requirements (Tables I, III, IV). All 12 described planar-segments remain intact whether recording axes are orthogonal, partially orthogonal, or completely non-orthogonal. If planar-segments prove to be clinically useful, any triplet of widespread electrode pairs could be used to record.

The robustness of 3-CLT planar-segment formation strongly suggests that planar-segments provide a more direct representation of generator activity than can be obtained from analyzing waveforms from any single channel. Each planar-segment reflects activity from all three contributing channels. The fact that segments of points along the Lissajous trajectory form a plane is not trivial and indicates a predictable relationship of generator activity over the duration of the planar-segment. Thus, the formation of planar-segments may indicate that it is possible to derive information about the time course and topography of activity underlying the ABR. The formation of planar-segments cannot be intuitively predicted by single-channel X, Y, and Z recordings (Martin et al, 1983a).

Another way in which the 3-CLT can be shown to provide more information is illustrated in Figure 2. In this case, activity occurring between 3 and 5 ms shows reduced amplitude in the Y channel, whereas the X and Z channels both show large positive peaks during this time period. The reason activity can be present in one or two channels and not in the other(s) is a consequence of the fact that ABRs are recorded differentially. In a given channel, activity at one electrode is subtracted from activity recorded at the other electrode. The ABR is therefore the difference in surface potentials between each electrode pair. Activity which is equal in voltage at both recording electrodes would be canceled, which could be interpreted in the ABR as an absence of neural activity. This may occur when a potential is generated by neural pathways that lie equidistant between recording electrodes, or when the algebraic sum of all generator activity at the given electrodes is zero. Therefore, isopotential portions of single-channel ABRs may not be indicative of an absence or even a decrease in neural activity! They may only indicate a distribution of potentials in an orientation which a particular electrode pair records as zero. The converse of this may also be true, that is, an absence of change in the amplitude of an ABR peak does not mean that a change in underlying generator activity has not occurred. It only indicates that the particular electrode configuration

employed did not record potential changes. Thus, negative results (i.e., minimal change in ABR waveforms with clinical pathology or experimental condition) from any single-channel ABR are non-conclusive. It would appear from theoretical considerations (Jewett, 1983) that three electrode "pairs" is a minimum number in order to be sure to detect any generator in the volume conductor, but limitations of signal to noise may require a larger number. At present the optimal number is not known.

The 3-CLT also provides all of the time and amplitude information available in a surface potential mapping study in one concise form. Mapping studies are not only tedious to record, but difficult to analyze, interpret and present data in a usable format (see Plantz et al, 1974; and Starr and Squires 1982). Also, apex-latency and 3-CLT amplitude information may be standardized across laboratories because these aspects of the 3-CLT do not appear to be dependent on electrode position. Indeed, computerized objective algorithms can be envisaged to automate measurements of planar-segment parameters.

Furthermore, the 3-CLT provides information which can also improve ABR single-channel analysis techniques. 3-CLT techniques may be used to identify or predict electrode configurations which may increase our ability to

detect specific pathologies. For example, if a given pathology affects the lateralization of the 3-CLT, the best single-channel electrode configuration will be one which maximizes the effect of the lesion on the potential (e.g., an ear-to-ear recording configuration). Different pathologies may require different "optimal" single-channel electrode positions for early diagnosis.

In conclusion, the 3-CLT of the ABR is robust and generator dependent rather than electrode position dependent. It provides more useful information than any single-channel ABR and has potential as a clinical and research tool. Parametric manipulation and lesion experiments support this conclusion (Martin et al, 1983c).

SUMMARY

Three-channel Lissajous trajectories (3-CLTs) of the auditory brain stem response (ABR) were recorded from six anesthetized adult cats using two different orthogonal and three different non-orthogonal recording configurations. Click stimuli were presented monaurally at 70 dB impulse SPL. Planar-analysis identified 12 planar-segments in all recording conditions. Planar-segment boundaries, apex-latencies, and durations were relatively unchanged by recording axis position in sharp contrast to changes in

single-channel ABR peak latencies and amplitudes. 3-CLT shape was maintained in voltage space when changes in electrode positions were made, provided the recording axes remained orthogonal. Non-orthogonal recording axes resulted in 3-CLTs which differed in shape from 3-CLTs recorded from orthogonal recording axes. These results indicate that planar-segment formation, boundaries, apex-latencies and duration are generator dependent and electrode position independent, and suggest that the 3-CLT can provide surface potential information in a concise form which usually requires extensive mapping experiments.

TABLE LEGEND

Table I.

Boundaries, apex-latencies, and durations for planar-segments recorded from one animal using chi electrode placements are compared to the ranges of the same values recorded from the same animal over a six hour period using the psi (control) electrode placements. All chi recorded apex-latencies were within the range of psi values as were 79 percent of the chi boundary values.

Table II.

Comparison of sight vector positions recorded using psi (control), chi, and Z2 recording axes. An estimate of sight vector position variability within one animal is presented in the first column. The numeric values represent the smallest and largest included angles observed between the same sight vectors from sequential recordings (e.g., a1 in trial 1 was compared to a1 in trial 2). Four pairs of sequential recordings were compared in determining the ranges presented. The large range in d3 position (47) was recorded during the last test in the six hour experiment.

Included angles between corrected chi sight vectors and psi sight vectors are presented for each planar-

segment in the second column. Chi values were corrected by rotating sight vectors counter-clockwise 45 degrees (see equations in Methods-Analysis section). Ten of the included angles between psi and corrected chi sight vectors are within the range of psi variability indicating little change in 3-CLT shape with rotation of orthogonal recording configurations. All values in the first and second columns were results from the same animal. The range of included angles between corrected chi and psi sight vectors across four animals is presented in the third column for comparison with the within-animal results.

Changes in 3-CLT shape as a function of recording configuration are indicated in the fourth column. Included angles between sight vectors from psi (orthogonal) recorded and Z2 (non-orthogonal) recorded data are presented for comparison with psi sight vector variability (first column). Data in the first, second, and fourth columns were recorded from the same cat. Column four values which exceeded the psi range in column one were indicative of changes in 3-CLT shape resulting from psi to Z2 recording axes changes.

Table III.

Boundaries, apex-latencies, and durations for planar-segments recorded from one animal using Z2 electrode placements are compared to the ranges of the same values recorded from the same animal over a six hour period using the psi (control) electrode configuration. All but one Z2 recorded apex-latency were within the range of psi values and 91 percent of the Z2 boundary values were within the range of psi values. This result indicates that orthogonal to non-orthogonal recording axes changes has little effect on these time related elements.

Table IV.

Boundaries, apex-latencies, and durations for planar-segments recorded from psi (control), NO1, and NO2 recording axes in one animal. Seventy-five percent of all NO1 and NO2 values were within 0.1 ms of the psi values supporting results presented in Table III and further indicating that planar-segment boundaries, apex-latencies, and duration values are independent of recording axes orthogonality.

FIGURE LEGENDS

Figure 1

Electrode locations for psi and chi recording configurations. Electrode pairs are orthogonal in relationship

(i.e., perpendicular to each other). In the psi configuration, X electrode locations are bridge of nose (positive) and occiput, Y locations left (positive) and right mastoids, Z locations Cz (positive) and throat. In the chi configuration the Y and Z electrode pairs have been rotated clockwise 45 degrees around the X electrode pair axis. In their new positions they are called V and W respectively.

Figure 2

Electrode locations for psi and Z2 recording configurations. In the psi configuration, X electrode locations are bridge of nose (positive) and occiput, Y locations left (positive) and right mastoids, Z locations Cz (positive) and throat. The Z2 configuration places the negative Z electrode 3 cm. towards the stimulated (right) ear.

Figure 3

Non-orthogonal electrode configuration NO1 and NO2. All electrode pairs are non-orthogonal in relation to each other, i.e., no two electrode pairs are perpendicular to each other. The configurations only differ in the S and T recording pairs.

Figure 4

Single-channel ABRs recorded from psi (X,Y,Z) and chi (X,V,W) electrode configurations (Figure 1). The arrowhead indicates stimulus onset. Note the change in single-channel waveforms with changes in electrode position. When Z is rotated to W, the major area changed is between 1-3 ms. in latency. When Y is changed to V, the major change occurs between 3-5 ms. latency. Planar-segment boundaries for a1, b2, and d3 are indicated by vertical cursors. Broken cursors indicate psi boundaries and solid cursors indicate chi boundaries. Planar-segments a1 and a2 are typical examples and show relatively little change in boundaries with change in electrode position. Segment d2 is an example of the greatest change due to changes in orthogonal recording axis position.

Figure 5

Comparison of 3-CLTs recorded from psi (X,Y,Z) and chi (X,V,W) electrode configurations. The chi plot on the right has been rotated clockwise 45 degrees to correct for the 45 degree rotation of the Y and Z recording electrodes. The positive X axis is coming out of each illustration towards the viewer. The open circle near the origin indicates the beginning of the response, and the arrowheads indicate the direction of the trajectory. These waveforms were derived from single-channel data

presented in Figure 4. Note the remarkable similarity in 3-CLT shape compared to the differences present in single-channel waveforms.

Figure 6

Single-channel ABRs recorded from psi (X,Y,Z) and Z2 electrode configurations. Note the change from a biphasic Wave I for Z (psi) to a monophasic Wave I for Z2. Arrows indicate click stimulus. As in Figure 4, planar-segments a1 and b2 are presented as typical examples of changes in boundaries that accompany changes in electrode configuration. Segment d3 is again the most altered by electrode position. Broken cursors indicate psi boundaries and solid cursors indicate Z2 boundaries.

Figure 7

Single-channel ABRs recorded from orthogonal psi (X,Y,Z) and non-orthogonal NO1 (Q,R,S) and NO2 (Q,R,T) configurations. Planar-segments a1 and b2 are typical examples of changes in boundaries that accompany changes in electrode configuration. Segment d3 is one example of the greatest change. Solid cursors at the top are psi planar-segment boundaries, broken cursors (middle) are NO1 planar-segment boundaries, and solid cursors at the bottom (T only) indicate NO2 planar-segment boundaries. Note the dependence of single-channel waveform and independence of

planar-segment boundaries on recording axes position and orientation.

PSI VS. CHI BOUNDARIES, LATENCIES, AND DURATIONS IN ONE ANIMAL					
(Values in milliseconds)					
Planar-segment		Beginning	Ending	Latency	Duration
a1	CHI	1.4	1.9	-	0.5
	PSI range	1.3 - 1.5	1.9 - 2.0	-	0.5 - 0.6
a2	CHI	1.7	2.1	1.8	0.4
	PSI range	1.7 - 1.8	2.1 - 2.2	1.8 - 1.9	0.4 - 0.5
b1	CHI	1.9	2.3	2.1	0.4
	PSI range	1.9 - 2.0	2.3 - 2.4	2.1 - 2.2	0.3 - 0.5
b2	CHI	2.1	2.6	2.4	0.5
	PSI range	2.1 - 2.2	2.6 - 2.7	2.4 - 2.4	0.4 - 0.7
c1	CHI	2.4	3.0	2.6	0.6
	PSI range	2.3 - 2.5	2.7 - 3.0	2.6 - 2.6	0.3 - 0.6
c2	CHI	2.6	3.3	2.8	0.8
	PSI range	2.6 - 2.7	2.9 - 3.1	2.8 - 2.8	0.3 - 0.5
c3	CHI	2.6	3.3	3.1	0.7
	PSI range	2.8 - 3.0	3.3 - 3.4	3.1 - 3.2	0.3 - 0.5
c4	CHI	3.1	3.4	3.3	0.3
	PSI range	3.1 - 3.2	3.5 - 3.7	3.3 - 3.4	0.3 - 0.6
d1	CHI	3.5	3.8i	3.6	0.4
	PSI range	3.2 - 3.5	3.7 - 4.0	3.5 - 3.6	0.5 - 0.7
d2	CHI	3.6	4.2	3.9	0.7
	PSI range	3.4 - 3.7	4.3 - 4.6	3.9 - 4.0	0.6 - 1.1
d3	CHI	4.0	5.1	4.6	1.2
	PSI range	4.1 - 4.3	5.1 - 6.1	4.6 - 4.9	1.0 - 2.0
d4	CHI	4.2	6.1	5.3	1.8
	PSI range	4.1 - 4.8	5.5 - 6.6	5.2 - 5.5	0.9 - 2.2

Table I.

SIGHT VECTOR POSITIONS (Values in included angle degrees)									
Planar-segment	Psi Test-retest Range			Psi vs. Corrected Chi	Across Animal Range			Psi vs. Z2
a1	2	-	14	5	5	-	14	22
a2	4	-	9	7	7	-	11	31
b1	1	-	28	3	1	-	16	8
b2	2	-	8	8	1	-	8	34
c1	2	-	9	9	2	-	10	19
c2	6	-	29	20	5	-	20	16
c3	0	-	4	6	4	-	12	24
c4	6	-	13	5	4	-	15	20
d1	5	-	13	21	11	-	21	23
d2	1	-	5	4	1	-	3	14
d3	1	-	47	16	7	-	17	12
d4	6	-	17	5	5	-	13	24

Table II.

PSI VS. Z2 PLANAR-SEGMENT BOUNDARIES, LATENCIES AND DURATIONS FOR ONE ANIMAL

(Values in milliseconds)

Planar-segment		Beginning	Ending	Latency	Duration
a1	Z2	1.4	2.0	-	0.6
	PSI range	1.3 - 1.5	1.9 - 2.0	-	0.5 - 0.6
a2	Z2	1.7	2.1	1.8	0.5
	PSI range	1.7 - 1.8	2.1 - 2.2	1.8 - 1.9	0.4 - 0.5
b1	Z2	1.9	2.3	2.2	0.4
	PSI range	1.9 - 2.0	2.3 - 2.4	2.1 - 2.2	0.3 - 0.5
b2	Z2	2.2	2.6	2.4	0.5
	PSI range	2.1 - 2.2	2.6 - 2.7	2.4 - 2.4	0.4 - 0.7
c1	Z2	2.4	2.8	2.6	0.4
	PSI range	2.3 - 2.5	2.7 - 3.0	2.6 - 2.6	0.3 - 0.6
c2	Z2	2.7	3.0	2.8	0.4
	PSI range	2.6 - 2.7	2.9 - 3.1	2.8 - 2.8	0.3 - 0.4
c3	Z2	2.9	3.3	3.2	0.4
	PSI range	2.9 - 3.0	3.3 - 3.4	3.1 - 3.2	0.3 - 0.5
c4	Z3	3.2	3.5	3.3	0.3
	PSI range	3.1 - 3.2	3.5 - 3.7	3.3 - 3.4	0.4 - 0.6
d1	Z2	3.3	3.6	3.5	0.4
	PSI range	3.2 - 3.5	3.7 - 4.0	3.5 - 3.6	0.5 - 0.7
d2	Z2	3.7	4.6	4.0	0.9
	PSI range	3.4 - 3.7	4.3 - 4.6	3.9 - 4.0	0.6 - 1.1
d3	Z2	4.1	5.3	4.6	1.2
	PSI range	4.1 - 4.3	5.1 - 6.1	4.6 - 4.9	1.0 - 2.0
d4	Z2	4.7	6.3	5.2	1.6
	PSI range	4.1 - 4.8	5.5 - 6.6	5.2 - 5.5	0.9 - 2.2

Table III.

PSI VS. NON-ORTHOGONAL BOUNDRIES, LATENCY, AND DURATION IN ONE ANIMAL					
(Values in milliseconds)					
Planar-segment	Config-uration	Beginning	Ending	Latency	Duration
a1	PSI	1.0	1.6	-	0.6
	NO1	1.0	1.7	-	0.7
	NO2	1.0	1.7	-	0.7
a2	PSI	1.4	1.9	1.5	0.4
	NO1	1.4	2.0	1.5	0.6
	NO2	1.4	1.9	1.5	0.5
b1	PSI	1.7	2.2	1.9	0.5
	NO1	1.8	2.2	2.0	0.4
	NO2	1.7	2.2	2.0	0.4
b2	PSI	1.9	2.3	2.2	0.4
	NO1	2.0	2.3	2.2	0.4
	NO2	1.9	2.3	2.2	0.4
c1	PSI	2.2	2.6	2.4	0.5
	NO1	2.2	2.6	2.4	0.5
	NO2	2.2	2.7	2.4	0.5
c2	PSI	2.4	3.0	2.7	0.6
	NO1	2.5	3.0	2.7	0.5
	NO2	2.5	3.0	2.7	0.6
c3	PSI	2.8	3.3	3.1	0.5
	NO1	2.8	3.3	3.1	0.5
	NO2	2.7	3.3	3.1	0.7
c4	PSI	3.1	3.6	3.3	0.6
	NO1	3.1	3.8	3.4	0.7
	NO2	3.0	3.7	3.4	0.7
d1	PSI	3.4	3.7	3.6	0.4
	NO1	3.4	4.1	3.7	0.7
	NO2	3.4	4.1	3.7	0.7
d2	PSI	3.8	4.6	4.1	0.8
	NO1	3.8	4.7	4.2	1.0
	NO2	3.7	4.7	4.2	1.0
d3	PSI	4.1	5.6	4.7	1.5
	NO1	4.5	5.1	4.7	0.6
	NO2	4.4	5.1	4.7	0.7
d4	PSI	5.0	6.7	5.3	1.7
	NO1	5.0	6.1	5.5	1.2
	NO2	5.0	6.5	5.5	1.6

Table IV.

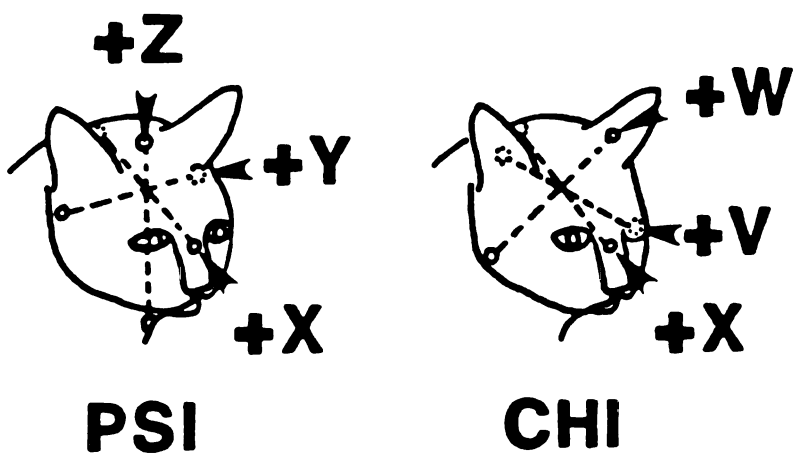

Figure 1

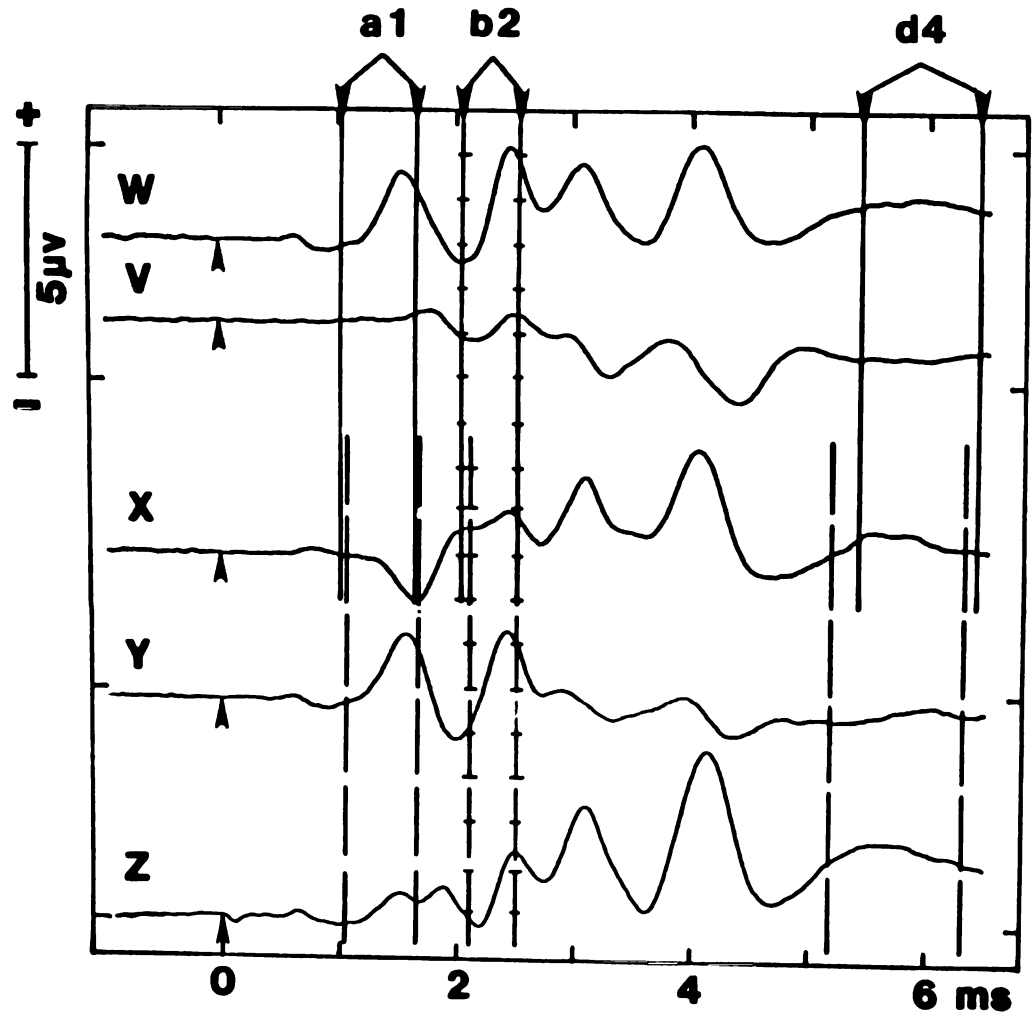

Figure 2

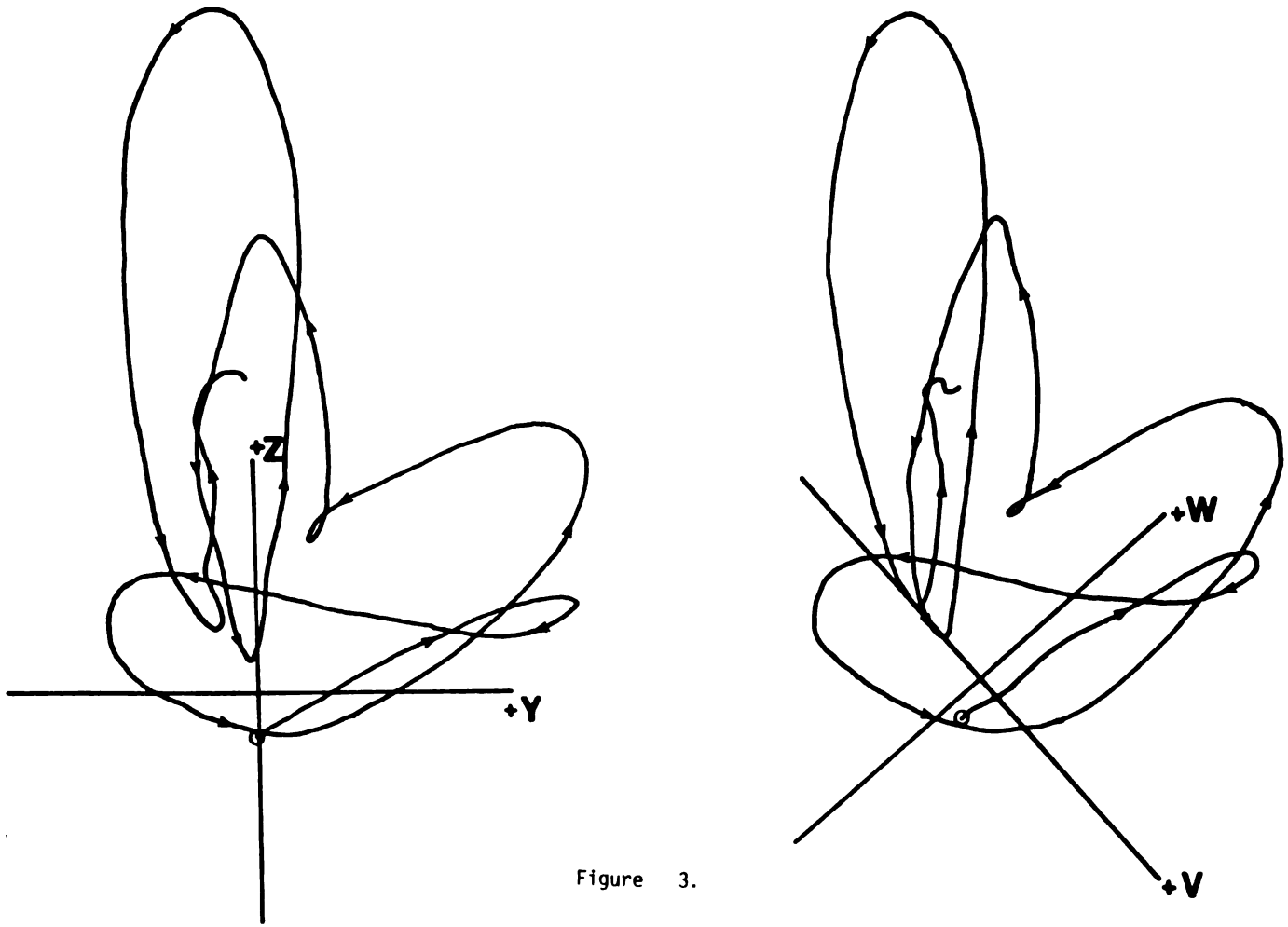

Figure 3.

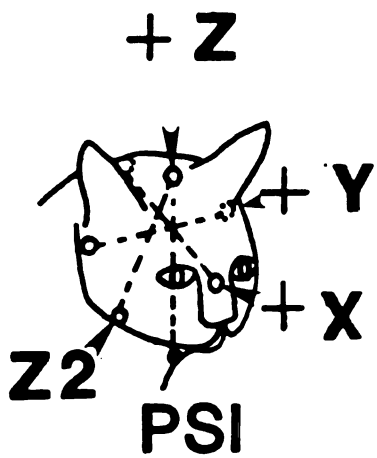

Figure 4

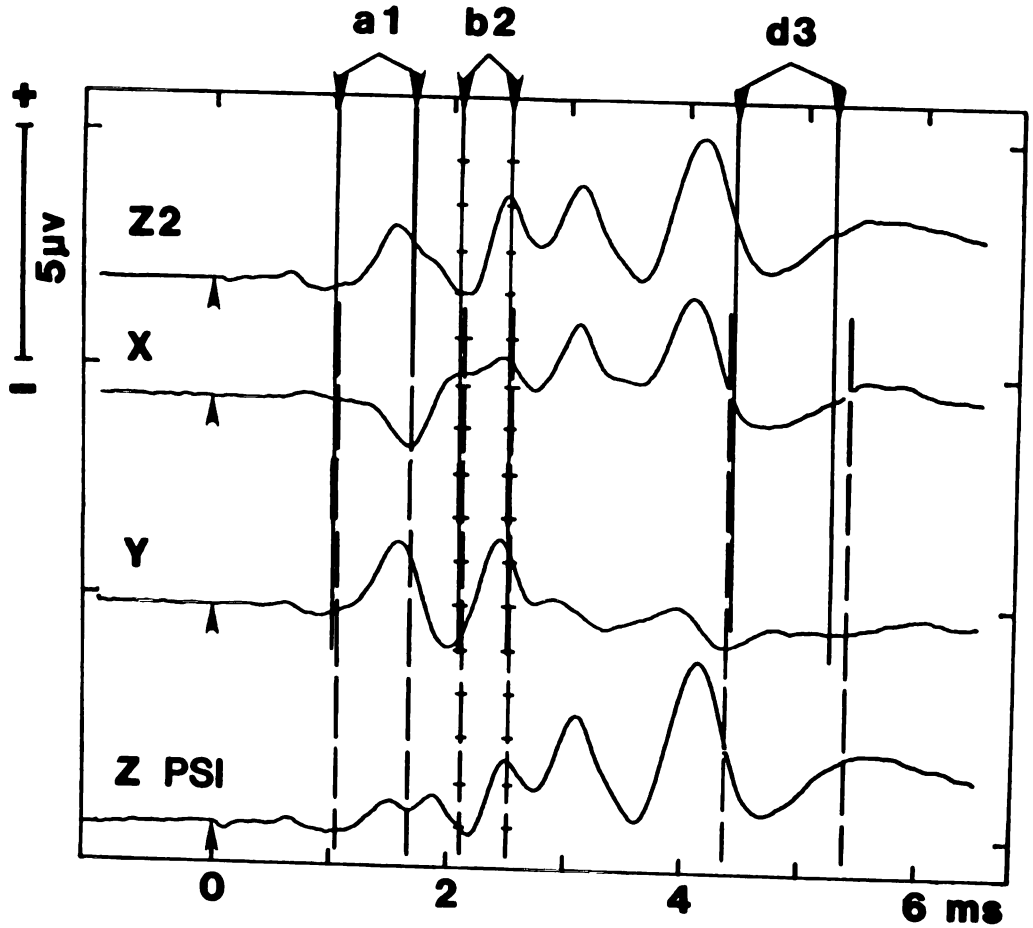

Figure 5

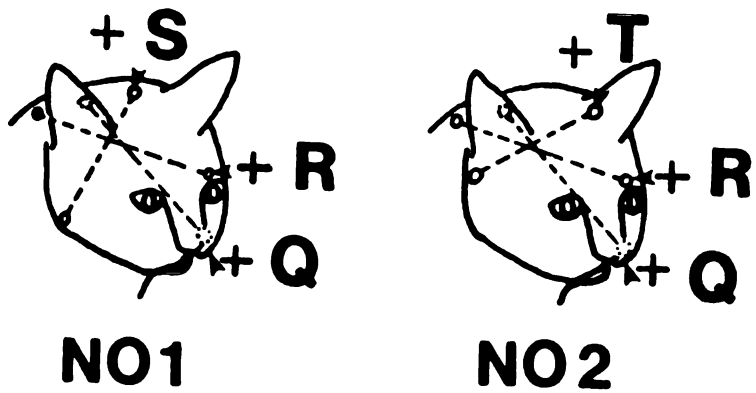

Figure 6

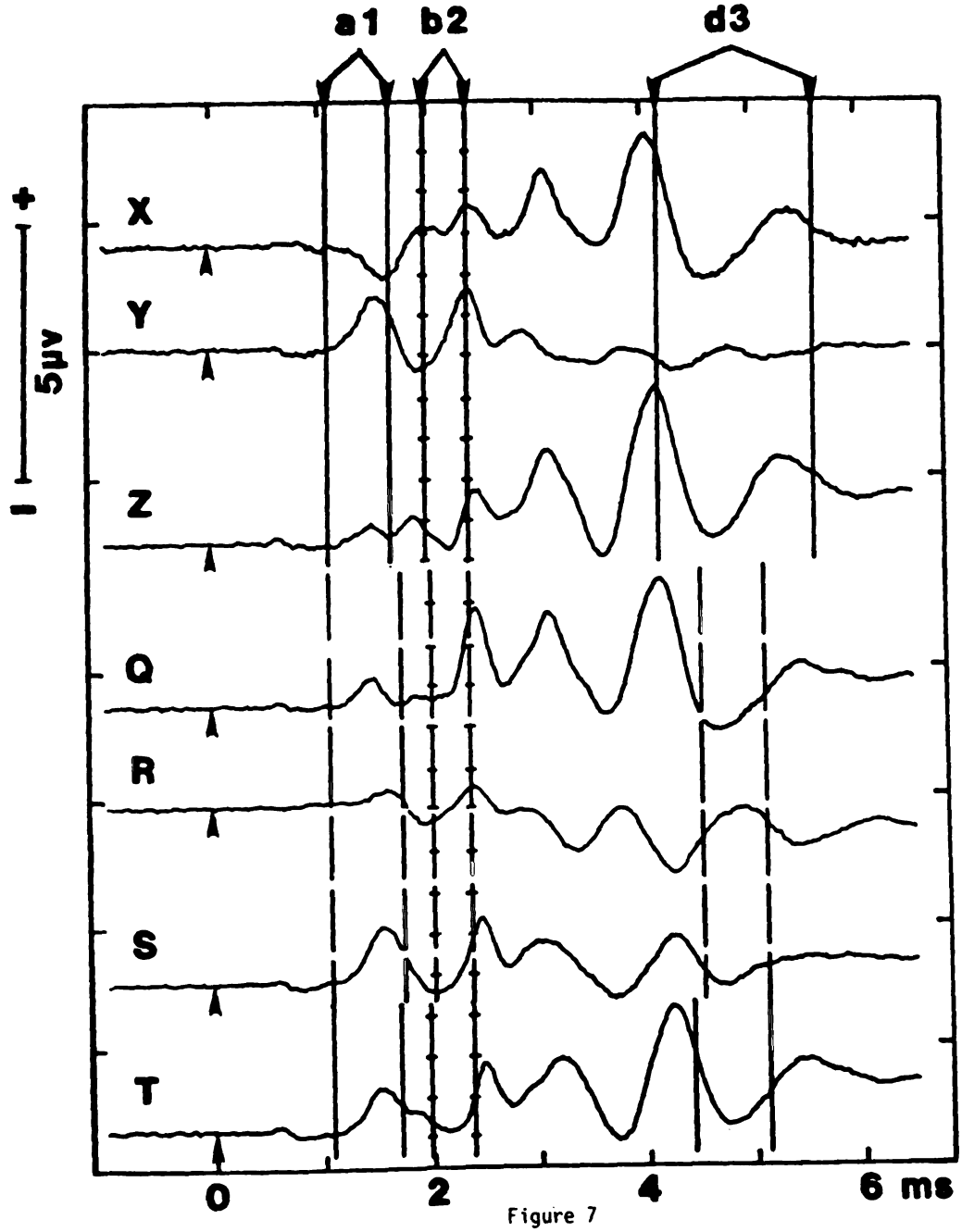

Figure 7

CHAPTER 4

THE EFFECTS OF STIMULUS INTENSITY

INTRODUCTION

Three-channel Lissajous trajectory

The three-channel Lissajous trajectory (3-CLT) of the auditory brain stem response (ABR) has been recorded in the guinea pig (Williston et al, 1981), cat (Martin et al, 1983a, b), and man (Pratt et al, 1983). In all three species, segments of the voltage trajectory had a planar characteristic. Because of this feature, these distinguishable segments are called planar-segments. To date, the majority of research efforts have been directed at the cat, in which 12 planar-segments are recorded during the first 10 milliseconds following a 70 dB impulse SPL click stimulus. Planar-segments were relatively consistent in number, shape, apex-latency, boundaries, duration and position in voltage space, both within and across subjects (Martin et al, 1983a). Planar-segment number, apex-latency, boundaries, and duration appeared to be unaffected by large changes in recording electrode configuration, in sharp contrast to changes observed in the peaks and valleys of single-channel ABRs recorded under similar conditions (Martin et al, 1983b). Thus, planar-segments

appear to be generator dependent, not electrode position dependent, and therefore offer a more direct means of evaluating the generator activity of the ABR.

Effects of Stimulus Intensity on the ABR

One of the most useful characteristics of the single-channel ABR has been that it allows for an evaluation of the integrity of the auditory pathway in a non-invasive manner. Knowledge of the approximate neural generators combined with simple parametric manipulations has increased both clinical and research capabilities. The recording of ABRs at different stimulus intensities is one of the primary strategies of evaluating auditory system status (Galambos and Hecox, 1977). The effect of stimulus intensity on the ABR was reported in early publications describing the response (Jewett et al, 1970; Jewett and Romano, 1972). One basic observation has been that latency decreases and amplitude increases as stimulus intensity is increased. This has been confirmed by a number of investigators (Lev and Sohmer, 1972; Leiberman et al, 1973; Sohmer and Feinmesser, 1973; Terkildsen et al, 1974; Hecox and Galambos, 1974; Picton et al, 1974; Schulman-Galambos and Galambos, 1975; Starr and Achor, 1975; Pratt and Sohmer, 1976; Starr et al, 1977; Don et al, 1977; Allen and Starr, 1978; Stockard et al, 1978; Mair et al, 1978; Huang and Buchwald, 1978; Rowe, 1978;

and Stockard et al, 1979) and by countless practitioners. Most published studies reported that the first five waves (in the human) vary in latency and amplitude, proportional to the stimulus intensity. Stockard et al (1979), however, reported that Wave I latency was more affected by stimulus intensity than was the latency of other waves. This does not agree with previous studies (Jewett et al, 1970; Jewett and Romano, 1972; Starr and Achor, 1975). They also suggested that interpeak latency changes as a result of varying stimulus intensity, reflecting changes in the neuronal population active in the auditory nerve at different stimulus levels.

The purposes of this study were to determine the changes in the 3-CLT of the cat resulting from systematic variation of stimulus intensity and to thereby establish a basis upon which to further understand the relationships between recorded planar-segments and the generators of the ABR.

METHODS

Experimental Conditions

The four adult cats used in this were the same as described in our previous reports (Martin et al, 1983a, b). All experimental conditions, including anesthesia,

recording parameters, and electrode positions have been earlier described in detail (Martin et al, 1983a).

Intensity Series

Computer generated 100 microsecond square waves were fed to an electrically shielded headphone (Stax model SR84) and presented monaurally via a plastic earbar at rates of 10/sec. The acoustic signal was calibrated using a sound-level meter (B&K model 2209) equipped with a 1/2" condenser microphone coupled directly to the output end of the plastic earbar. All stimulus intensities are reported in decibels of impulse sound pressure level (dB impulse SPL). Stimulus level was regulated with a Hewlett Packard attenuator (model 350-D for dB volts). The time/pressure waveform of a 70dB acoustic click is shown in Figure 1. Fast Fourier transformation of this waveform indicated primary energy peaks at 3 and 5 kHz with a smaller peak between 11 and 15 kHz and is shown in Figure 2. The higher frequency peak is about 24dB down from the 5 kHz peak amplitude. A large low frequency component is seen on the FFT. It may be due to the type of FFT sampling window used (rectangular) and/or to the low frequency ringing from 2 to 6 milliseconds after the stimulus onset which was included in the FFT sample and is probably due to the resonance characteristics of the plastic earbar. ABRs were recorded from X, Y, and Z channels using stimuli

from threshold to 70dB impulse SPL. The number of sweeps acquired for a single-channel average was increased at lower stimulus intensities to improve the signal-to-noise ratio of the response. At stimulus intensities above 30dB, 500 sweeps were averaged. At lower intensities, from 4000 to 25,000 sweeps were averaged.

Analysis

The X, Y, and Z channel data recorded at each stimulus intensity were interpreted using planar analysis as described by Martin et al,(1983a). Planar segments were evaluated at each stimulus level in terms of number of distinguishable segments, shapes, apex-latencies, boundaries, durations, and positions in voltage space. For a description of the analysis method and terminology definitions, see Martin et al, (1983a).

RESULTS

Intensity Series

Single-channel ABRs recorded from the X, Y, and Z electrode configurations systematically changed with changes of stimulus level. As intensity was decreased the number and amplitude of grossly visible positive peaks decreased and the peak latencies increased as previously reported in cats (Jewett, 1970; Jewett and Romano, 1972).

Also, the inter-peak latencies appeared to remain constant across the range of stimulus levels tested. Representative X, Y, and Z configuration single-channel waveforms from one cat are shown as a function of stimulus intensity in Figures 3a, b, and c. Note the decrease in latency and increase in amplitude as the stimulus level was raised.

Three-channel Lissajous trajectories (3-CLTs) were formed when X, Y, and Z single-channel ABRs recorded at each intensity were combined and plotted in three-dimensional voltage space. Planar-segments were identified in the 3-CLTs recorded at all stimulus levels. However, the numbers, shapes, apex-latencies, durations and positions of the planar-segments were dependent upon the intensities of stimuli presented.

Number of Planar-segments vs. Stimulus Level

Near ABR threshold (in most cats between 10 and 20dB impulse SPL) four discrete planar-segments could be identified. They have been labeled 'a', 'b', 'c' and 'd'. The X, Y, and Z single-channel ABRs recorded at 10dB impulse SPL as well as their planar-segment boundaries, are illustrated in Figure 4. There was an overlap of boundaries for all four planar-segments. The single-channel waveforms recorded near threshold typically showed at most three gross positive peaks, however four discrete planar-

segments could be defined using planar analysis.

As stimulus level was increased, the initial four planar-segments differentiated into a progressively greater number of "descendant" planar-segments. Typically there were 5 to 7 planar-segments at 20dB SL (i.e., 20dB above the level at which no ABR could be recorded within the experimental conditions), 8 to 9 at 30dB SL, and 9 to the maximum of 12 from 40 to 70dB SL. In some cases, as the stimulus level was increased, data points which formed two planar-segments at one intensity formed a single planar-segment at a higher intensity. As the stimulus level was further increased, the data points again divided into two planar-segments. An example of this is shown in Figure 5b. At 30dB, c4 and d1 exist independently and have an included angle between them of 68 degrees (Figure 6). C4 and d1 combine at 40 and 50dB to form one planar-segment and divide in two again at 60 and 70dB. In this particular animal, d3 and d4 also combined at 60dB (only) to form a combination planar-segment. This variability was consistent with the type reported both within and across animals at 70dB (Martin et al, 1983a), but did not occur in the in the results from the other three subjects used in this study.

The included angles between adjacent planar-segments at each stimulus intensity are presented in Figure 6. All

but four of the include angle values presented exceed the test-retest included angle range for the individual sight vectors at 50dB presented at the bottom of the figure. This range was the maximum position difference between any two of three sight vectors for a given planar-segment which were recorded over a two hour period. That the included angles between adjacent sight vectors typically exceeds the range of variability for the individual sight vectors suggests that the adjacent planar-segments lie in different planes.

Changes in the number of planar-segments with parametric manipulation was also observed in a preliminary study using high-pass masking to obtain derived narrow-bands of response (after Don and Eggermont, 1978). The derived narrow-band 3-CLTs recorded from the cat using a 50dB impulse SPL click and a white-noise masker high-pass filtered at 96dB/octave varied in complexity as a function of the frequency of the derived band. While all 12 planar-segments could be identified in some narrow-band 3-CLTs, as few as four planar-segments were found in others.

Planar-segment Shape vs. Stimulus Level

Planar-segment shape also depended upon stimulus level. Examples of the "broadside" views of all planar-

segments recorded at all stimulus intensities from one animal are shown in Figures 5a and b just as with the single-channel ABRs in Figures 3a, b, and c. All planar-segments increased in size as the stimulus intensity was increased (note the change in scale factor at the right side of the figure). Qualitatively, the size of each planar-segment increased most rapidly from 10 to 30dB impulse SPL. Above 30dB, the proportional increases in size as a function of intensity were more gradual. This animal was chosen as the example because it was typical of the shapes observed in all of the subjects and because it was the least contaminated by noise at the lower intensities.

Group 'a'

Planar-segment 'a' (Figure 5a) typically demonstrated a hairpin shape which doubled in size and changed in curvature between 10 and 30dB. The data points which would make up planar-segment 'a' (determined by tracing 'a' boundaries from lower intensities), formed two new planar-segments, a1 and a2, at 40dB. Both a1 and a2 had a unique shape which differed from its ancestor. From 40 to 70dB, there were only slight variations in the curvature of a1 and a2.

Group 'b'

There was little change in the curvature of planar-segment 'b' at 10dB and 20dB. At 30dB, 'b' changed shape, there resembling segment b2 recorded at higher stimulus levels. As in the 'a' group, data points formed two new planar-segments at 40dB. B1 and b2 shapes were similar from 40 to 70dB.

Group 'c'

At 10dB, planar-segment 'c' had apices and landmarks which could be traced to equivalent landmarks on planar-segments (c1, c2, c3) and c4 at higher stimulus levels (Figure 7a). At 20dB, the apices on planar-segment (c1,c2,c3) became more pronounced and c4 formed an independent planar-segment. C1, c2, c3 and c4 each formed an independent planar-segment at 30dB, and their basic shapes were relatively unchanged as stimulus intensity was increased to 70dB compared to lower intensities. At 40 and 50dB, c4 and d1 combined to form a single planar-segment, but the data points from c4 (shorter in post-stimulus latency) which contributed to the c4, d1 combination segment approximated the curvature of their c4 ancestors and descendants.

Group 'd'

The 10dB 'd' planar-segment was a complex elliptically shaped curve with apices and landmarks which could

be traced to equivalent components on descendant planar-segments d1, d2, d3, and d4 (Figure 7b). At 20dB, d1 and d4 formed independent planar-segments while d2 and d3 remained combined (as a (d2,d3) complex). The shape of (d2,d3) remained constant from 20 to 40dB. D1 changed markedly in shape at 30dB, forming a hairpin turn which was seen up to 70dB. D4 was unidentifiable at 30dB, but reappeared in various shapes from 40 to 70dB. D4 was also not identified at 30dB in one other subject. At 50dB, d2,d3 divided into d2, which resembled its ancestors and descendants; and d3, which varied somewhat in shape up to 70dB.

Summary

In general, by about 40dB each planar-segment acquired its "high intensity" shape, which was approximately maintained as stimulus level was increased. The most dramatic curvature changes occurred below 40dB. However, in some planar-segments, particular shape patterns indicative of apices were preserved from 10 to 70dB (Figures 7a, 7b). The preservation of curvature characteristics (e.g., apices) was more profound in groups 'c' and 'd' than in 'a' and 'b'.

Apex-latency vs. Stimulus Level

Apices which could be easily traced from 10 to 70dB were measured. They revealed a progressive decrease in apex-latency as stimulus level was increased (Table I). The net change over the 60dB range was approximately 1 millisecond, which is comparable to the changes in single-channel peak latencies as illustrated in Figures 3a, b, and c over the same intensity range. The relative time between apices changes relatively little. For example, the inter-apex latencies between c1 and d2 at 10, 40, and 70dB are 1.9, 1.9, and 1.8 milliseconds respectively. Apex-latencies and boundaries for all planar-segments recorded from one animal at all stimulus intensities are listed in Table II. Across subjects, the boundaries and apex-latencies varied depending on the number of planar-segments identified at any given stimulus intensity.

Planar-segment Duration vs. Stimulus Level

An example of planar-segment duration as a function of stimulus level for one representative animal is shown in Figure 8. The durations of individual planar-segments as well as planar-segment To determine the duration of a 'group', the duration was measured from the first data point of the first planar-segment in the group to the last point of the last planar-segment in the group. It is important to note that the duration of a group was not the same as the sum of the durations of all planar-segments

within that group. Since planar-segment boundaries overlap, the group duration is always less than the summed duration. As stimulus intensity was increased, the initial four planar-segments were divided into smaller subsegments, each of which had shorter duration, but which were also planar. Although there was a slight trend toward duration reduction, the combined durations of groups of descendant planar-segments were similar to those of their original ancestors. There was an occasional overlap between groups as stimulus level was increased (e.g. the (c4,d1), complex) which made it difficult to follow group duration changes across all stimulus intensities. An example of this maintenance of duration phenomenon across stimulus intensities is demonstrated by planar-segment at 10dB while the combined duration for the 'c group' (including c1, c2, c3, and c4) at 70dB is also 1.3 milliseconds.

The nomenclature used in this study (as well as Martin et al, 1983a and b) is based primarily based on the grouping of planar-segments relative to their lower intensity ancestors. Groupings of planar-segments at higher intensities was done by first determining the boundaries of the four planar-segments at the lowest possible stimulus level in all subjects. As stimulus intensity was increased, the boundaries were decreased in latency an

appropriate amount which was determined by apex-latency shift and by single-channel peak latency shift. Planar-segments which fell within the adjusted boundaries were considered members of that group. This method proved to be consistent across all four animals and was supported by the maintenance of shape characteristics found in high intensity planar-segments which could be traced to the same characteristics in the near threshold ancestors.

Planar-segment Position vs. Stimulus Level

An example of sight vector azimuth and elevation values from one animal recorded over the 60dB range of stimulus intensities is presented in Figure 9. Also the variability in sight vector position at stimulus intensities of 10, 20, 40, and 70dB is shown in table III. The variability was estimated by calculating the range of across animal included angles for each sight vector. The included angles were measured comparing responses from three animals. The results suggest that planar-segment with shorter latencies (which are in groups 'a' or 'b') decrease in variability as the stimulus level is raised, but the later groups tend to vary more at higher stimulus levels when compared to lower. When compared to the within animal test-retest range at 50dB presented at the bottom of Figures 6, 10, 11, and 12, the values in Table III may appear unusually large. Two factors which may

contribute to this difference are; first, that the across animal sight vector variability is generally twice that of the within animal (Martin et al, 1983a) and second, at stimulus intensities below 40dB planar-segments change in position and in number over a relatively small range of stimulus intensities. Unless subjects are perfectly matched for equal sensation level, it is possible that the variability may be a result of small intensity differences which affect planar-segment number and position.

As stimulus level was increased, the positions of planar-segment sight vectors varied in a complex manner. To illustrate these changes a series of intensity/position trees is presented (Figures 10, 11 and 12).

Position Changes re Intensities

Included angles (see Martin et al, 1983a) between planar-segment sight vectors at successive 10dB stimulus increments from one cat are presented in Figure 10. Each sight vector is compared to the sight vector(s) at 10dB above and below its own stimulus level. Therefore, the included angle value indicates the amount of sight vector position change (in degrees) for a 10dB change in stimulus level. For comparison, the ranges of test-retest variability for all planar-segments within the same animal are presented. The stimulus intensity was 50dB. Underlined

values in Figure 10 emphasize included angles which were less than or equal to the test-retest variability for that particular sight vector. This was determined by calculating the maximal included angle between any two of three sight vectors corresponding to the same planar-segment which were recorded over a two hour period. The stimulus intensity at which variability was determined was 50dB. This variability standard was used for evaluating all position change comparisons.

Group 'a'

Sight vector 'a' may have changed position between 10 and 20dB, but due to the high variability indicated for that planar-segment at that intensity (Table III) subtle changes cannot be detected with certainty. Little change in position was recorded between 20 and 30dB. Between 30 and 40dB, 'a' differentiated into a1 and a2, each of which differed in position from its parent segment. Sight vectors a1 and a2 remained in approximately the same positions for successive intensities from 40 to 70dB, a range over which there was less shape change.

Group 'b'

No change in the position of sight vector 'b' was observed between 10 and 20dB. Between 20 and 30dB as well as 30 and 40dB, position changes were recorded. At 40dB,

planar-segment 'b' divided into b1 and b2 whose sight vector positions remained unchanged for successive intensities from 40 to 70dB (as in group 'a').

Group 'c'

Between 10 and 20dB, planar-segment position of sight vector (c1,c2,c3) was unchanged while c4 was changed dramatically, when compared to test-retest variability values. During the next intensity decade, c1, c2, and c3 formed independent planar-segments. In this transition, there was a large sight vector position change for c1, and little change for c2 and c3. Like c1, sight vector c4 was also not changed in position by the 10dB increase. Additional sequential 10dB increases in stimulus intensity failed to significantly alter the positions or shapes of sight vectors c1, c2, c3 or c4.

Group 'd'

Between 10 and 20dB, planar-segment 'd' differentiated into d1,(d2,d3) and d4, of which only sight vector (d2,d3) remained constant in position. No change in sight vector position was observed for d1 and (d2,d3) between 20 and 30dB. Segment d4 was not identified at 30dB. At 40dB, d1 combined with c4 to form a combination planar-segment with a new sight vector position, while d2,d3 was again unchanged compared to its ancestor. Between 40 and

50dB, sight vector c4,d1 did not change in position. At 50dB, (d2,d3) divided into a separate d2 in the same position, and a separate d3 in a new position. Sight vector d4 also shifted in position by increments in stimulus intensity from 40 to 50dB. From 50-60dB, the positions of d1, d2, and d3 did not change. At 60dB, d3 and d4 formed a combination planar-segment which was similar in position to its d3 ancestor but different in position to its d4 ancestor. Between the highest intensities tested (60 to 70dB), there was only a small change in the positions of d1, d2, and d3, and a slight change in the d4 position as the (d3,d4) combination again divided into two discrete planes.

Summary

Two observations were made from examining position changes at sequential 10dB intensity levels. First, with the exception of sight vectors d3 and d4 between 40 and 50dB, a 10dB intensity difference at or above 40dB resulted in little or no change in sight vector position in any component. However, below 40dB, the same increment of intensity change resulted in an increased number of sight vectors which changed position. Therefore, somewhere between 30 and 40dB stimulus level appeared to mark a transition range for sight vector position. At roughly 40dB, sight vectors appeared to reach a stable "high-

intensity" position.

Second, some sight vectors appeared to remain relatively unchanged in position from 10dB to 70dB, at least when measured in 10dB increments. An example is the progression of planar-segment 'c' to (c1,c2,c3) to c2. The maximal change in sight vector position is only 12 degrees between (c1,c2,c3) at 20dB and c3 at 30dB. Another example was that of 'd' to (d2,d3) to d2. In this case the maximal sequential sight vector position change was 17 degrees (between 60 and 70dB). Therefore, some sight vector positions appear to be little affected by stimulus level.

To evaluate these two observations more thoroughly, changes in sight vector position resulting from changes in stimulus level were considered in two other ways. The possible presence of a 40dB stimulus level turning point was evaluated by comparing the position of all sight vectors at all stimulus levels with the equivalent sight vector at 40dB. The possibility that some sight vectors do not change position with increased stimulus level was evaluated by comparing all sight vector positions at higher stimulus levels with the position of their 10dB ancestors.

Position Changes re 40dB Position

Included angles between sight vectors at each stimulus level and the equivalent sight vector at 40dB are presented in Figure 11. The included angle indicates the amount of position change for a given sight vector as the stimulus level is raised above or lowered below 40dB.

Group 'a'

Sight vector 'a' recorded at 10, 20, or 30dB was in a position which differed from either a1 or a2 recorded at 40dB. However, sight vectors from planar-segments recorded from 50 to 70dB were in positions similar to those of their 40dB ancestors. These observations parallel shape changes within the same group.

Group 'b'

The 'b' group revealed the same trend. Ancestors to the 40dB b1 and b2 sight vectors were in different locations while descendants from 50 to 70dB were unchanged in position. Also, as in group 'a', position and shape changes were parallel.

Group 'c'

Sight vector 'c' at 10dB differed in position markedly from sight vectors c1 and c4 at 40dB. However, there was little or no change in position when comparing 'c' at 10dB to c2 or c3 at 40dB. Two planar-segments were

present in the 'c' group at 20dB. The 20dB (c1,c2,c3) sight vector differed in position from the c1 sight vector at 40dB, but did not greatly differ from the 40dB c2 or c3 sight vectors. C4 at 20dB was in a similar position to its 40dB counter part, but was less similar at 30dB. This was in part because c4 and d1 combined at 40dB to form a combination (c4,d1) planar-segment. Sight vectors c1, c2, and c3 at 30, 50, 60, and 70dB remained in similar positions to their counterparts at 40dB, with the one possible exception of the location c2 at 70dB. Above 40dB, c4 also remained in the same position as its 40dB ancestor from 50 to 70dB.

Group 'd'

Sight vector 'd' at 10dB was similar in position to d1 and (d2,d3) at 40dB but different in position from d4 at 40dB. When d1, (d2,d3) and d4 at 20dB were compared to their 40dB counterparts, only (d2,d3) was unchanged in position. The same was true at 30dB for d1 and (d2,d3), but d4 was unidentified and therefore not evaluated. As the stimulus intensity was increased, position changes relative to the 40dB sight vectors continued to be complex. Planar-segments c4 and d1 combined to form a combination planar-segment at 40dB whose sight vector remained unchanged in position at 50dB. Planar-segment (d2,d3) differentiated into separate segments d2 and d3 at 50dB.

The 50dB d2 sight vector was unchanged in position from its parent, while the 50dB d3 deviated from its 40dB counterpart. At 60dB, c4 and d1 were again independent planar-segments with sight vectors similar in position to the 40dB values. However, planar-segments d3 and d4 formed a combination planar-segment whose sight vector differed from that of either of its 40dB ancestors. Sight vectors d1 and d4 at 70dB were different than their 40dB ancestors, but 70dB d2 and d3 were only slightly changed in position compared to their 40dB ancestors.

Summary

Comparing sight vectors recorded at 40dB with those recorded at lower intensities revealed relative position changes in all but c2, c3, and (d2,d3). Comparing 40dB sight vectors with their higher intensity descendants showed that most of them do not change in position above 40dB. Exceptions include c2 and d1 at 70dB and d3 and d4 at 60dB. In general, many sight vectors attain a relatively stable "high intensity" position at 40dB. It is interesting to note that several sight vectors (specifically c2, c3, (d2,d3) and its descendant d2), remain in about the same position at all stimulus levels. This is further illustrated in the next section.

Position Changes re 10dB

Sight vector positions at each stimulus level were compared with those at 10dB to determine the cumulative change in position as a function of stimulus intensity. The included angles between each sight vector at a given intensity and the counterpart sight vector at 10dB were calculated and are presented in Figure 12.

Group 'a'

All descendant sight vectors recorded at intensities from 20 to 70dB differed in position with that recorded at 10dB.

Group 'b'

In the 'b' group, increasing the stimulus intensity from 10 to 20dB did not result in a sight vector position change. However a position change was observed when sight vectors recorded at all higher intensities were compared to those recorded at 10dB.

Group 'c'

At 20dB, planar-segment 'c' divided into two individual segments, (c1,c2,c3) and c4. C4 sight vectors at intensities 20 to 70dB differed in position from their ancestor same position as its 10dB ancestor. At 30dB, planar-segment (c1,c2,c3) differentiated into three subsegments (c1, c2, and c3). Sight vector c1 differed

markedly from 'c' at 10dB at intensities from 30 to 70dB. Sight vector positions for c2 and c3 were similar to the 10dB 'c' position at intensities from 20 to 60dB. At 70dB, the c2 and c3 sight vectors differed in position from the 10dB 'c' position, but not greatly.

Group 'd'

Planar-segment 'd' formed a single plane at 10dB. At 20dB, 'd' was divided into d1, (d2,d3) and d4. Sight vectors of planar-segments d1 and d4 changed in position relative to their 10dB ancestor 'd' sight vector as stimulus level was increased, while sight vector (d2,d3) did not. At 40dB, (d2,d3) formed separate d2 and d3 segments. Between 40 and 60dB, 'd2' was similar in position to its 10dB ancestor, but by 70dB d2 had changed its relative position. Sight vector d3 only marginally changed position compared to 'd' from 40 to 70dB.

Summary

In general, planar-segments changed position as a function of stimulus level. There were, however, four exceptions. Sight vectors of planar-segments c2, c3, d2, and d3 changed relatively little in position as stimulus levels were increased from 10dB to 60dB. At 70dB, only d3 was unchanged relative to 10dB.

CONCLUSIONS

Number of Planar-segments

Increasing the stimulus intensity increased the complexity of the 3-CLT in the cat. One index used to estimate the complexity of the 3-CLT waveform is the number of planar-segments at any given stimulus level

Near threshold, there appeared to be four sequential planar-segments of discrete duration and time locked to the stimulus. As the stimulus level is increased, these initial four components progressively differentiated into a total of 12 planar-segments. These changes may well be consistent manifestations of progressive changes in the behavior of auditory system neurons that are time-lock-activated by clicks. The interesting fact is that these modifications result in sub-units of sequential activity which is also planar in voltage space.

The increase in planar-segment number could in part be due to the increased spread of activation along the basilar membrane as a function of increasing stimulus intensity. Certainly this increase in spread results in factors which could affect planar-segment formation. As stimulus level is increased, the size of the active fiber population is also increased (Pfeiffer and Kim, 1974). These additional fibers are from different best-frequency

regions of the cochlea (Eggermont, 1976). Because the auditory system is tonotopically arranged, a change in stimulus intensity results in a change in the spatial distribution of the active fibers. Due to the traveling wave time, a phase shift in the time during which those fibers are active (Yoshie, 1976) also occurs as stimulus level is varied. Theoretically, the position of a plane in voltage space can be influenced by the spatial orientation of its neural generators, or the phase relationship in activity between them (Jewett, 1983). The above mentioned cochlear processes could fulfill both of these requirements as stimulus level is increased. Tonotopicity could induce spatial changes in the generators while traveling wave time could induce the necessary relative phase shift. The observation that the number of planar-segments reaches its maximum around 40dB suggests that these processes plateau at that level.

It is interesting to note that single-channel ABRs recorded with use of near-threshold stimuli show a maximum of only three easily identifiable peaks (Figures 3a, b, c, and 4). The latencies of these peaks is dependent upon the recording electrode positions. However, at 10dB, the 3-CLT has four constant planar segments which can be identified and used for evaluation of the auditory system. This becomes important in clinical situations where wave V is

delayed at low stimulus levels and wave I is absent in the single-channel ABR. In these cases, electrocochleography (ECochG) must be performed to determine if the wave V shift is due to cochlear dysfunction or due to an increased central conduction time indicative of brain stem lesions (Starr and Hamilton, 1976). Misdiagnosis of this type can lead to over estimation of the conductive component of an impairment. The presence of short (1-2ms) and longer latency (3-6ms) planar-segments at low stimulus intensities provides additional information unavailable in a single-channel ABR.

Shape

Broadside views of planar-segments revealed changes in shape as a function of stimulus level. These changes were of two types; first the curvature of the segment and second, the size.

Changes in curvature are qualitatively demonstrated in Figures 5a, 5b, 7a and 7b. One cause of curvature changes is the fact that planar-segments differentiate into sub-segments at higher stimulus levels. This results in descendant planar-segments each having their own shape, but retaining some characteristics of their ancestor. The apex of some planar-segments can be traced to inflections on planar segments at 10dB (Figures 7a and b). This indi-

cates that some aspect of the generator activity near threshold is maintained in the three-dimensional waveform over a 60dB stimulus range. Curvature changes which are not due to planar-segment differentiation probably reflect the same processes which were suggested to affect planar-segment number, namely generator orientation and phase. In vectorcardiography, changes in the shape of the VCG loop have proven to be the most useful index of cardiopathology (Wartak, 1970). The majority of planar-segments do not change in curvature at or above 40dB, supporting the hypothesis that the factors which determine planar-segments change and stabilize at about that level.

Size changes probably reflect the size of the neural population active at any given stimulus level. As stimulus level is raised above 40dB, the rate of size change diminishes. This suggests that the rate of adding active fibers also decreases above 40dB. Planar-segment size reflects the same processes underlying single-channel peak amplitude and therefore has the potential to be applied clinically. The advantage of using planar-segment size over peak amplitude is that an additional two dimensions of voltage distribution are considered in the planar-segment which could be more sensitive to amplitude variations in directions perpendicular to a single-channel electrode pair (Martin et al, 1983b).

Apex-latency

The apex-latencies of planar-segments are three-dimensional indicators of the same physiologic processes underlying single-channel peak latency. The advantage of apex-latencies over peak latency is that the apex of a planar-segment is that the apex of a planar-segment is determined by three channels of voltage information and is relatively independent of electrode placement, therefore providing a direct information about the time course of generator activity than any single-channel ABR (Martin et al, 1983b). Several apices can be identified on planar-segments at 10dB and tracked as stimulus level is increased (Table I). The similarity in the net changes of apex-latencies over a 60dB intensity range in Table I, indicates that apex-latency changes reflect cochlear mechanisms. Apex-latency did not decrease at the same rate as stimulus level was increased. At higher levels, the rate of apex-latency change diminished supporting the hypothesis of cochlear process saturation at high stimulus intensities.

Duration

The duration of the initial four planar-segments is maintained by the boundaries of their descendants as stimulus level is increased (Figure 8). There is a slight

decrease in duration of "groups" 'a', 'b' and 'd' which is reasonably expected in view of increased synchrony of neural activity as a function of increasing stimulus level (Antoli-Candela and Kiang, 1978). However, this does not account for the increase in traveling wave time at higher stimulus levels which could possibly increase the duration of a planar event (Pfeiffer and Kim, 1974). The maintenance of "group" duration over a 60dB range suggests a cochlear process which is independent of stimulus level, or a delicate balance between the increasing synchrony of neural firing and the traveling wave time.

Sight Vector Position

The three primary observations concerning planar-segment position vs. stimulus were that; (1.) the majority of planar-segments change position as a function of stimulus level, (2.) that change occurs mainly at stimulus intensities less than 40dB, and (3.) some planar-segment positions do not change as a function of stimulus level. That planar-segments change position as a function of stimulus level is not surprising in light of the theoretical basis for planar-segment position (Jewett,1983) and the changes in population size, phase relation, and orientation of the generators previously discussed (Pfeiffer and Kim, 1974; Eggermont, 1976; and Yoshie, 1976). The relative invariance in sight vector

position above 30dB is consistent with the other findings of this study and may be a result of two different processes. Both processes are based on a three-phase response pattern of the compound action potential (CAP) a stimulus level is increased. At low intensities (0-45dB HL), fibers which are sensitive to low level stimuli (L population) are the sole contributors to the CAP. AT high stimulus intensities (60-100dB HL) fibers which are insensitive to low level stimuli are activated (H population). At stimulus levels between 45 and 65dB HL, a transition period occurs during which the H activity is added to the L activity (Yoshie, 1976). Yoshie (1976) presents two hypotheses to account for this phenomenon which can be related to our position findings.

The first hypothesis proposes that at high stimulus intensities, high frequency fibers in the region above 4,000 Hz are fired synchronously and contribute to the H component of the response. At lower stimulus levels the primary region of activation is more apically located, between 1,500 and 4,000 Hz, and forms the L component. Therefore, intensity information is coded in frequency distribution along the basilar membrane. This could result in changes in sight vector position because as intensity is increased a new population of fibers having a new tonotopic distribution is being added to a lower intensity

population which has a different tonotopic distribution. Also, as the high frequency fibers are added, there is a time differential between when the stimulus activates the high frequency and low frequency fibers. Once both populations are excited the spatial orientation, and phase relationship of the generators would be established, resulting in less changes in sight vector position with further increase in stimulus level.

The second hypothesis proposes that there are two populations of sensory units which are differentially sensitive to stimulus intensity at the same region of the basilar membrane. This corresponds to the results seen in studies on the responses of inner and outer hair cells. In this condition, the outer hair cells would represent the L population and the inner hair cells the H group. Applied to changes in sight vector position, the inner and outer hair cell fibers would be activated simultaneously and have similar tonotopic distribution. Therefore, if the H and L populations were inner and outer hair cells, we would not expect changes in sight vector position as a function of stimulus level.

General Summary

Planar-segments provide stimulus related information about neural generator activity of the ABR in two

categories. First, dynamic information, resulting from changes in generator activity, and reflected in changes in planar-segment number, shape, apex-latency and position in voltage space. In all cases, these intensity related changes stabilize near 40dB impulse SPL providing both low and high stimulus level information defined by a relatively narrow transition level. Dynamic information may be clinically useful for determining subtle changes in auditory processing, since most of the changes which are observed can be based in cochlear and neural processes involving tonotopicity, phase relation, and synchrony of firing. These processes interact over a range of stimulus levels in a predictable manner. Either excessive or insufficient changes in planar-segment indices at a given intensity could be used as indicators of pathology.

The second category is invariant information, resulting from generator activity which is either stable or at a delicate state of equilibrium across stimulus levels. Invariant information is reflected in an absence of change in inter-apex latency and duration, as well as shape and sight vector position for some planar-segments. This type of information could be useful in detecting gross abnormalities such as morphological alterations or changes in conduction velocities. Both dynamic and invariant characteristics of planar-segments are generator dependent, and

not electrode position dependent (Martin et al, 1983b), thus increasing their utility in a clinical setting.

TABLE LEGENDS

Table I

An example of planar-segment apex-latency vs. stimulus level from one animal. Apices which were identified at 10dB and could be traced at each increasing stimulus level were measured for their post-stimulus level were measured for their post-stimulus latency. In cases where one planar- segment had multiple apices, each apex was measured and noted by an asterisk. The net change is the time difference, in milliseconds, between the latency of a given apex at 10dB and the latency of that same apex at 70dB.

Table II

An example of the planar-segment boundaries and apex-latencies of each planar-segment at each stimulus intensity from one cat.

Table III

The range in sight vector position variability across three subjects at 10, 20, 40 and 70dB. The range of variability in sight vector position is estimated by calculating the included angles between each pair of sight vectors for the same planar-segment from each of three different cats. The maximum and minimum included angles are

presented.

FIGURE LEGENDS

Figure 1

The time/pressure waveform of a 100 microsecond click transduced by an electrically shielded Stax SR84 headphone coupled to a plastic earbar.

Figure 2

Fast fourier transform using a rectangular window of the stimulus waveform presented in Figure 1.

Figure 3a

X single-channel ABRs recorded using stimuli ranging from 10 to 70dB in intensity. The arrowhead indicates the stimulus onset. The 10 and 20dB waveforms have been multiplied by a factor of five. Note that at 10dB (average of 25,000 sweeps) two positive peaks are easily identified. However small inflections can be seen at 10dB which, when traced to higher intensities, form distinct peaks.

Figure 3b

Same as 3a, but for Y channel.

Figure 3c

Same as 3a, but for Z channel.

Figure 4

Single-channel X,Y, and Z waveforms recorded at 10dB & with planar-segment boundaries. The stimulus onset was at the first point (far left) of each trace. Note that the planar-segment boundaries overlap and do not correspond to the peaks or valleys of any of the single-channel waveforms.

Figure 5a

Planar-segment shape as a function of stimulus level. The broadside view of planar-segments 'a' and 'b' and their higher intensity descendents are illustrated. At 40dB, the data points which contribute to 'a' and 'b' divide into two separate planar-segments, each with its own shape and position in voltage space (see Figures 9 and 10). The multiplication factor indicates that the waveform has been magnified the indicated number of times before plotting. Note the relative invariance in planar-segment curvature and size at and above 40dB compared to lower stimulus levels.

Figure 5b

Shape as a function of stimulus level for 'c' and 'd' planar-segment groups. For most planar-segments, planar-

segment shape changes are less above 40dB than below. The primary exception is d4 which is the least stable in shape across intensities. The basic curvature of d2 remains more consistent at all stimulus levels that most other planar-segments.

Figure 6

Included angles, in degrees, between the sight vectors of adjacent planar-segments at each stimulus level. The size of the included angle is an indicator of how two adjacent planar-segments differ in orientation in voltage space relative to one another (Martin et al, 1983a).

Figure 7a

Apices from planar-segments c1, c2, c3, and c4 at 10dB and 70dB. At 10dB, planar-segment 'c' has four curvature characteristics which can be traced as stimulus intensity is increased much like peaks in the single-channel ABR (upper figure). At 70dB, the original 10 dB inflections correspond to the apices of four separate planar-segments (lower figures).

Figure 7b

A second example of apices which can be traced from 10 to 70dB. In this case, planar-segment 'd' at 10 dB (upper figure) has four apices which can be identified as

apices of individual planar-segments d1, d2, d3, and d4 at 70dB (lower figures).

Figure 8

Individual and group planar-segment durations, in milliseconds, from one animal. Each black dot on a horizontal line represents a planar-segment at that given intensity (compare to Figures 9, 10, 11, and 12). The values above a line indicate the duration of the individual planar-segment at that intensity. The values below a line indicate the duration of the group of planar-segments enclosed by the brackets. Group durations are shorter in duration than the sum of the durations of the group members because adjacent planar-segments within a group usually have overlapping boundaries (Table II, Martin et al, 1983a).

Figure 9

Planar-segment azimuth and elevation as a function of stimulus level for one animal. As in Figure 9, each dot on the horizontal lines represents a planar-segment at that particular intensity. Below the dots, the azimuth for that planar-segment's sight vector is presented immediately over the elevation. At 30dB, d4 was not identified.

Figure 10

Sequential planar-segment position changes as a function of stimulus level. Dots on horizontal lines are planar-segments at each intensity. The values on the vertical lines between the dots are the included angles between the sight vectors at each 10dB increment. For example, there is 38 degrees difference in the position of 'a' at 10dB compared to 'a' at 20dB. Also there is 50 degrees difference between d1 at 30dB and (c4d1) at 40dB. As an indicator of normal variability, test-retest included angle ranges for each individual sight vector at 50dB are included for comparison with sight vector changes as a result of stimulus level differences. The included angle values in the figures which are underlined were within the range of variability for the same planar-segment in this cat at 50dB. Note that the majority of position changes occur below 40dB and that c2, c3, and d2 do not show large changes between any two sequential stimulus levels.

Figure 11

Planar-segment positions at higher and lower stimulus levels relative to 40dB. In this figure a planar-segment at each intensity is compared to its counterpart at 40dB. The included angles between the sight vector at 40dB and

the sight vectors at other stimulus levels are on the lines connecting the planar-segment dots. For example sight vector (c1c2c3) at 20dB was in a location which differed from the 40dB sight vectors of c1 by 73 degrees, c2 by 2 degrees, and c3 by 14 degrees. Included angles which were with the test-retest range of variability for that sight vector at 50dB are underlined. In general, sight vectors at higher intensities have smaller position changes relative to 40dB than do lower intensity sight vectors, the exceptions being d3 and d4.

Figure 12

Planar-segment positions at higher stimulus levels relative to 10dB. This is an example in which all planar-segment sight vector positions at higher intensities were compared with the positions of their ancestor planar-segments at 10dB. For example, d3 at 50dB is 30 degrees different in position than increasing stimulus level, however some planar-segments namely c2, c3, d2, d3 are to some degree invariant over a large part of the intensity range.

PLANAR-SEGMENT APEX-LATENCY						
(Values in milliseconds)						
dB	Planar-Segment					
	c1	c2	c3	d1	d2	d3
10	3.4*	3.7*	4.0*	4.7*	5.4*	6.0*
20	3.1*	3.3*	3.7*	4.5	4.9	5.5*
30	3.0	3.1	3.6	4.3	4.7*	5.3*
40	2.7	3.0	3.5	4.0*	4.5*	5.0*
50	2.6	2.9	3.3	3.9*	4.4	5.0
60	2.5	2.7	3.2	3.8	4.3	4.9*
70	2.4	2.6	3.1	3.7	4.2	4.7
Net Change	1.0	1.0	0.9	1.0	1.2	1.3

* - Indicates that the planar-segment had multiple apices at that stimulus intensity.
Table I.

PLANAR-SEGMENT BOUNDARIES AND APEX-LATENCIES VS. STIMULUS LEVEL IN ONE ANIMAL

(Values in milliseconds)

dB	Boundaries	Latency	Boundaries	Latency	Boundaries	Latency	Boundaries	Latency
10	a) 1.5-2.8	a) 2.5	b) 2.6-3.3	b) 3.0	c) 3.3-4.5	c1) 3.4 c2) 3.6 c3) 4.0	d) 4.2-7.3	d1) 4.6
20	a) 1.4-2.5	a) 2.1	b) 2.3-3.0	b) 2.6	c1c2c3) 3.0-4.1 c4) 3.8-4.4	c1) 3.1 c2) 3.3 c3) 3.6 c4) 4.1	d1) 4.2-4.8 d4) 5.6-7.4	d1) 4.5 d4) 6.5
30	a) 1.6-2.5	a) 1.9	b) 2.4-3.0	b) 2.7	c1) 2.7-3.5 c2) 2.8-3.4 c3) 3.2-3.8 c4) 3.6-4.1	c1) 3.0 c2) 3.1 c3) 3.6 c4) 3.9	d1) 4.1-4.5 d2d3) 4.3-5.5 d4) NR	d1) 4.3 d2) 4.6
40	a1) 1.4-1.9 a2) 1.7-2.2	a2) 1.8	b1) 1.9-2.4 b2) 2.3-2.6	b1) 2.3 b2) 2.3	c1) 2.5-3.0 c2) 2.7-3.4 c3) 3.0-3.7 c4d1) 3.4-4.5	c1) 2.7 c2) 3.0 c3) 3.4 c4d1) 3.7	c4d1) 3.4-4.5 d2d3) 4.0-5.9 d4) 5.2-6.5	c4d1) 4.0 d2) 5.0 d4) 5.8
50	a1) 1.2-1.7 a2) 1.6-2.0	a2) 1.7	b1) 1.9-2.2 b2) 2.1-2.5	b1) 1.7 b2) 2.3	c1) 2.4-2.7 c2) 2.5-3.2 c3) 3.0-3.5 c4d1) 3.4-4.3	c1) 2.5 c2) 2.8 c3) 3.3 c4d1) 3.6	c4d1) 3.4-4.3 d2) 3.9-4.9 d3) 4.7-5.2 d4) 5.4-6.5	c4d1) 3.9 d2) 4.4 d3) 4.9 d4) 5.7
60	a1) 1.2-1.7 a2) 1.5-1.9	a2) 1.7	b1) 1.8-2.2 b2) 2.0-2.4	b1) 2.0 b2) 2.2	c1) 2.3-2.5 c2) 2.5-2.9 c3) 2.9-3.4 c4) 3.2-3.8	c1) 2.5 c2) 2.7 c3) 3.2 c4) 3.4	d1) 3.4-5.1 d2) 3.7-4.6 d3d4) 4.6-6.3	d1) 3.8 d2) 4.2 d3) 4.8
70	a1) 1.1-1.6 a2) 1.5-1.9	a2) 1.6	b1) 1.7-2.1 b2) 2.0-2.3	b1) 2.0 b2) 2.2	c1) 2.3-2.5 c2) 2.4-2.8 c3) 2.9-3.3 c4) 3.2-3.6	c1) 2.4 c2) 2.6 c3) 3.1 c4) 3.3	d1) 3.5-3.9 d2) 3.8-4.6 d3) 4.5-4.3 d4) 5.0-6.4	d1) 3.7 d2) 4.2 d3) 4.7 d4) 5.4

Table II.

SIGHT VECTOR VARAIBILITY RANGE ACROSS ANIMALS (Values in degrees)												
dB	'a'		'b'		'c'				'd'			
10	9-76		45-66		26-48				4-25			
20	41-69		12-67		9-55				12-29			
40	12-17	8-19	10-25	27-55	24-41	19-48	9-23		30-67	16-45	9-90	42-85
70	19-22	8-21	5-7	24-38	33-72	26-55	7-39	17-37	36-95	10-53	12-53	54-115
	a1	a2	b1	b2	c1	c2	c3	c4	d1	d2	d3	d4

Table III.

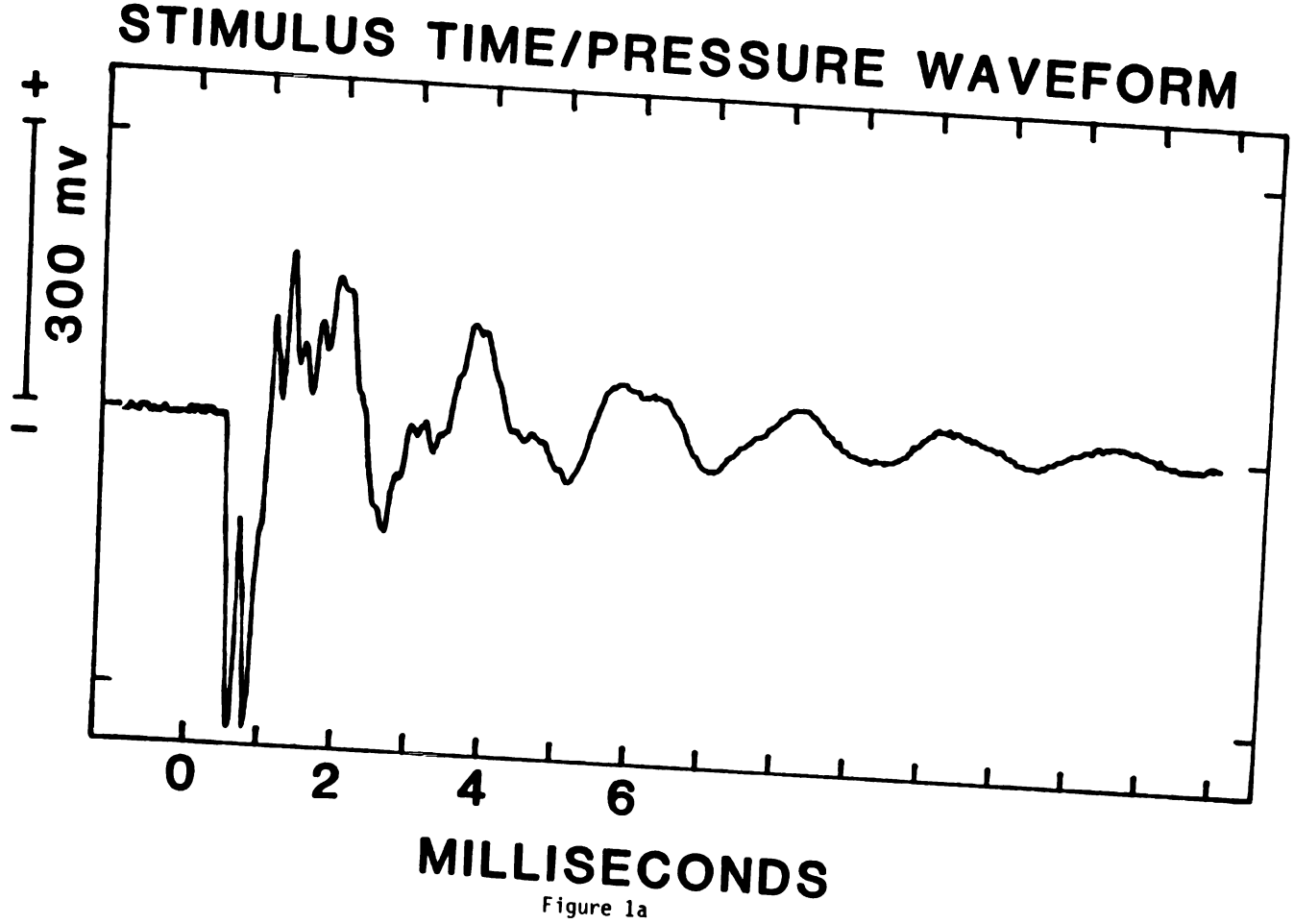

Figure 1a

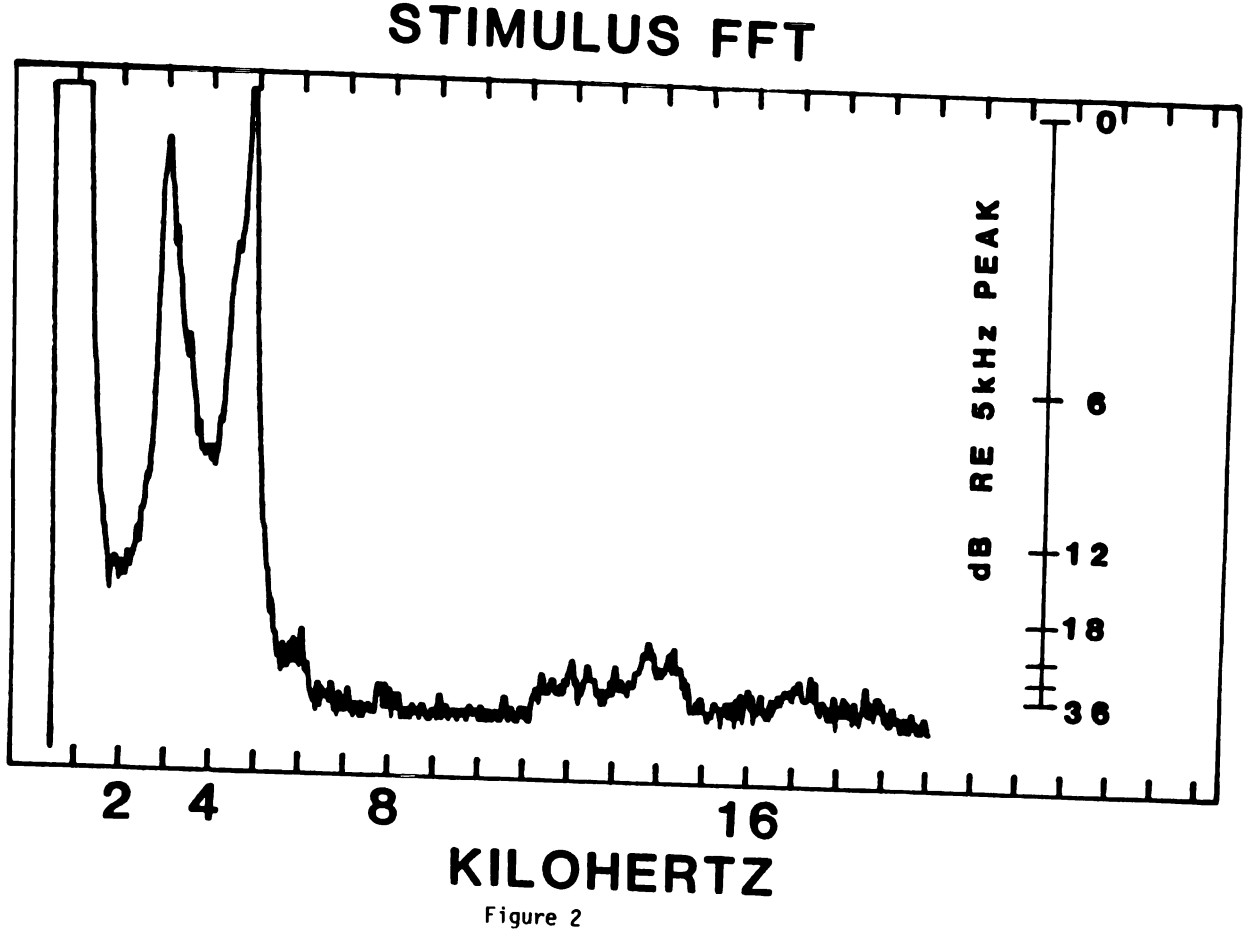

Figure 2

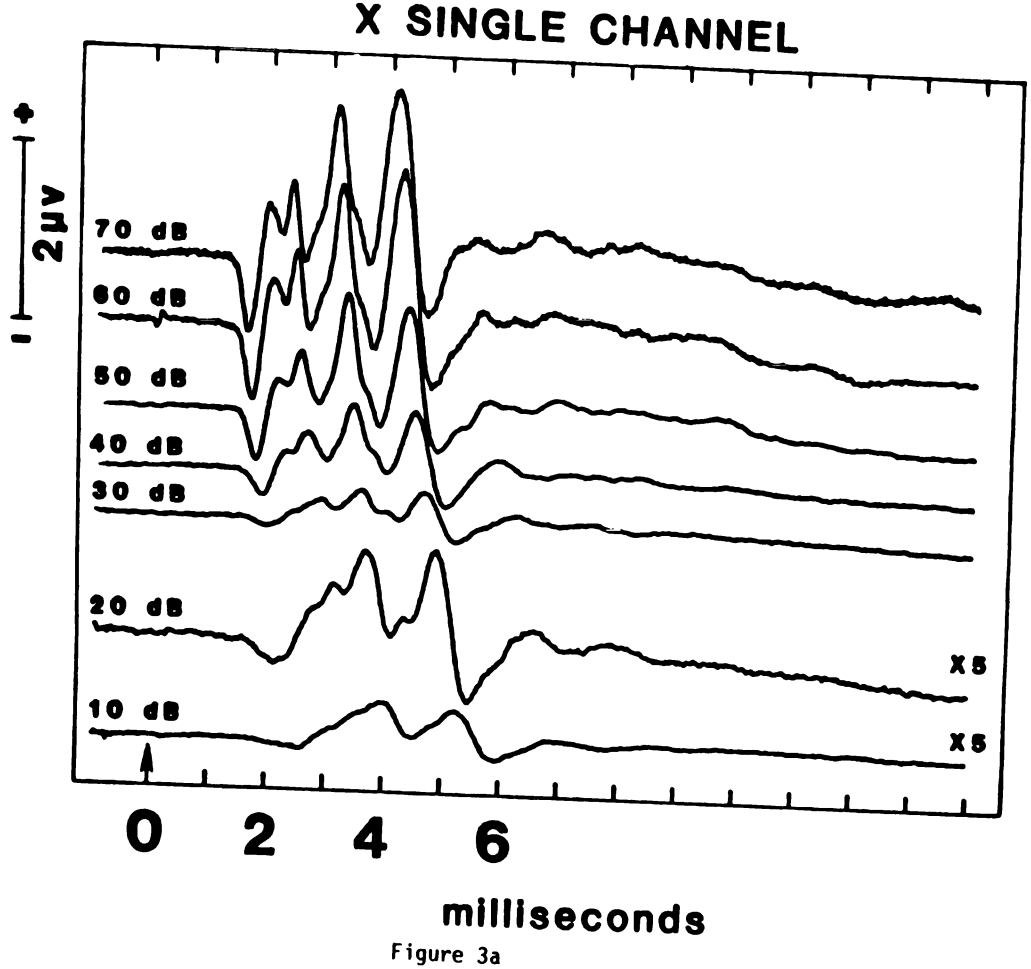
X SINGLE CHANNEL
+
2μv
-
70 dB
60 dB
50 dB
40 dB
30 dB
20 dB
10 dB
X5
X5
0
2
4
6
milliseconds

Figure 3a

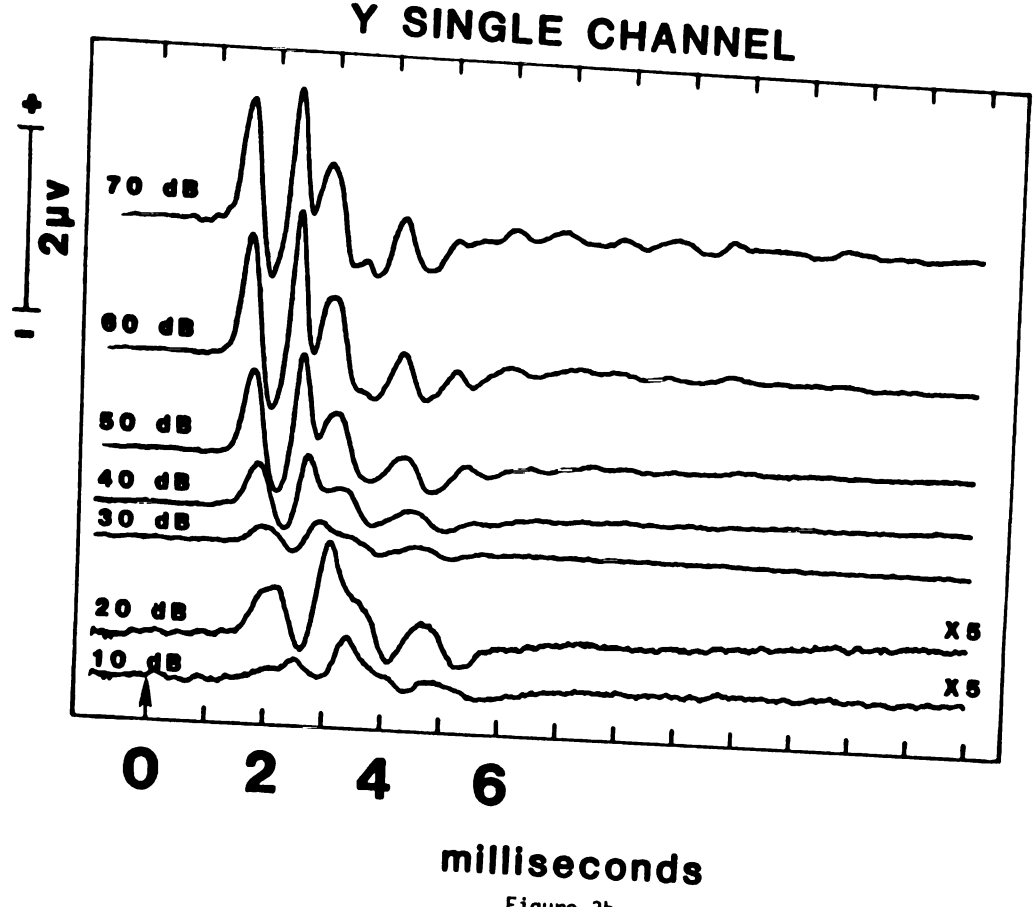
Y SINGLE CHANNEL
+
2μv
-
70 dB
60 dB
50 dB
40 dB
30 dB
20 dB
10 dB
X5
X5
0
2
4
6
milliseconds

Figure 3b

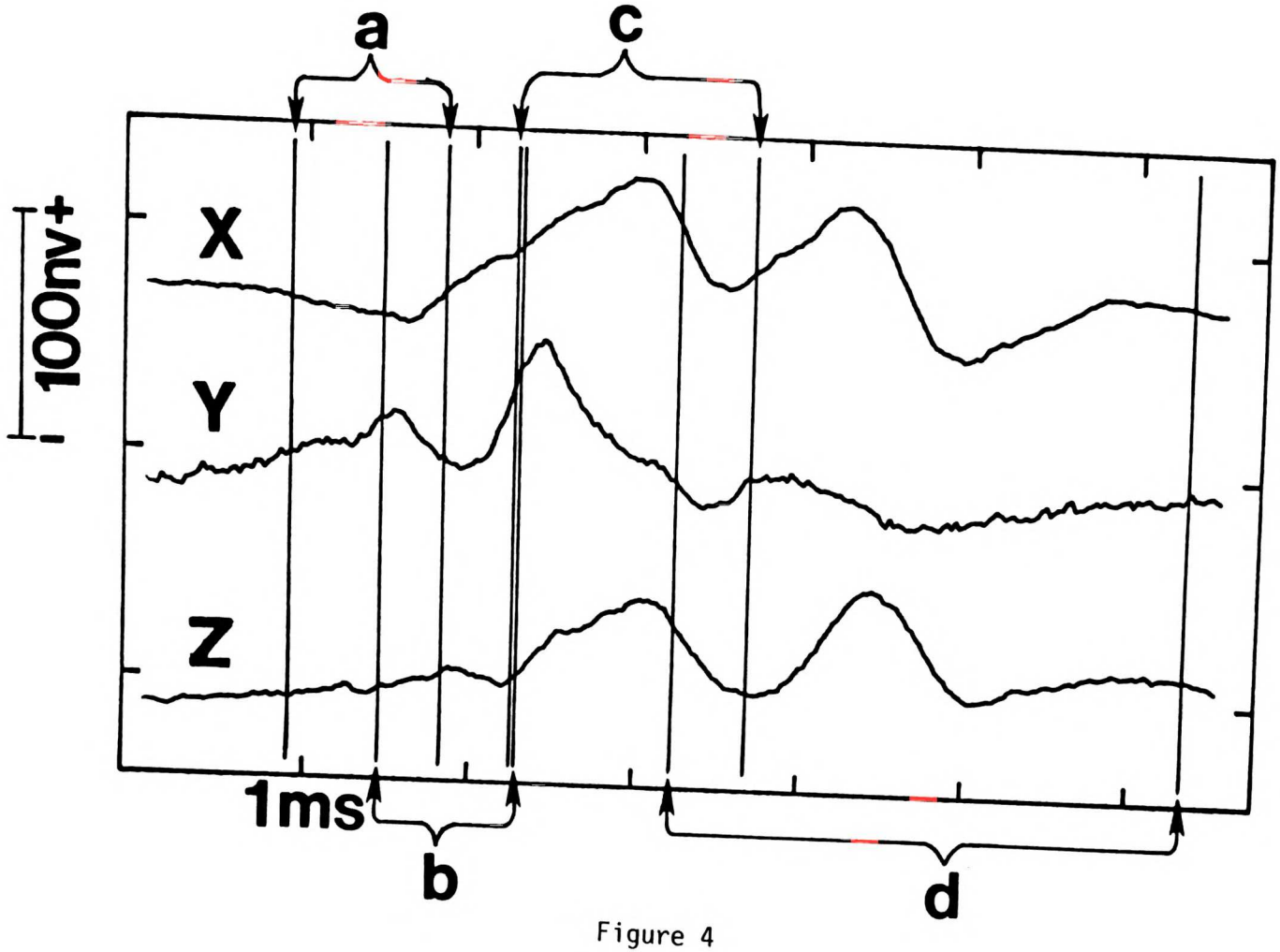

Figure 4

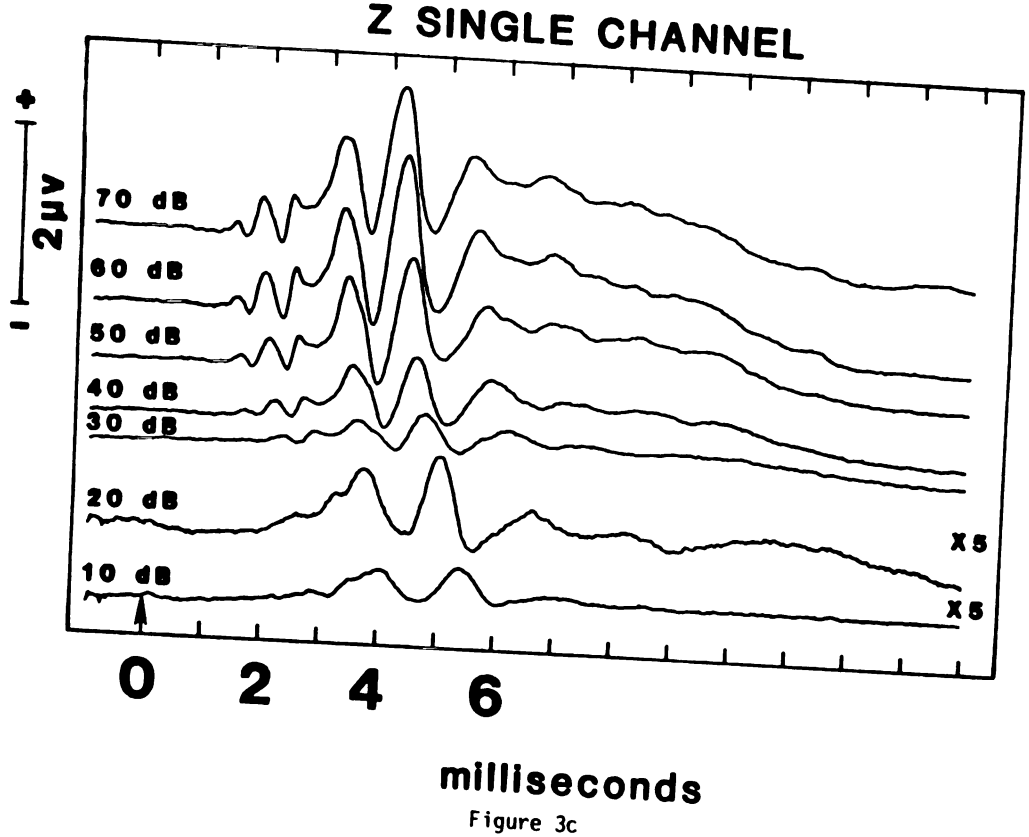
Z SINGLE CHANNEL
+
2μv
-
70 dB
60 dB
50 dB
40 dB
30 dB
20 dB
10 dB
X5
X5
0
2
4
6
milliseconds

Figure 3c

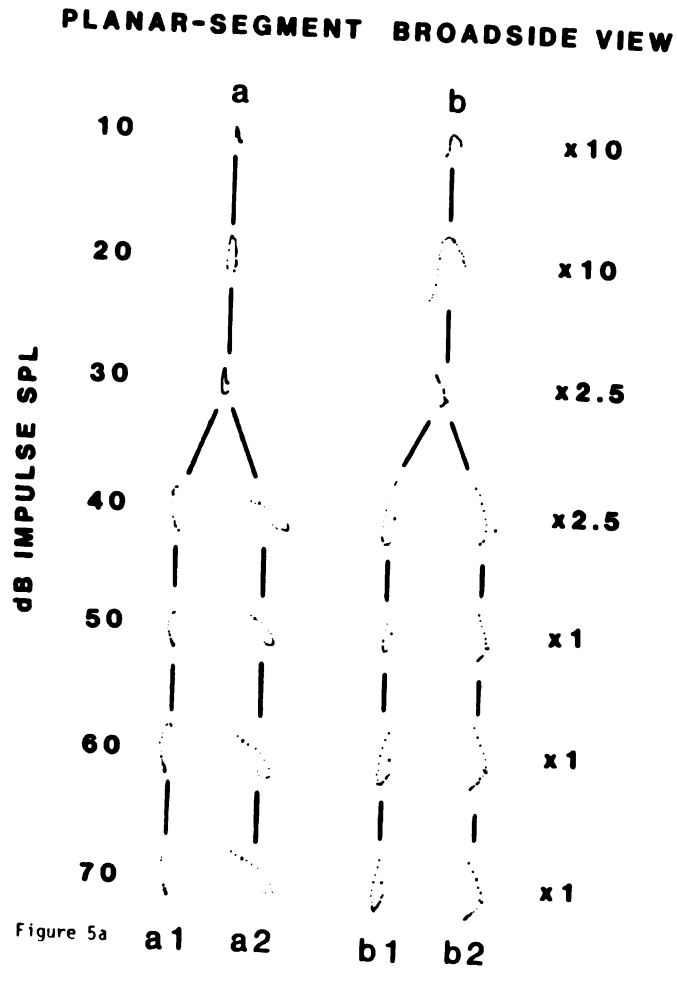
PLANAR-SEGMENT BROADSIDE VIEW
dB IMPULSE SPL
10
20
30
40
50
60
70
a
b
x10
x10
x2.5
x2.5
x1
x1
x1
a1
a2
b1
b2

Figure 5a

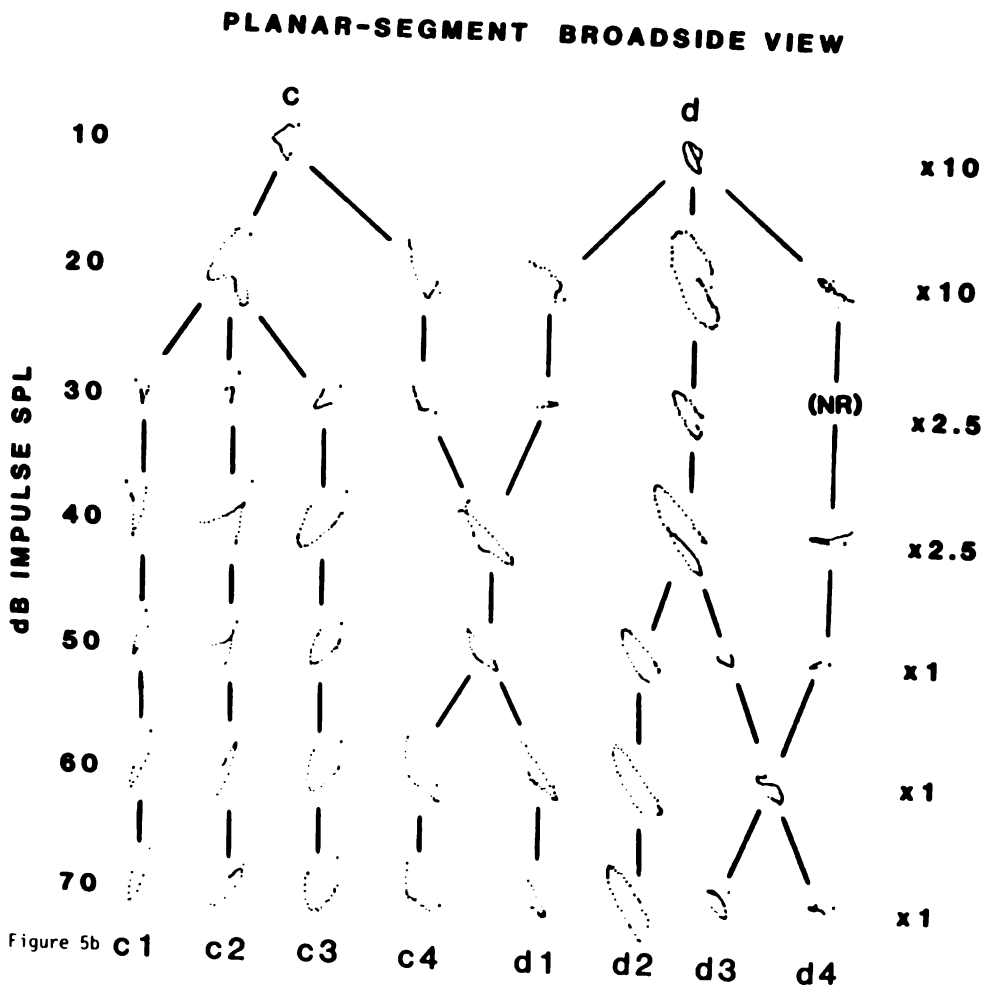
PLANAR-SEGMENT BROADSIDE VIEW
dB IMPULSE SPL
10
20
30
40
50
60
70
c
d
x10
x10
x2.5
x2.5
x1
x1
x1
(NR)
c1
c2
c3
c4
d1
d2
d3
d4

Figure 5b

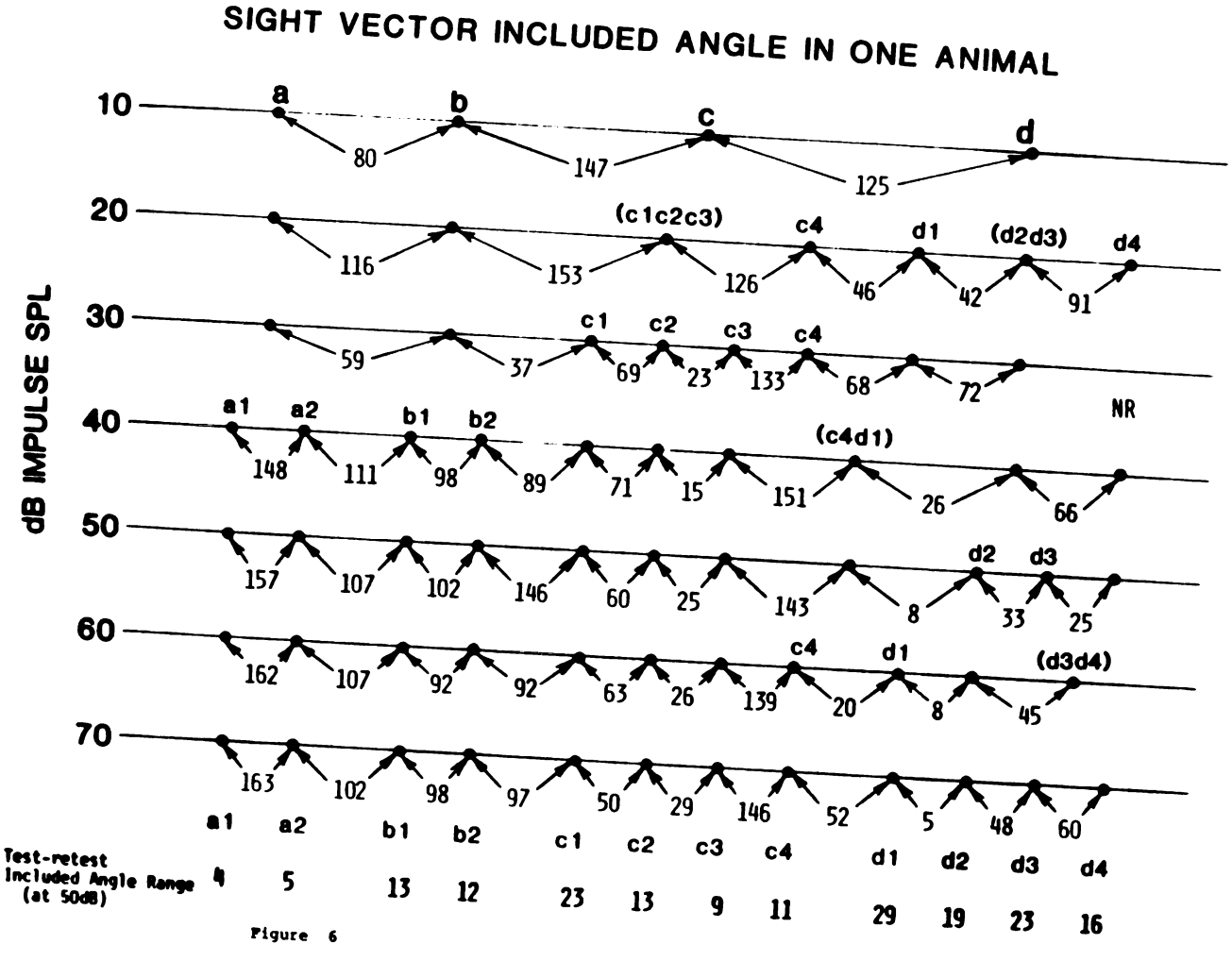
SIGHT VECTOR INCLUDED ANGLE IN ONE ANIMAL
dB IMPULSE SPL
10
20
30
40
50
60
70
a
b
c
d
80
147
125
(c1c2c3)
c4
d1
(d2d3)
d4
116
153
126
46
42
91
c1
c2
c3
c4
59
37
69
23
133
68
72
NR
a1
a2
b1
b2
(c4d1)
148
111
98
89
71
15
151
26
66
d2
d3
157
107
102
146
60
25
143
8
33
25
c4
d1
(d3d4)
162
107
92
92
63
26
139
20
8
45
163
102
98
97
50
29
146
52
5
48
60
a1
a2
b1
b2
c1
c2
c3
c4
d1
d2
d3
d4
Test-retest
Included Angle Range
(at 50dB)
4
5
13
12
23
13
9
11
29
19
23
16

Figure 6

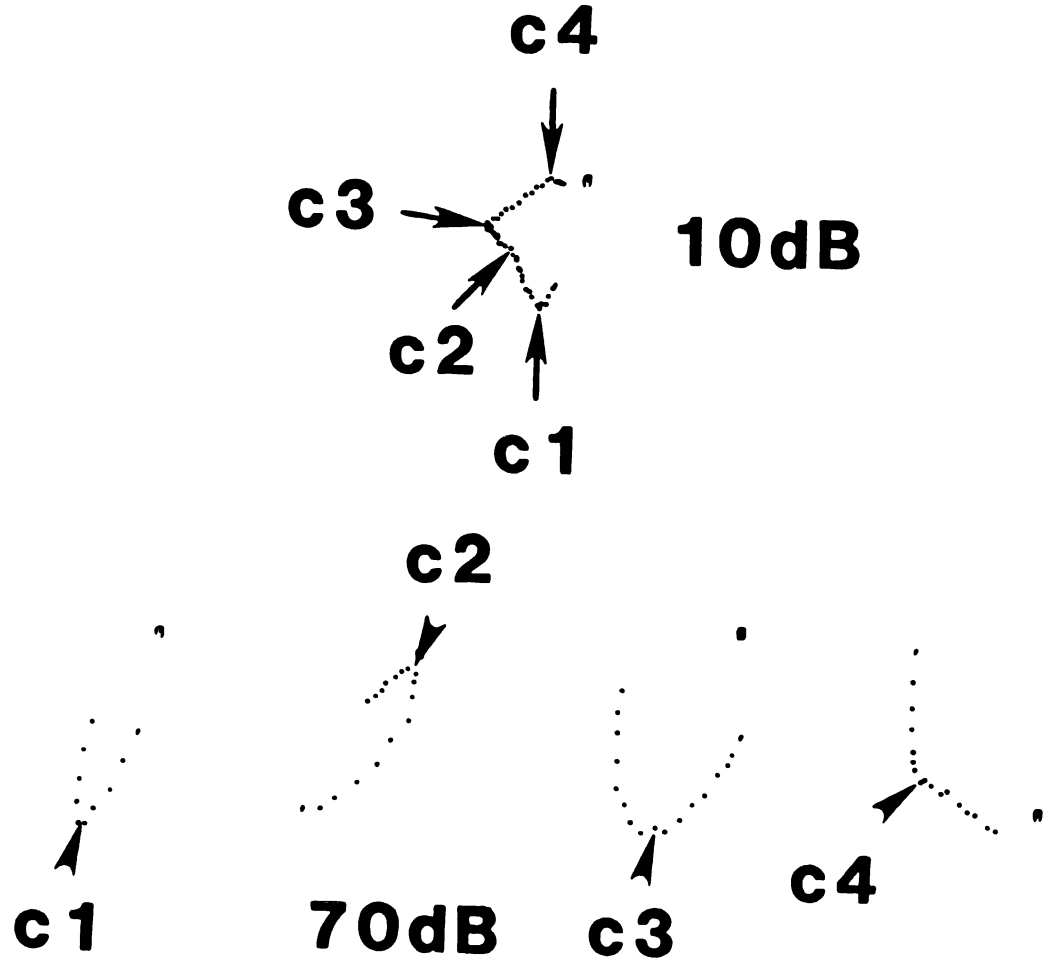

Figure 7a

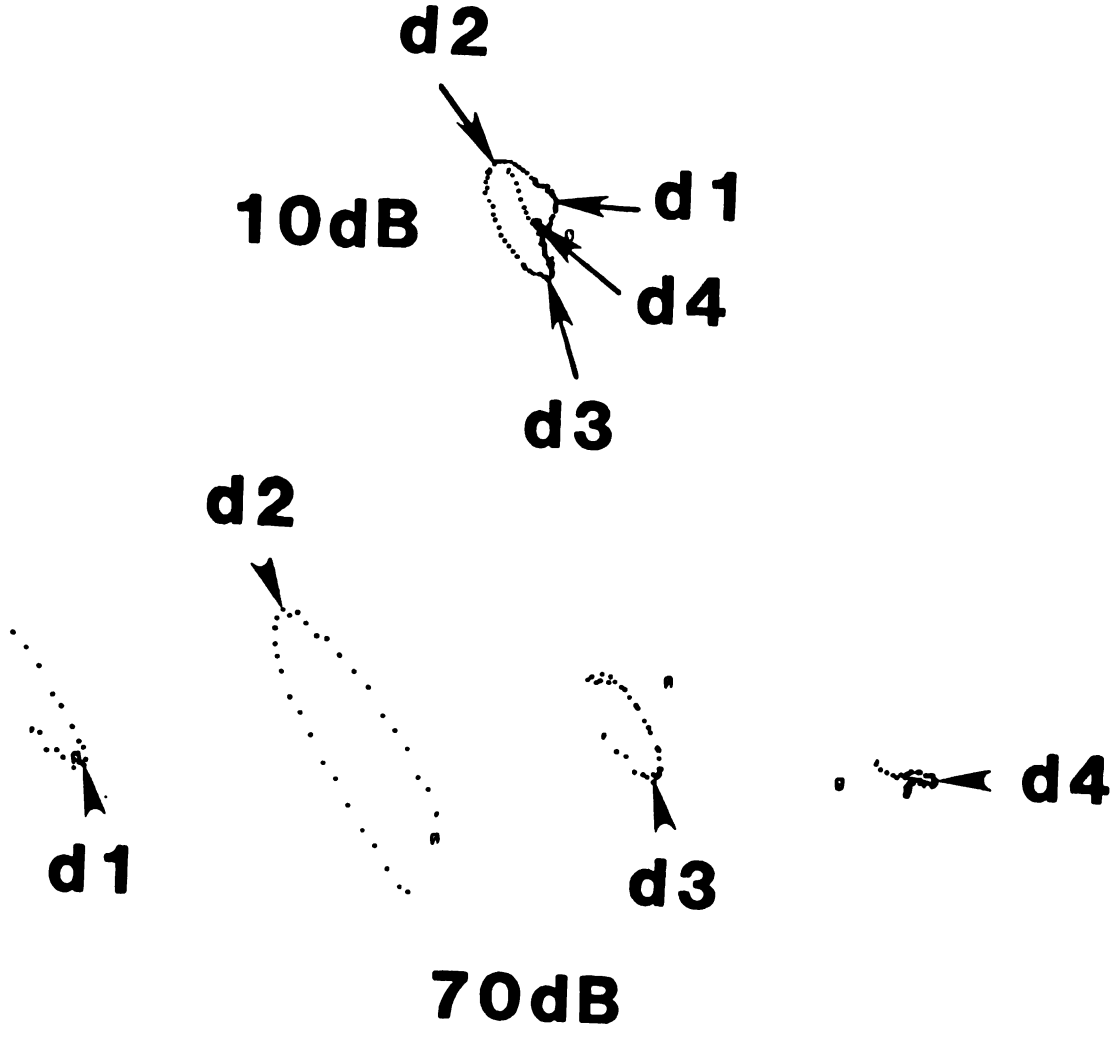

Figure 7b

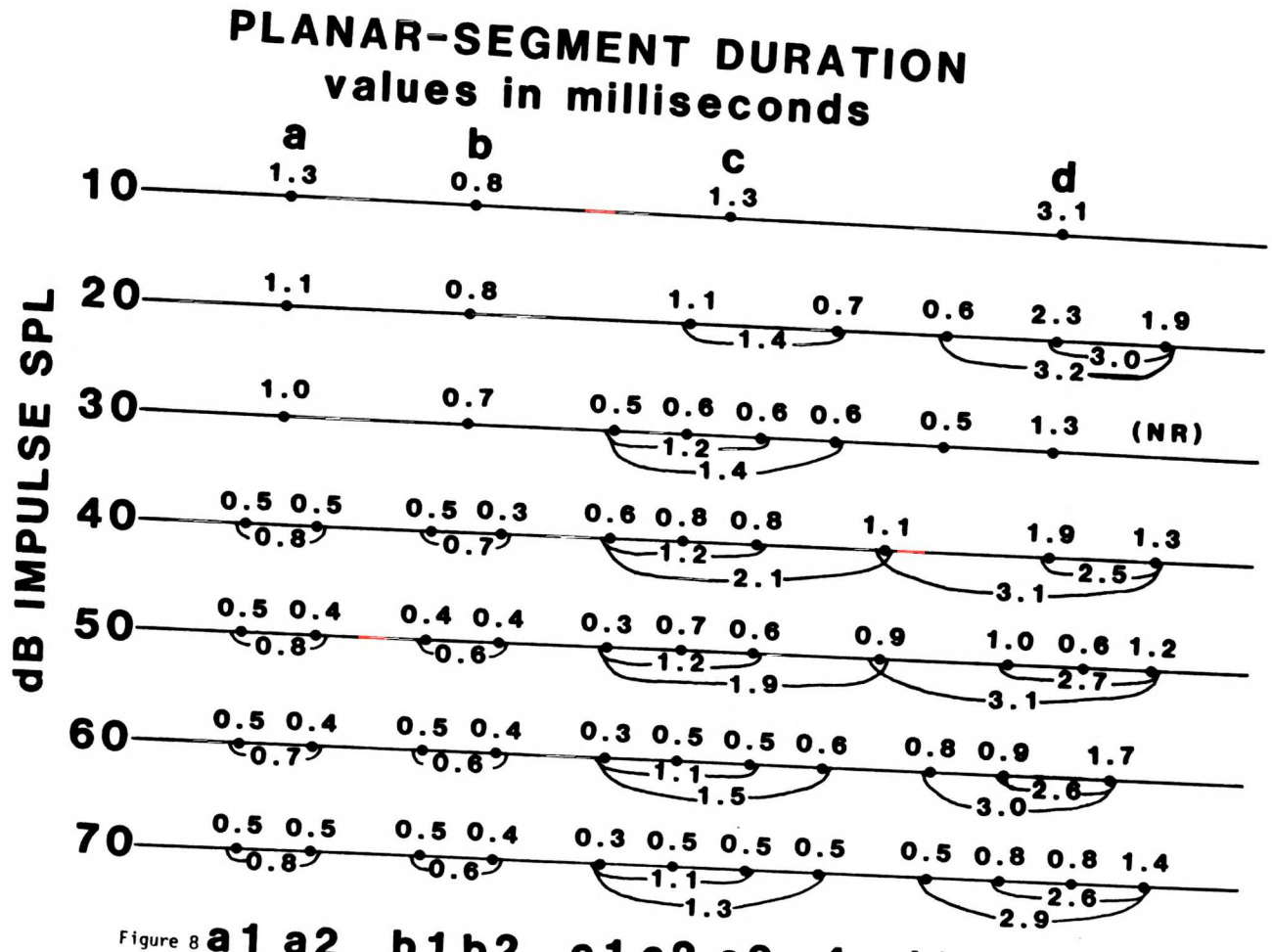
PLANAR-SEGMENT DURATION
values in milliseconds
dB IMPULSE SPL
a
b
c
d
10
20
30
40
50
60
70
1.3
0.8
1.3
3.1
1.1
0.8
1.1
0.7
0.6
2.3
1.9
1.4
3.2
3.0
1.0
0.7
0.5
0.6
0.6
0.6
0.5
1.3
(NR)
1.2
1.4
0.5 0.5
0.5 0.3
0.6 0.8
0.8
1.1
1.9
1.3
0.8
0.7
1.2
2.1
2.5
3.1
0.5 0.4
0.4 0.4
0.3 0.7
0.6
0.9
1.0
0.6
1.2
0.8
0.6
1.2
1.9
2.7
3.1
0.5 0.4
0.5 0.4
0.3 0.5
0.5
0.6
0.8
0.9
1.7
0.7
0.6
1.1
1.5
2.6
3.0
0.5 0.5
0.5 0.4
0.3 0.5
0.5
0.5
0.5
0.8
0.8
1.4
0.8
0.6
1.1
1.3
2.6
2.9
a1 a2 b1 b2 c1 c2 c3 c4 d1 d2 d3 d4

Figure 8

PLANAR-SEGMENT POSITION IN ONE ANIMAL

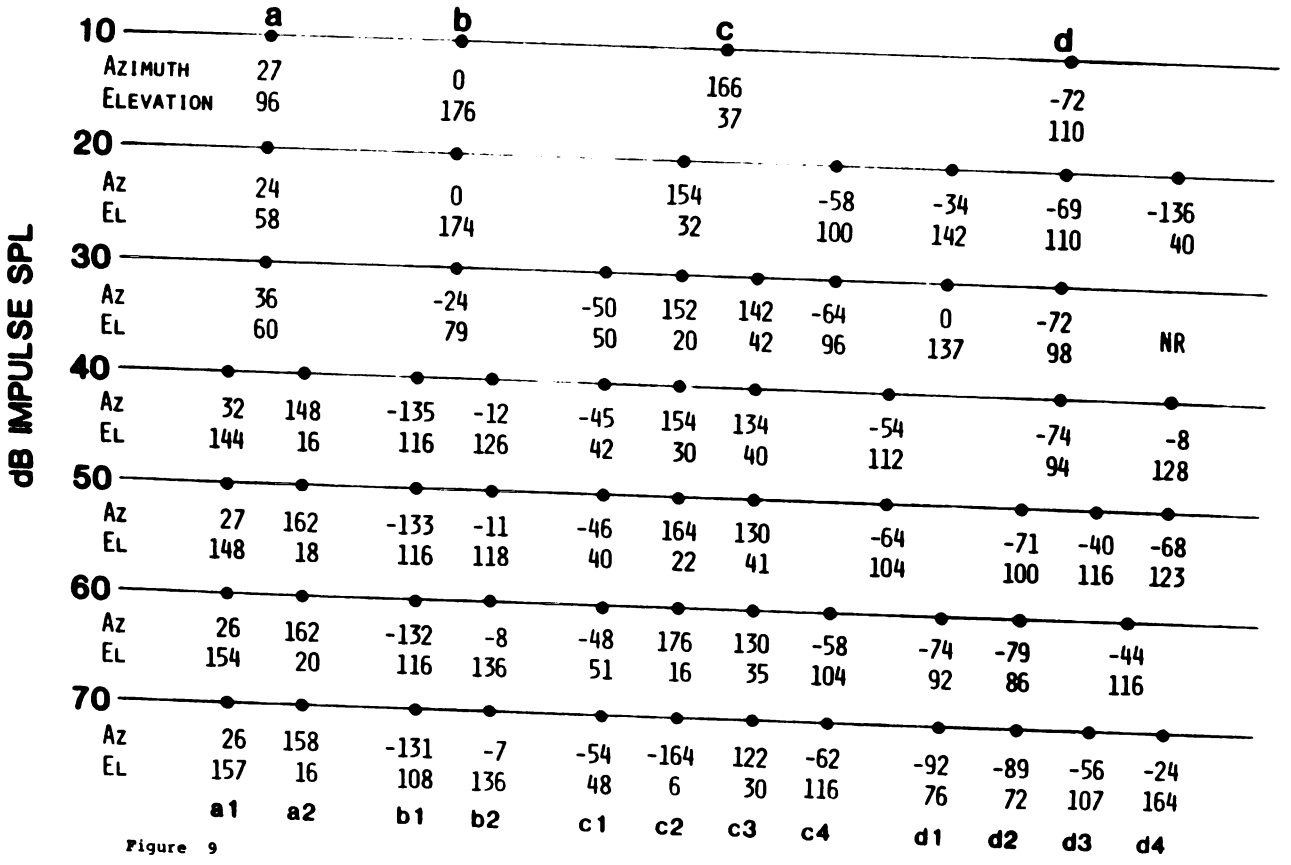

Figure 9

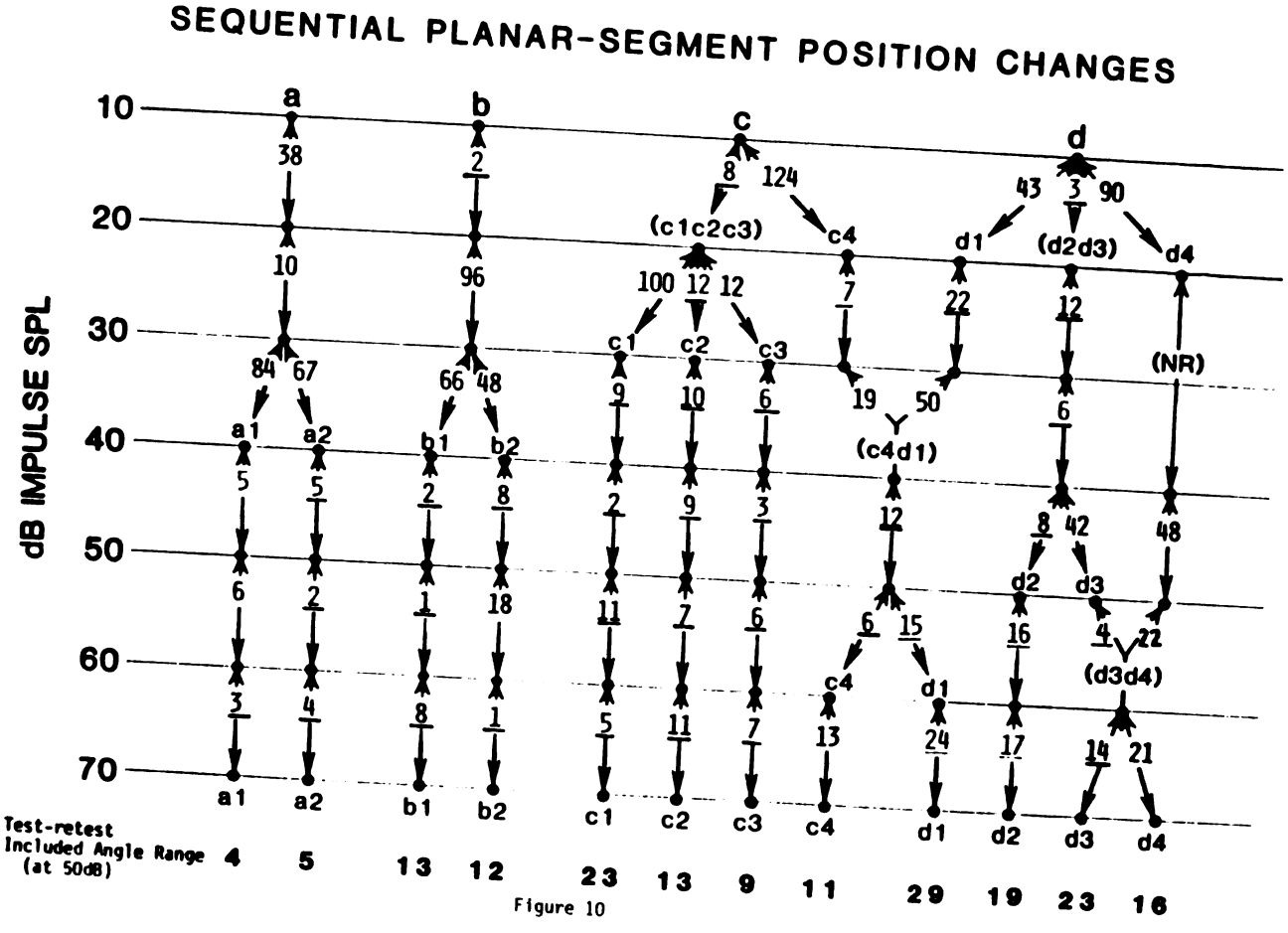
SEQUENTIAL PLANAR-SEGMENT POSITION CHANGES
dB IMPULSE SPL
10
20
30
40
50
60
70
a
b
c
d
38
2
8
124
43
3
90
(c1c2c3)
c4
d1
(d2d3)
d4
10
96
100
12
12
7
22
12
c1
c2
c3
(NR)
84
67
66
48
19
50
9
10
6
6
a1
a2
b1
b2
(c4d1)
5
5
2
8
2
9
3
12
8
42
48
d2
d3
6
2
1
18
11
7
6
6
15
16
4
22
(d3d4)
3
4
8
1
5
11
7
13
24
17
14
21
a1
a2
b1
b2
c1
c2
c3
c4
d1
d2
d3
d4
Test-retest
Included Angle Range
(at 50dB)
4
5
13
12
23
13
9
11
29
19
23
16

Figure 10

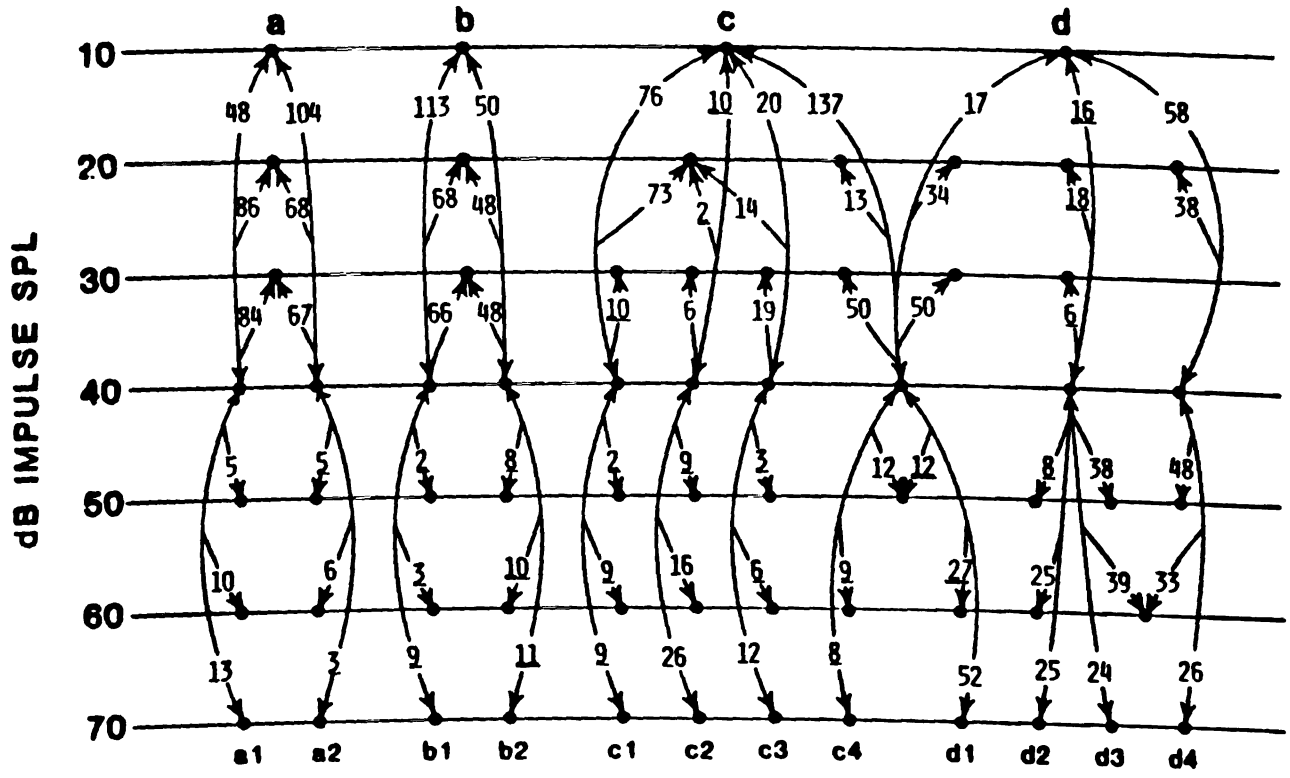
PLANAR-SEGMENT POSITION RE:40dB
dB IMPULSE SPL
10
20
30
40
50
60
70
a
b
c
d
a1
a2
b1
b2
c1
c2
c3
c4
d1
d2
d3
d4
Test-retest Included Angle Range (at 50dB)
4
5
13
12
23
13
9
11
29
19
23
16

Figure 11

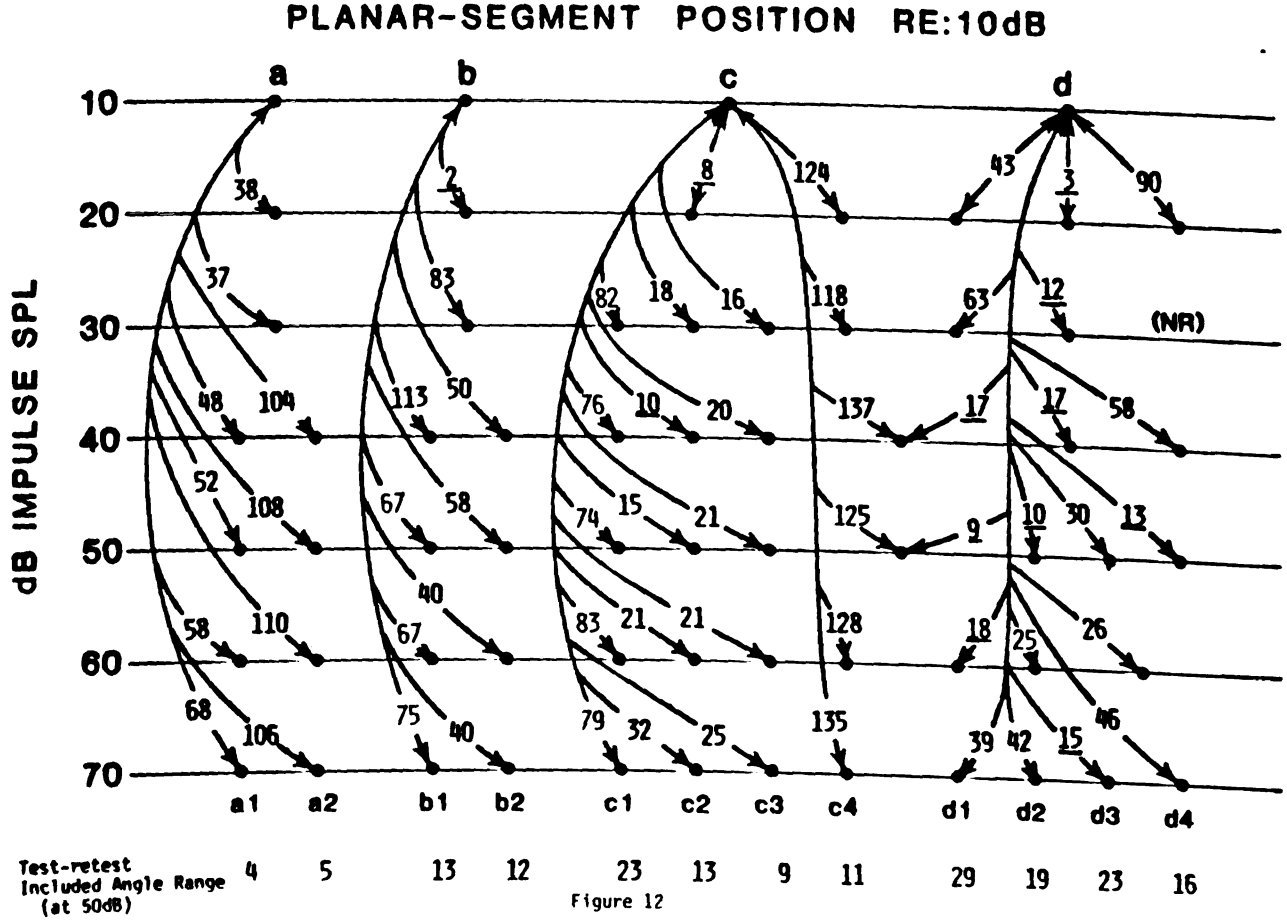
PLANAR-SEGMENT POSITION RE:10dB
dB IMPULSE SPL
10
20
30
40
50
60
70
a
b
c
d
38
37
48
104
52
108
58
110
68
106
2
83
113
50
67
58
40
67
75
40
8
124
82
18
16
118
76
10
20
137
74
15
21
125
83
21
21
128
79
32
25
135
43
3
90
63
12
(NR)
17
17
58
9
10
30
13
18
25
26
39
42
15
46
a1
a2
b1
b2
c1
c2
c3
c4
d1
d2
d3
d4
Test-retest Included Angle Range (at 50dB)
4
5
13
12
23
13
9
11
29
19
23
16

Figure 12

CHAPTER 5

CONCLUSION

The planarity of an electrophysiologic response is a phenomenon which can result from at least two completely different types of active generators, cardiac muscle and neurons of the auditory pathway. In both cases, shape, degree of planarity, and position of the plane of data points are directly related to the generator activity (Burger and Vaane, 1958; Pipberger and Carter, 1962; Martin et al, 1983a, b, c). That planarity of response results from two different generator types suggests that the basis of planarity is not unique to any particular generator type, but that planarity is a result of some basic principles functioning in both generator types. Therefore, we might expect that any electrophysiologic generator source sharing these basic principles would have a planar distribution of activity in voltage space.

What are these principles? From vectorcardiography, we have a clinical model from which we can derive some ideas about planarity. The QRS loop has been reported to be planar in the 'normal' case, with some exceptions (Schellong, 1937; Schellong, 1938; Burger and Vaane, 1958; Pipberger and Carter, 1962; Abel, 1965; Mark and Arbeit, 1968; Hannien, 1967; and Wartak, 1970). The orientation of

the QRS plane relative to the anatomical axes was reported by Pipberger and Carter (1962) to be the best indicator between normal and pathological VCG records. Types of pathologies which affected the orientation of the plane include old myocardial infarctions, ventricular hypertrophy,and ventricular conduction defects. The degree of planarity in children was predominantly altered by hypertrophy of heart muscle (Mark and Arbeit,1965). In adults, right ventricular conduction defects caused disruptions of planarity, but in general planarity of the QRS was not the most effective index for identifying pathology (Pipberger and Carter, 1962). Although variations in loop shape were noted in normal individuals, abnormal shape patterns were useful in identifying hypertrophy and conduction defects, and in identifying infarctions (Pipberger and Carter, 1962). Hypertrophy changes the physical size of the generators and therefore their spatial distribution and possible phase relationship. Myocardial infarctions and conduction defects result in asynchronous depolarization of the heart tissue which also disrupts the phase relationship between the generators.

In the studies presented in this paper three observations were made: 1) the planar-segments identified were similar in characteristics across animals (chapter 2), 2) their positions in voltage space were generator dependent

and not recording electrode position dependent (chapter 3), and 3) changes in generator activity elicited by parametric manipulation were reflected in planar segment number, shape, apex-latency, duration and position in voltage space. Since the planar-segments are reliable and reflect generator activity, their behavior can be said to reflect the processes within those generators which lead to planar-segment formation. If we are certain that changes in spatial distribution and phase relationship of generators occur as stimulus level is increased, then alterations of the planar-segment can be assumed to reflect those principles. Thus, both theory and practice indicate that planar characteristics of electrophysiologic responses in general, rely on the time related aspects of generator activity, such as synchrony and relative phase, and on the spatial orientation of the generators.

BIBLIOGRAPHY

Abel, H. Vectorcardiographic alterations and efficiency of the cardiovascular system after myocardial infarction. In Vectorcardiography, 1965 North Holland Publishing Co., Amsterdam, 1966.

Allen, A.R., and Starr, A. Auditory brain stem potentials in monkey (M. mulatta) and man. Electroenceph. Clin. Neurophysiol., 1978, 45: 53-63.

Antoli-Candela, F., and Kiang, N. Y.-S. Unit activity underlying the N_1 potential. In R.F. Naunton and C. Fernandez (Eds.), Evoked electrical activity in the auditory nervous system. New York: Academic Press, 1978.

Buchwald, J.S. Generators. In Moore (Ed.), Basis of auditory brain-stem evoked responses. New York: Grune and Stratton, 1983.

Burger, H.C., and Vaane, J.P. A criterion characterizing the orientation of a vectorcardiogram in space. Am. Heart J., 1958, 56: 29-35.

Coats, A.C., and Martin, J.L. Human auditory nerve action potentials and brain stem evoked responses. Arch. Otolaryngol., 1977, 103: 605-622.

Cohen, M. M. Coronal topography of the middle latency auditory evoked potentials (MLAEPs) in man. Electroencephal. Clin. Neurophysiol., 1982, 53: 321-336.

Davis, H. Principles of electric response audiometry. Annals Oto. Rhin. and Laryn., (suppl.), 1976, 28: 1-96.

DePasquale, N., and Burch, G.E. The spatial vectorcardiogram in left bundle branch block and myocardial infarction, with autopsy studies. Am. J. Med., 1960, 29: 633-639.

Don, M., Allen, A.R., and Starr, A. Effect of click rate on the latency of auditory brain stem responses in humans. Ann. Otol. Rhinol. Laryngol., 1977, 86: 186-196.

Don, M., and Eggermont, J.J. Analysis of the click-evoked brainstem potentials in man using high-pass noise masking. J. Acoust. Soc. Am., 1978, 63: 1084-1092.

Dum, N., Schmidt, U., and Von Wedel, H. Scalp distribution of the auditory evoked brainstem potentials in the guinea pig during monaural and binaural stimulation. Hear. Res., 1981, 5: 271-284.

Eggermont, J.J. Analysis of compound action potential responses to tone bursts in the human and guinea pig cochlea. J. Acoust. Soc. Amer., 1976, 60: 1132-1139.

Frimpter, G.W., Scherr, L. and Ogden, D. The spatial vectorcardiogram in complete left bundle branch block with special reference to the initial component. Am. Heart J., 1958 55: 220-230.

Hannien, P. Vectorcardiographic studies in newborn infants. Acta Paediatrica Scand., 1967, Suppl. 175: p.27.

Hashimoto, I., Ishiyama, Y., Yoshimoto, T., et al. Brainstem auditory evoked potentials recorded directly from human brain-stem and thalamus. Brain, 1981, 104: 841-859.

Hecox, K. and Galambos, R. Brainstem auditory evoked responses in human infants and adults. Arch. Otolaryngol., 1974, 99: 30-33.

Hodgman, C.D., editor in chief, Handbook of chemistry and physics, forty-second edition. The Chemical Rubber Publishing Co., Cleveland, Ohio, 1960.

Huang, C.M., and Buchwald, J.S. Factors that affect the amplitudes and latencies of the vertex short latency acoustic responses in the cat. Electroencephal. Clin. Neurophysiol., 1978, 44: 179-186.

Hugenholtz, P.G., Whipple, G.H. and Levine, H.D. A clinical appraisal of the vectorcardiogram in myocardial infarction. I. The cube system. Circulation, 1961, 24: 808-824.

Ino, T. and Mizoi, K. Vector analysis of auditory brain stem responses (BSER) in human beings. Arch. Otolaryngol., 1980, 226: 55-62.

Jewett, D.L. Averaged volume-conducted potentials to auditory stimuli in the cat. Physiologist, 1969, 12:262.

Jewett, D.L. Volume conducted potentials in response to auditory stimuli as detected by averaging in the cat. Electroencephal. and Clin. Neurophysiol., 1970, 28: 609-618.

Jewett, D.L. Personal communication, 1983.

Jewett, D.L., and Romano, M.N. Neonatal development of auditory system potentials averaged from the scalp of rat and cat. Brain Res., 1972, 36: 101-115.

Jewett, D.L., Romano, M.N., and Williston, J.S. Human auditory evoked potentials: Possible brain stem components detected on the scalp. Science, 1970, 167: 1517-1518.

Jewett, D.L., and Williston, J.S. Auditory-evoked far fields averaged from the scalp of humans. Brain, 1971, 94: 681-696.

Kodera, K., Yamane, H., Yamada, O., and Suzuki, J-I. Brain stem response audiometry at speech frequencies. Audiology, 1977, 16: 469.

Leiberman, A., Sohmer, H., and Szabo, G. Standard values of amplitude and latency of cochlear audiometry (electrocochleography) responses in different age groups. Arch. Klin. Exp. Ohren Nasen Kehlkopfheilk, 1973, 203: 267-273.

Lev, A., and Sohmer, H. Sources of averaged neural responses recorded in animals and human subjects during cochlear audiometry (Electro-cochleogram). Arch. Klin. Exp. Ohren. Nasen Kehlkopfheilk, 1972, 201: 79-90.

Mair, I.W.S., Elverland, H.H., and Laukli, E. Bilateral recording of early auditory evoked responses in the cat. Hear. Res., 1978, 1: 11-23.

Mark, H., and Arbeit, S. The resolved vector loop in children. In Vectorcardiography, 1965. North Holland Publishing Co., Amsterdam, 1966.

Martin, W.H., Jewett, D.L., Morris, J.H., Williston, J.S.,and Gardi, J.N. The three-channel

Lissajous trajectory of the auditory brain stem response I: Planar-segment formation, analysis, and reliability. In preparation, Electroencephal. Clin. Neurophysiol., 1983.

Martin, W.H., Jewett., D.L., Randolph, M.G., Williston, J.S. and Gardi, J.N. The three-channel Lissajous trajectory of the auditory brain stem response II: Effects of electrode position. In preparation, Electroencephal. Clin. Neurophysiol, 1983.

Martin, W.H., Gardi, J.N., and Jewett, D.L. The three-channel Lissajous trajectory of the auditory brain stem response III: Effects of stimulus intensity. In preparation, Electroencephal. Clin. Neurophysiol., 1983.

Mayer, H.W., Castellanos, A., and Lemberg, L. The spatiovectorcardiogram in peri-infarcton block. Am. J. Cardiol., 1963, 11: 613-621.

McFee, R., Wilkinson, R.S., and Abildskov, J.A. On the normalization of the electrical orientation of the heart and the representation of electrical axis by means of an axis map. Am. Heart J., 1961, 3: 391-397.

Moore, E.J., editor. Bases of auditory brainstem evoked responses. New York: Grune and Stratton. 1983.

Morrison, D.F. Multivariate statistical methods. New York: McGraw-Hill, 1976.

Parker, D. Dependence of the auditory brainstem response on electrode location. Arch. Otolaryngol., 1981, 107: 367-371.

Pfeiffer, R., and Kim, D.O. Cochlear fiber response: Distribution along the cochlear partition. J. Acoust. Soc. Am., 1974, 58: 867-869.

Picton, T.W., high, S.H., and Krauz, H.J. et al. Human auditory evoked potentials. I. Evaluation of components. Electroencephal. Clin. Neurophysiol., 1974, 36: 179-190.

Pipberger, H.V. and Carter, T.N. Analysis of the normal and abnormal vector cardiogram in its own reference frame. Circulation, 1962, 25: 827-840.

Plantz, R.G., Williston, J.S., and Jewett, D.L. Spatio-

temporal distribution of auditory far field potentials in rat and cat. Brain Res., 68: 55-71.

Plonsey, R. Bioelectric phenomena. New York: McGraw-Hill Book Co., 1969.

Prasher, D.K., and Gibson, W.P.R. Brain stem auditory evoked potentials: Significant latency differences between ipsilateral and contralateral stimulation. Electroencephal. Clin. Neurophysiol., 1980, 50: 240-246.

Pratt, H., Har'el, Z., and Golos, E. Three channel Lissajous' trajectory of human auditory brain stem evoked potentials. In press, Electroencephal. Clin. Neurophysiol., 1983.

Pratt, H., and Sohmer, H. Intensity and rate functions of cochlear and brainstem evoked responses to click stimuli in man. Arch. Oto. Rhino. Laryngol., 1976, 212: 85-93.

Rowe, M.J. Normal variability of the brain-stem auditory evoked response in young and old adult subjects. Electroencephal. Clin. Neurophysiol., 1978, 44: 459-470.

Schellong, F., Schwingel, E., and Herman, G. Die praktisch-Klinische Meth der Vektordiagraphie and das normale Vektordiagramm. Archiv fur Kreislaufforschung., 1937, 2: 1-5.

Schellong, F. Vektordiagraphie des Herzens als Klinische Meth. Klinische Wochenschrift., 1938, 17: 453-457.

Schulman-Galambos, C., and Galambos, R. Brainstem auditory-evoked responses in premature infants. J. Speech Hear. Res., 1975, 18: 456-465.

Shipley, C., Buchwald, J., Norman, R., and Guthried, D. Brainstem auditory evoked response development in the kitten. Brain Res., 1980, 182: 313-326.

Sohmer, H., and Feinmesser, M. Cochlear action potentials recorded from the external ear in man. Ann. Otol. Rhinol. Laryngol., 1967, 76: 427-435.

Sohmer, H., and Feinmesser, M. Routine use of Electrocochleography (cochlear audiometry) on human

subjects. Audiology, 1973, 12: 167-173.

Sohmer, H., Feinmesser, M., and Szabo, G. Sources of electrocochleographic responses as studied in patients with brain damage. Electroenceph. Clin. Neurophysiol., 1974, 37: 663-669.

Starr, A., and Achor, L.J. Auditory brainstem responses in neurological disease. Arch. of Neurol., 1975, 32: 761-768.

Starr, A., Amlie, R., Martin, W., and Saunders, S. Development of auditory function in newborn infants revealed by auditory brainstem potentials. Pediatrics, 1977, 60: 831-839.

Starr, A., and Brackmann, D.E. Brain stem potentials evoked by electrical stimulation of the cochlea in human subjects. Ann. of Oto. Rhino. Laryngol., 1979, 88: 550-556.

Starr, A., and Hamilton, A. Correlation between sites of neurological lesions and abnormalities of far-field auditory brainstem responses. Electroencephal. Clin. Neurophysiol., 1976, 41: 595-608.

Starr, A., and Squires, K. Distribution of auditory brainstem potentials over the scalp and nasopharynx in humans. Ann. NY Aca. Sci., 1982, 427-442.

Stockard, J., and Rossiter, V. Clinical and pathological correlates of brain stem auditory response abnormalities. Neurology, 1977, 316-325.

Stockard, J.E., Stockard, J.J., Westmoreland, B.F., and Corfits, J.L. Normal variation of brainstem auditory-evoked responses as a function of stimulus subject characteristics. Arch. Neurol., 1979, 36: 823-831.

Streletz, L.J., Katz, L., and Hohenberger, M. Scalp recorded auditory evoked potentials and Sonomotor responses: An evaluation of components and recording techniques. Electroencephal. Clin. Neurophysiol., 1977, 43: 192-206.

Szelenberger, W. Vector analysis of auditory evoked potential in the brain stem. Int. J. Bio-Medical Computing, 1982, 13: 263-269.

Terkildsen, K., Osterhammel, P., Huis, N.T., and Veld, F.

Far field electrocochleography, electrode positions. Scand. Audiol., 1974, 3: 123-129.

Wartak, J. Simplified Vectorcardiography. Philadelphia: J.B. Lippincott Co., 1970.

Williston, J., Jewett, D.J., and Martin, W.H. Planar curve analysis of three-channel auditory brain stem response: a preliminary report. Brain Res., 1981, 223: 181-184.

Yoshie, N. Electrocochleographic classification of sensorineural defects: Pathological pattern of the cochlear nerve compound action potential in man. In Electrocochleography. Baltimore: University Park Press, 1976.